STUDIES ON VIA COUPLING ON MULTILAYER PRINTED CIRCUIT BOARDS

TIMO TARVAINEN

Department of Electrical Engineering

OULU 1999

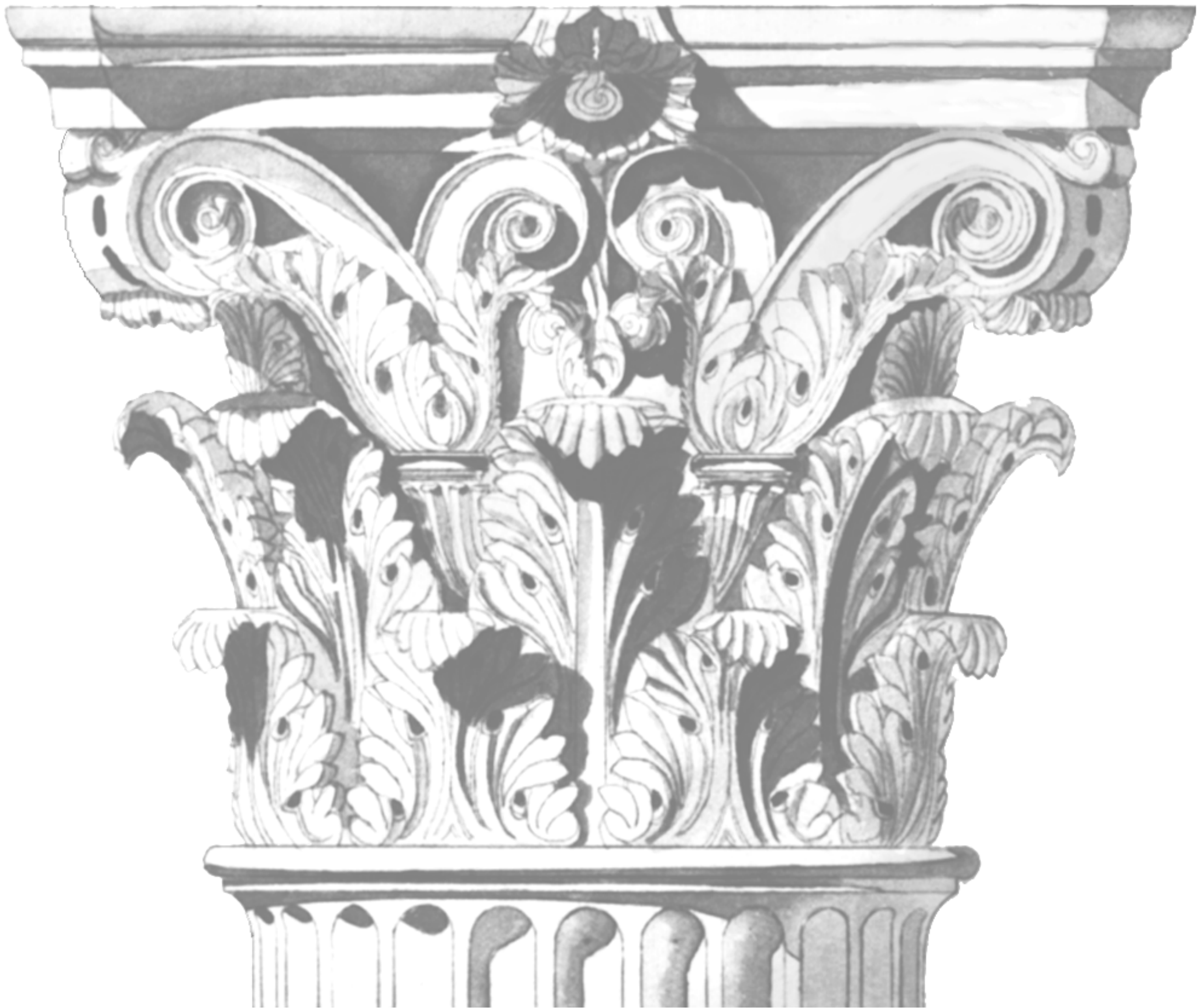

TIMO TARVAINEN

STUDIES ON VIA COUPLING ON MULTILAYER PRINTED CIRCUIT BOARDS

Academic Dissertation to be presented with the assent of the Faculty of Technology, University of Oulu, for public discussion in Oulunsali (Auditorium L5), Linnanmaa, on April 23rd, 1999, at 12 noon.

OULUN YLIOPISTO, OULU 1999

Copyright © 1999
Oulu University Library, 1999

Manuscript received 22.3.1999
Accepted 23.3.1999

Communicated by
Professor Lauri Kettunen
Professor Raimo Sepponen

ISBN 951-42-5189-X
(URL: http://herkules.oulu.fi/isbn951425189X/)

ALSO AVAILABLE IN PRINTED FORMAT

ISBN 951-42-5188-1
ISSN 0355-3213 (URL: http://herkules.oulu.fi/issn03553213/)

OULU UNIVERSITY LIBRARY
OULU 1999

Tarvainen Timo, Studies on via coupling on multilayer printed circuit boards
Department of Electrical Engineering, University of Oulu and Esju Oy, Oulu, FIN-90570, Oulu, Finland
1999
Oulu, Finland
(Manuscript received 22 March 1999)

Abstract

Design and manufacturing techniques of printed circuit boards (PCB's) have advanced from early one or two-layer structures to the multilayer boards where ten or more layers are no longer uncommon. These give additional routing space, potential decrease in device size and various design possibilities like solid ground and power planes. Unfortunately multilayer boards are vulnerable to high coupling between signal vias especially due to PCB resonances.

In this study via crosscoupling is investigated on multilayer PCB's. Special attention is given to the coupling due to resonances and vertically aligned blind vias. Problem is approached from the electromagnetic compatibility (EMC) point of view and high accuracy of measurements or models is not the objective. Instead ways to increase isolation are considered important. EMC is considered to include internal functionality of the device.

Analytical methods are used to calculate resonant frequencies, fields and quality factors for simple rectangular structures. The PCB cavity is reduced to two-dimensions for numerical calculation of same quantities. Aplac finite-difference time-domain simulator is used to model coupling due to PCB resonances. Isolation between vertically aligned blind vias is estimated analytically. A quasi-static numerical model is used to study a coaxial via structure. Multilayer test boards are constructed for measurement purposes. Simplified resonator structures on two-layer boards are used to test different methods to increase isolation.

Measurements show that high coupling between vias may occur due to PCB resonances. This leads to the situation, where previously used isolation methods between vias are not necessarily effective enough. Several means to reduce effects of PCB resonances are described in this study. Measured and modelled results agree well from an EMC point of view. Coupling due to vertically aligned blind vias is also shown to be high. A simple capacitance model may be used to approximate this up to frequencies where the dynamic wave nature of the board starts to be important. From a PCB designer's point of view these results mean that when the board size is not small compared to the wavelength, there is a possibility of resonances and reduction methods have to be taken into account. Also placement of the vias have to be carefully selected especially if blind or buried vias are used.

Keywords: crosscoupling, electromagnetic compatibility

Acknowledgements

This study was carried out in Esju Oy, Oulu, Finland, during the years 1997-1998 as a part of the research project for Nokia Radio Access Systems considering isolation on printed circuit boards. I owe a great dept of gratitude to my colleague Pekka Adolfsen whose interest in the physical behaviour of the PCB's gave me the possibility to conduct this research, which is reported in this thesis and also for his continuous encouragement during the study.

I wish to express my deepest gratitude to my supervising Professor Kalevi Kalliomäki for his advice and guidance, which were needed to complete this thesis.

I wish to thank Professor Lauri Kettunen and Professor Raimo Sepponen for refereeing this thesis and giving many valuable comments. I am truly grateful to Mr. Malcolm Musgrave for his revision of the English of the manuscript.

I am grateful to Tommi Ahosola, Marko Kuusikko and Jukka Luomala for realising layout drawings from the sketches and Päivi Pajala for dimensional measurements of the PCB cross-section. Marko Kuusikko also raised interesting questions in consideration of isolation on PCB's and one of these questions initiated the study of the vertically aligned blind via structure.

I wish to thank all other wonderful individuals who have helped me during this study and especially Timo Ahonpää, Jari Kolehmainen, Eero Koukkari, Docent Markku Moilanen, Lauri Pesola, Simo Piiroinen, Matti Syrjä and Markus Vahtola.

I also wish to thank the Tauno Tönning Foundation and the Jenny and Antti Wihuri Foundation for their financial support.

I am most indebted to my parents for their encouragement already in my early childhood research projects from 'fishing of whales' to 'structurally improved LEGO castles', which gave a spark for the future research work. Finally, I want to thank Hanna for her patience and support, which were especially needed during writing process of this thesis.

Oulu, March 1999 Timo Tarvainen

List of symbols and abbreviations

Latin letters

A	amplitude coefficient
a	radius of the coaxial line centre conductor, diameter of a ground via
b	radius of the coaxial line outer conductor
C'_{d1}	model parameter for calculation of shunt capacitance
C_{series}	series discontinuity capacitance
C_{shunt}	shunt discontinuity capacitance
C_{tot}	total per unit length capacitance
D	coaxial outer conductor diameter, amplitude parameter
D_a	diameter for placement of coaxial ground vias G1 and G4
D_b	diameter for placement of coaxial ground vias G2, G3, G5 and G6
d	coaxial inner conductor diameter
E_x, E_y, E_z	components of electric field intensity
$E_z(i, j)$	z-directed electric field intensity at a node (i, j)
$E_z^r(i, j)$	most recent value of z-directed electric field intensity at a node (i, j)
$E_z^{n+1}(i, j)$	updated value of z-directed electric field intensity at a node (i, j)
f_r	resonant frequency
f_{Smn}	resonant frequency corresponding to the measured coupling between ports m and n
H	height of the cavity
H_t	tangential magnetic field intensity
H_{tot}	total magnetic field intensity
H_x, H_y, H_z	components of magnetic field intensity
$H_x(i, j)$	x-directed magnetic field intensity at a node (i, j)
$H_y(i, j)$	y-directed magnetic field intensity at a node (i, j)
h	discretization factor
i	simulation node location at x-direction

$imax$	the largest simulation node index at x-direction
j	simulation node location at y-direction
$jmax$	largest simulation node index at y-direction
j	imaginary unit
k	wave number
k_c	cut-off wave number
L	length of the cavity
$(L_A)_r$	attenuation through the cavity at resonance [dB]
m	resonant mode number indicator in x-direction, number of nodes in x-direction
n	resonant mode number indicator in y-direction, number of nodes in y-direction
P_c	power lost to the cavity walls
p	resonant mode number indicator in z-direction
Q	quality factor
Q_{1cop}, Q_{2cop}, Q_{3cop}, Q_{4cop}	measured loaded quality factors for a cavity which sidewalls are metalled
Q_{1via}, Q_{2via}, Q_{3via}, Q_{4via}	measured loaded quality factors for a cavity which sidewalls are formed by via fences
Q_c	quality factor due to wall losses
Q_d	dielectric quality factor
Q_l	loaded quality factor
Q_r	radiation quality factor
Q_u	unloaded quality factor
$R(i, j)$	residual at a node (i, j)
R_s	surface resistivity
r	acceleration factor, relaxation coefficient
s	gap length in a coaxial line
S	ground via grid separation parameter
U	stored energy, stored energy per unit length
$V(i, j)$	potential at a node (i, j)
$V^r(i, j)$	most recent value of potential at a node (i, j)
$V^{n+1}(i, j)$	updated value of potential at a node (i, j)
W	width of the cavity
W_e	time averaged energy stored in electric field
x, y, z	Cartesian coordinates
Z_0	characteristic impedance

Greek letters

α	model parameter for calculation of shunt capacitance
Δ	separation of ground vias along width of the resonator
Δf	3 dB bandwidth of the resonance
ΔU	energy enclosed in a unit area per unit length
δ_s	skin depth

ε	permittivity
ε_0	permittivity of vacuum
ε_r	relative permittivity
$\varepsilon_{r,2}$	relative permittivity of dielectric support bead
$\varepsilon_{r,1}$	relative permittivity of coaxial line filling
η_0	characteristic impedance of free space
λ	wavelength
λ_{Smn}	wavelength corresponding to the measured coupling value between ports m and n
μ	permeability
μ_0	permeability of vacuum
σ	conductivity
ω	angular frequency
ω_r	angular frequency at resonance

Abbreviations

2-D	two-dimensional
3-D	three-dimensional
BMA	blind mate connector (coaxial surface mount RF connector)
div	division
EM	electromagnetic
EMC	electromagnetic compatibility
EMI	electromagnetic interference
FDTD	finite difference time-domain
FR4	epoxy/ glass substrate material
G1, G2, …, G6	numbering of coaxial ground vias
GND	ground
HPGL	Hewlett Packard graphics language
IFBW	intermediate frequency bandwidth
P1, P2, P3, P4	numbering of the measurement ports
PC	personal computer
PCB	printed circuit board
RES1, RES2, …, RES6	indicators of different ground via structures for coupled resonators
RGH_{rms}	surface roughness (root mean square)
RF	radio frequency
S_{11}, S_{21}, S_{12}, S_{22}	two port S-parameter set
SMA	coaxial connector with outer conductor diameter of 3.5 mm
TM	transverse magnetic
$\tan\delta$	dielectric loss tangent

Contents

Abstract
Acknowledgements
List of symbols and abbreviations
1. Introduction 13
 1.1. Background 13
 1.2. Purpose of the study 14
 1.3. Contribution 15
 1.4. Contents of the thesis 16
2. Resonant cavities and via coupling inside multilayer PCB's 17
 2.1. Introduction to the multilayer PCB's 17
  2.1.1. Description of multilayer PCB's 17
  2.1.2. Description of the via types 18
  2.1.3. EMI view to the multilayer boards and vias 19
 2.2. Description of the PCB cavity as a short circuited waveguide 20
  2.2.1. Description of ground via configurations and related boundary conditions 20
  2.2.2. Waveguide types for different boundary conditions 22
  2.2.3. Simplification to the two-dimensional waveguide problem 22
3. Descriptions of the structures to be studied 23
 3.1. Structures on multilayer boards 23
  3.1.1. Isolated cavities 23
  3.1.2. Stacked cavities 25
  3.1.3. Transitions between shielded sections 25
  3.1.4. Coupling between opposite open ended blind vias 27
 3.2. Simplified cavities on two-layer boards 28
  3.2.1. Isolated cavities 28
  3.2.2. Coupled cavities 30
4. Modelling 31
 4.1. Purpose of modelling in this study 31
 4.2. Analytical models 31
  4.2.1. Approximation of resonant frequencies and fields 31
  4.2.2. Approximation of Q-values 35
  4.2.3. Coupling between opposite open ended blind vias 37

4.3. Numerical models 40
4.3.1. Two-dimensional modelling of PCB cavities in the frequency domain 40
4.3.2. Approximation of unloaded Q-values 45
4.3.3. Three-dimensional modelling of PCB cavities in the time domain 46
4.3.4. Quasi static modelling of a coaxial via 48
5. Measured results 52
5.1. Description of the measurement methods 52
5.1.1. Coupling measurements 52
5.1.2. Q-value measurements 53
5.2. Measurements on multilayer boards 53
5.2.1. Isolated cavities 53
5.2.2. Stacked cavities 55
5.2.3. Transitions between shielded sections 56
5.2.4. Coupling between opposite open ended blind vias 56
5.3. Measurements on two-layer boards 59
5.3.1. Isolated cavities 59
5.3.2. Coupled cavities 73
6. Discussion 78
6.1. Measurement accuracy 78
6.2. Modelling accuracy 78
6.3. Comments on measured and modelled results 79
6.4. Improvement of isolation 81
7. Conclusions 84
References 86

1. Introduction

1.1. Background

Rising operating frequencies and complexity of telecommunications and computer systems offer a challenge for PCB designers and manufacturers. Usage of PCB's is preferred to the traditional microwave solutions like rectangular waveguide, because of their lower price and achievable device size reduction. In response to the increasing needs manufacturing techniques have advanced from simple two-layer circuit boards to the multilayer PCB's, where ten or more layers are no longer uncommon. An advantage of these is that they give additional routing space and offer the possibility for solid ground and power planes. These are important from the EMC point of view (Clayton 1992, Kiang 1990, Montrose 1996). In this study EMC is considered to include internal functionality of the device. In addition to this, various coupler and antenna designs are possible when multiple layers are available (Chen *et al.* 1996, Fujimoto & James 1994). Unfortunately there may exist unintentional cavity resonators buried inside this structure. The principle of resonant PCB is well known and it has been applied to permittivity measurements since the early seventies (Howell 1973, Landbrooke *et al.* 1973, Napoli & Hughes 1971). An undesired effect is that isolation between signal vias going through the cavity tends to decrease. This may cause devices with high dynamic ranges compared to the isolation to be out of their assumed specifications. Possible results are degraded attenuator performance, poor filter rejection responses and oscillating amplifiers. In digital circuitry fast data or clock signals may be victims of high crosscoupling.

Gu *et al.* (1994) have studied coupling between two vias in multilayer boards by using analytic model and measurements. However, results under resonant conditions are not shown. This is quite odd because board size used in their measurements should be large enough for resonances to appear. Measured results are shown at 1 GHz intervals and this might be the cause that no resonances were noted. Increasing via spacing is mentioned as a method to reduce crosscoupling. Effects of layer count and permittivity are also discussed. Coupling between open-ended vias between two parallel rectangular planes has been modelled by Parker (1997). This study mainly considers ground bounce between power and ground plane in the time domain although results may be applied in the frequency domain also. Hybrid model between conventional circuit and three-dimensional

electromagnetic (3-D EM) simulator has been also presented for characterisation of ground bounce or delta I noise (Yook *et al.* 1997a, Yook *et al.* 1997b). Properly placed decoupling capacitors are shown to suppress ground bounce. Van den Berghe *et al.* (1998) have shown capacitor fences or inductively separated power planes to be effective in case that switching noise is caused by power plane resonances. These methods seem to be far from reality, because parasitics of the capacitors and inductors are not considered in modelling. From the shielding point of view general idea of ground vias surrounding signal vias between different layers for controlling return currents and thus coupling have been proposed (Montrose 1996). More specific coaxial ground via structure is suggested to improve isolation between signal vias in multilayer boards (Pillai 1997). In this study possibility of resonances is mentioned, but no specific comments are made on the effect of these on isolation and match. Somewhat similar ideas are presented for ground access opening around signal via to improve matching (Daigle *et al.* 1993, Watson & Gupta 1996). Simulations without measurements are used in these studies. Reduction of coupling due to via fences between coplanar microstrips and striplines have been reported by Das (1996) and Ponchak *et al.* (1998), respectively. Similar ideas have been introduced for isolation between microstrips in form of a strip grounded by a via fence to the ground plane (Coetzee & Joubert 1996).

1.2. Purpose of the study

The complexity of modern telecommunications and computer systems offer a challenge for PCB designers and manufacturers, especially when operating frequencies are near 1 GHz or higher. One reason for this is crosstalk. The goal of this study is to find PCB design methods, which could help to avoid problems caused by crosstalk between vias on multilayer PCB's. The focus is firstly on a resonant coupling between vias and secondly on coupling between vertically aligned blind vias.

From a PCB designers point of view it is important to be able to estimate possible isolation problems already in a design phase. For this purpose two kinds of models are studied. These are described as follows:

1. Simple and fast methods to approximate: a) resonant frequencies and Q-values of a cavity inside a PCB and b) coupling between blind vias.
2. 3-D EM model, which can give estimation on coupling values between vias due to PCB resonances.

When a possible coupling problem is noticed we need also a way to solve it. For this purpose various means to reduce crosstalk are studied. This is carried out by using numerous measurements. As an application simulation models are used to give ideas for improvement of isolation. Measurements are used also to check the validity of the approximations done in modelling.

1.3. Contribution

This study considers some coupling mechanisms between two vias on multilayer PCB's. Methods to simply model and reduce coupling are presented. The focus of this study is on resonant coupling due to the dynamic wave nature of the fields inside a multilayer board. Here consideration is mainly given to the boards that have cavities formed by groundplanes connected with via grids. This selection is made, because previous studies concentrate on power plane resonances and thus on open-edges. Potential pitfalls using earlier presented methods to reduce via coupling are considered when board resonances are present. Coaxial via structure presented by Pillai (1997) is taken as a starting point in reducing via coupling. Via fences and metalled holes are applied to the division of a resonator to the smaller sections. Also coupling due to two opposite blind vias on a multilayer board is studied.

The measurements carried out show that the coaxial via structure described by Pillai (1997) may indeed reduce coupling and signal path loss. However, it does not necessarily increase isolation at some particular frequency. This may happen, because coaxial via tends to shift resonances to higher frequencies. Isolation at some frequency may even decrease in the worst case. Similarly it is shown that increasing separation between vias as suggested by Gu *et al.* (1994) may not help to reduce coupling.

Coaxial via is studied numerically by using a quasi-static approximation and the finite difference method (Booton 1992, Dworsky 1979). This study shows that the use of just two ground pins at a distance determined by a coaxial line approximation increases the characteristic impedance and does not approximate the coaxial mode well. The effect of this is decreased matching and increased leakage as indicated by measurements shown in this thesis and also by simulations given in an earlier study by Pillai (1997). The numerical method exploited is simple to implement and might be used to analyse fitness of different ground via structures as coaxial line approximations.

Analytical methods are shown for approximation of resonant frequencies, fields and Q-values of the cavity. As an application selection of division ratio of a cavity to get smaller sections with different resonant frequencies is done. Analytically calculated results are shown to match well with measured results from the EMC point of view. Two-dimensional numerical model for analysing resonant frequencies of a cavity with approximately electric or mixed boundaries is presented. Numerical approximation of Q-values of a cavity is also shown. Aplac finite-difference time domain (FDTD) simulator is used to approximate coupling between vias. Here it is noted that small thickness of a PCB layer at multilayer board compared to the transverse dimensions may lead simulations to be too time consuming to aid in PCB design process.

Cavities inside PCB's are studied on both eight and two-layer boards. Differently terminated (open, short and 50 ohms) vias are used as coupling probes. For measurements cavity is formed between centre layers of an eight-layer board. From EMC point of view this may be characterised quite well with two-layer cavity of equivalent size. This is important because making corrections like adding vias at testing phase is not a trivial task on a multilayer board. It should be noted that situation is more complicated with cavities on multiple layers. Termination of a via is shown to have a great effect on coupling as expected. Measurements and modelling show that Q-values of the studied resonators are below 100. Loss tangent of used glass/ epoxy (FR4) substrate and small cavity height with

conductor losses are main limitations to the Q-values. For a suggestion to reduce coupling thicker substrate is used to get exaggerated values of coupling and thus increased dynamic range of measurements. Several methods to reduce resonant coupling are described based on the analytical calculations, simulations, measurements and ideas from closely related studies. These include selection of coupling pin locations, coaxial via structures, increasing resonant frequencies with additional ground vias, splitting the cavities and reducing permittivity values.

Two analytical models for approximating coupling between vertically aligned blind vias are presented. First one is based on an approximation of a gap in a coaxial line. Usage of this may be reasoned when coaxial ground via structure is used. Second model consists of a simple series capacitance. This is considered to be formed between ends of blind vias and does not take fringing fields into account. Coupling values approximated with these models compare reasonably well with measured results up to slightly above 3 GHz.

1.4. Contents of the thesis

Chapter 2 of this thesis gives an overview of the resonant cavities and via coupling inside a PCB. This includes a description of a multilayer printed circuit board and different via types and how they form a cavity. An electromagnetic interference (EMI) view to the coupling between vias is also given. Chapter 3 describes both the two and eight-layer board structures that were constructed for measurement purposes. Chapter 4 focuses on the analytical and numerical models used to study different coupling structures. Analytical models include calculation of resonant frequencies, approximation of Q-values and coupling between vertically aligned open-ended blind vias. Two-dimensional numerical models are used to calculate resonant frequencies for analytically difficult structures. A method to evaluate Q-values numerically is also shown. 3-D modelling in the time domain is used to determine coupling between vias with different terminations. Coaxial via structure is studied by a two-dimensional (2-D) quasi-static model. Chapter 5 describes the measurement methods used and details also the S-parameter results. Chapter 6 gives a discussion of measurement and modelling accuracy, comparisons between measurements and models and highlights techniques to increase isolation in multilayer PCB’s. Chapter 7 presents the conclusion on the main aspects of this thesis.

2. Resonant cavities and via coupling inside multilayer PCB's

2.1. Introduction to the multilayer PCB's

2.1.1. Description of multilayer PCB's

By multilayer PCB we mean a printed circuit board which is constructed of two or more layers sandwiched together. These are separated by dielectric substrate material. Layer heights and even dielectric materials between different layers can vary. Routing or other kind of copper structures can be implemented at all layers. Surface mount components can be installed on both the top and bottom, which are the outermost layers of the board. In case that through hole components are used mounting holes are also needed. These form via like structures inside the board. Naturally integrated components like coils or capacitors can be placed also on the inside layers of the board. In this study layer indicator 1 refers to the top and n to the bottom of an n-layer board. Fig. 1 shows a simplified view of a multilayer board with shielding mechanics.

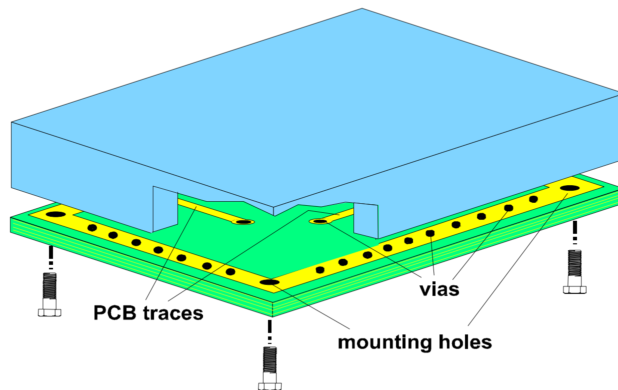

Fig. 1. Simplified example of a multilayer board with shielding mechanics.

Some advantages of multilayer PCB's compared to the simpler single layer structures are that they give additional routing space and offer the possibility for solid ground and power planes, which are important from an EMC point of view (Montrose 1996, Kiang 1990). Additionally various coupler and antenna designs are possible when multiple layers are available (Chen *et al.* 1996, Fujimoto & James 1994). Ample routing space also tends to decrease size of the device and a sandwiched structure gives mechanical rigidity to the board.

2.1.2. Description of the via types

Vias are required to interconnect traces on different PCB layers. This is to allow complex interconnections of components to take place without shorting traces together. Vias are also utilised to establish connections to the ground or power planes. Desired properties of the specific via depend on the purpose for which it is used. For example in high-speed signal routing, impedance matched transitions between layers are needed. In case that connection is to ground plane low impedance is probably desired. Also available space and board geometry in general determine how vias can be used.

Nowadays multiple types of vias namely through, blind and buried do exist. These are presented in Fig. 2. It can be seen that difference between via types comes from the way they penetrate through the PCB. Through via goes all the way from top to bottom layer. Blind via starts either from the top or bottom and ends inside the PCB. Buried via is located entirely inside the PCB. An advantage of blind and buried vias is that they enable more versatile high-speed transitions than through vias. In addition to this they also save component placement space, since they do not occupy both sides of the board like a through via does. Typically layers at which buried and blind vias can be used are somewhat restricted and depend on the board manufacturer. An example may be where a via transition from layer 1 (top) to layer 3 is desired, but the via has to be extended to the layer 4. This means that we have an unwanted extension in our via, which may cause mismatching and also lead to reduced isolation.

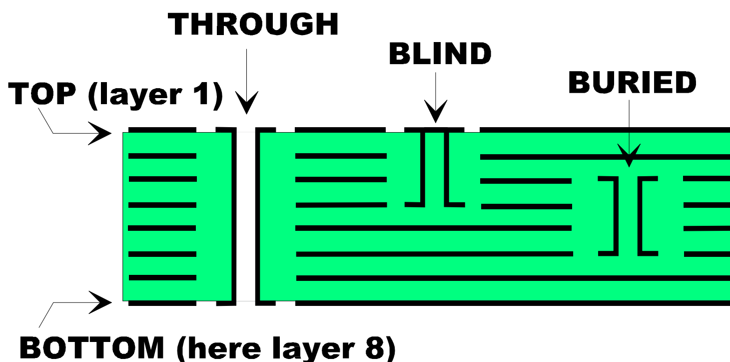

Fig. 2. Different types of vias on a multilayer board.

In general vias are challenging from the matching and isolation point of view particularly as frequencies rise to the gigahertz range. Possible problems may be seen as ringing in fast signal transmission, poor filter or amplifier performances due to inductive grounding and crosscoupling.

2.1.3. EMI view to the multilayer boards and vias

One unfortunate fact with multilayer PCB's is that unintentional cavity resonators may form due to two or more metalled layers. These are typically either ground or power planes. A simplified example of this kind of structure is shown in Fig. 3. Resonator is formed between two ground layers which are connected together only at the edges with through ground vias. Resonance effects between other ground planes are more or less reduced because they are connected together with blind ground vias in addition to the through vias at edges. Coupling to the cavity depends on the termination of the signal vias. In this study we consider shorted (magnetic), open ended (electric) and terminated via (combination of electric and magnetic) configurations.

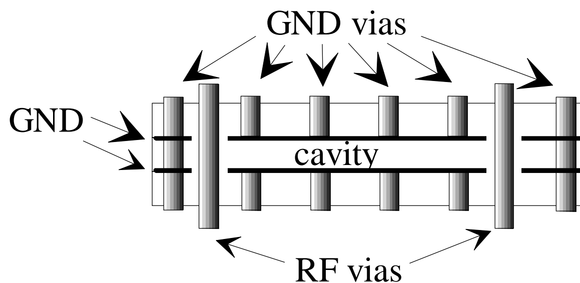

Fig. 3. Cross-sectional view of an unintentional cavity resonator formed inside a multilayer PCB. Only layers adjacent to the cavity are shown. Signal vias are shown to carry radio frequency (RF) signals.

We may be able to eliminate resonators inside the PCB itself, however they may still form between a metalled PCB plane and other reflective objects such as screening (Hoffman 1987, Robinson 1971). This kind of structure is shown in Fig. 1. If screws are separated with electrically long distances compared to the wavelength a cavity backed slot antenna may form which can be disastrous to the EMC emission performance (Li *et al.* 1997). Typically components and routings exist on the outer layers and this makes analytical evaluation of the previously described resonator difficult, if not impossible. This kind of cavity resonator tends to be loaded partially by substrate material which causes losses and shifts resonant frequencies compared to ideal rectangular cavity in homogenous media (Hoffman 1987).

Using blind or buried vias in the quest for a compact PCB may lead to the situation, where two via ends inside PCB are facing each other with nothing but dielectric material in between them. Now if coaxial vias recommended by Pillai (1997) are used we do have a structure, which looks approximately like a coaxial line with a gap, which is a well known filtering structure already in use several decades ago (Dawirs 1969). So, we have a coupling structure with basically a high pass response. Cross-section of this kind of via configuration is shown in Fig. 4.

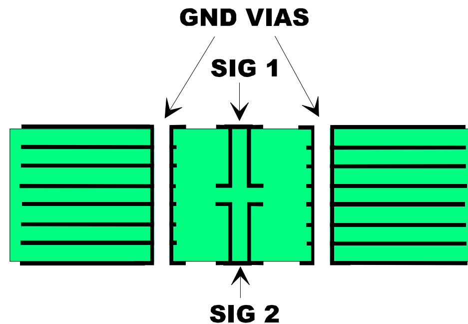

Fig. 4. Cross-section of a multilayer board with opposite blind vias.

2.2. Description of the PCB cavity as a short circuited waveguide

2.2.1. Description of ground via configurations and related boundary conditions

Here a basic idea of how a PCB cavity may be described for the modelling purposes is presented. To solve Maxwell's equations we define a calculation domain, in which surfaces satisfy either Dirichlet or Neumann boundary condition for the electric field. Hereafter these surfaces are called electric and magnetic walls, respectively. This approach leads to simpler solution of the resonant frequencies than an open problem and the solution may still be considered accurate enough from the EMC point of view (Howell 1973, Napoli & Hughes 1971, Van den Berghe *et al.* 1998). Note that at the frequency range of interest, which is up to 6 GHz, fields inside the cavity do not have significant variation in the direction perpendicular to the PCB plane.

In a PCB plane boundary surfaces are naturally formed by copper ground or power planes and perpendicularly by vias and dielectric surfaces. Walls of the cavity along PCB plane can be taken to be electric, because they are formed of copper planes. Inaccuracies in this model are basically caused by the following reasons: 1) copper is not an ideal conductor, 2) copper surface is not perfectly smooth and 3) there may be gaps in the copper plane. In the case that cavity walls perpendicular to the PCB plane are occupied by vias spaced with a small separation compared to the wavelength, then the boundary may be defined as electric. Small is considered to be about 0.1 λ or less. The reasoning for this is based on the measured results shown later in section 5.3.1 and especially in Fig.

36 p 62. Here an approximation is due to 1) discontinuities of the surface and 2) finite conductivity of the vias. Better approximation is possible if surfaces are uniformly metalled. It is also possible, that there are no vias at all and this leads to the magnetic boundary condition. This approximation has been used in measurement of permittivity of the substrate materials and modelling of power plane resonances (Napoli & Hughes 1971, Van den Berghe *et al.* 1998). Inaccuracy is caused by the fact, that fields are not completely enclosed inside the PCB. In case, that sidewalls are partially filled with vias and partially left open a combination of above boundary conditions may be used. This is referred here as a mixed boundary. Approximate boundary conditions for different via configurations are shown in Fig. 5.

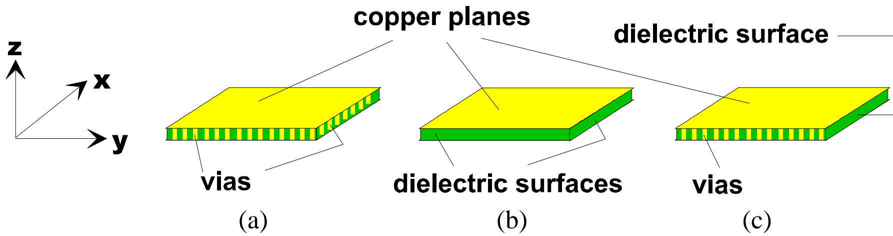

Fig. 5. Approximate boundary conditions for different ground via configurations. In all pictures the top and bottom walls are formed of uniform copper planes, which can be modelled as electric walls. Sidewalls are formed by via fences in (a), open dielectric surfaces in (b), and a combination of via fences and dielectric surfaces in (c). These form approximately electric, magnetic and mixed boundaries, respectively. Note that only two metalled layers forming a cavity and ground vias connecting them are shown.

We may also have ground vias inside the outer walls of the cavity. These can be taken into consideration by imposing the electric field boundary condition. It is also possible, that there are horizontal discontinuities inside the cavity, but these are not considered in this study. Conclusion and mathematical representation of boundary conditions is shown in Fig. 6. It is to be noted that these models consider unloaded cavities and do not include the effect of coupling pins.

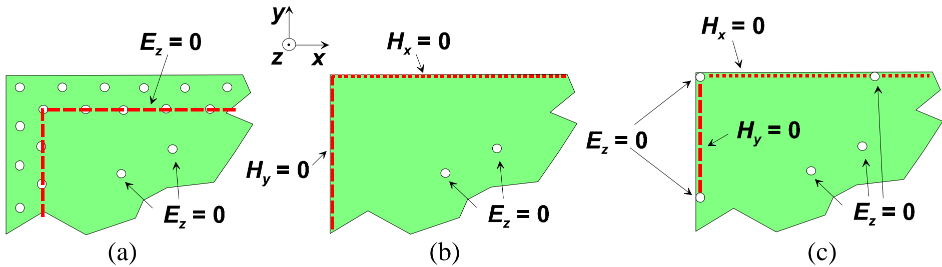

Fig. 6. Top view of a corner of a cavity describing boundary conditions for different ground via configurations. In (a) an electric field boundary at the sidewalls of the cavity is imposed as illustrated by the dashed line. In (b) a magnetic boundary is imposed as illustrated by dashed and dotted lines. In (c) a combination of these conditions is imposed i.e. electric field boundary at via locations and magnetic boundary at the other surfaces. It is assumed, that in (a) via spacing at the sidewalls is small compared to the wavelength and in (b) there are no vias at the sidewalls. Note that at the interior of the cavity ground vias are treated similarly in all cases i.e. electric boundary is imposed.

2.2.2. Waveguide types for different boundary conditions

The structures described in section 2.2.1 can be considered to be different kinds of waveguides. They are then terminated to electric or magnetic walls or combinations of these thus forming a cavity resonator. Now depending on the choice of direction of propagation and coordinate system we may end at seemingly different solutions. However, these solutions give similar resonant frequencies and overall performance of the cavity. For example if we look at structure in Fig. 5(b) and remember the approximate boundary conditions given in the previous section we may have the following descriptions of the guide.

1. Direction of propagation is along x- or y-axis. This makes our structure look like a parallel plate waveguide terminated at a magnetic wall.
2. Direction of propagation is along the z-axis. This gives an impression of a dielectric slab (with magnetic walls), which is terminated at an electric wall.

Similar analyses can be carried out for structures in Fig. 5(a) and (c). It is appropriate to ask if there is some preferred selection of direction of propagation that would simplify mathematical model for the given waveguide? By looking at structures in Fig. 5 it may be difficult to get clear answer to this question. However, if it is taken into account, that ground vias may be located also inside the outer walls of the cavity it seems to be appropriate to choose direction of propagation to be perpendicular to the PCB plane. This should be done, because waveguide with continuous cross-section along direction of propagation is formed. Termination of the guide is at electric walls. Advantages of this selection may still be a bit unclear from a 3-D modelling point of view, but if the model can be reduced to 2-D we note that the solution is far simpler. This is described in section 2.2.3.

2.2.3. Simplification to the two-dimensional waveguide problem

PCB cavities tend to have a structure where one physical dimension is much smaller than the other two. This is due to the fact that layer height to trace length ratio is high. So, at the frequency range of interest, which is up to 6 GHz, fields inside cavity do not have significant variation in direction perpendicular to the PCB plane. This leads to the simplification where fields and resonant frequencies for different modes can be solved using a 2-D instead of a 3-D model (Waldron 1967). To use a 2-D model for a waveguide a constant cross-section along direction of propagation is needed. Keeping this in mind it is evident how selecting this direction to be perpendicular to the PCB plane is advantageous in case that we have only vias in our cavity. Naturally if cavity is formed so, that there are striplines or other horizontal structures inside the cavity solution is not that simple. Here interest is directed to the coupling between vias due to resonant effects and these structures are selected not to include the transmission lines mentioned above.

3. Descriptions of the structures to be studied

3.1. Structures on multilayer boards

3.1.1. Isolated cavities

A resonator formed in a cavity between layers 4 and 5 of an 8-layer board is used in this study. For the sake of simplicity the board has only ground layers and a signal route to be studied. Blind mate connectors (BMA) on layers 1 and 8 are used as a measurement interface. Arrangement where input and output connectors are at opposite sides of the board is favoured to avoid coupling between via ends especially in case that they are left open-ended (Bird 1996). Coplanar microstrip line is used as a route from the BMA connector to the signal via, which goes through the board. Length of this line is 3 mm. Connector and signal via locations are shown in Fig. 7. Note that all dimensions in the figures are in millimetres unless otherwise stated. Via diameter is 0.5 mm. The termination is located on the other side of the board. Approximate short, open or load can be used as a termination. Load is manufactured by connecting two surface mount 100 ohms resistors of 0603 (indicates dimensions of 60 mils × 30 mils, which is about 1.52 mm × 0.76 mm) footprint in parallel. The open circuit is achieved simply by leaving probe end open. The short circuit is made by soldering piece of a copper tape to the ground plane with a 360° connection.

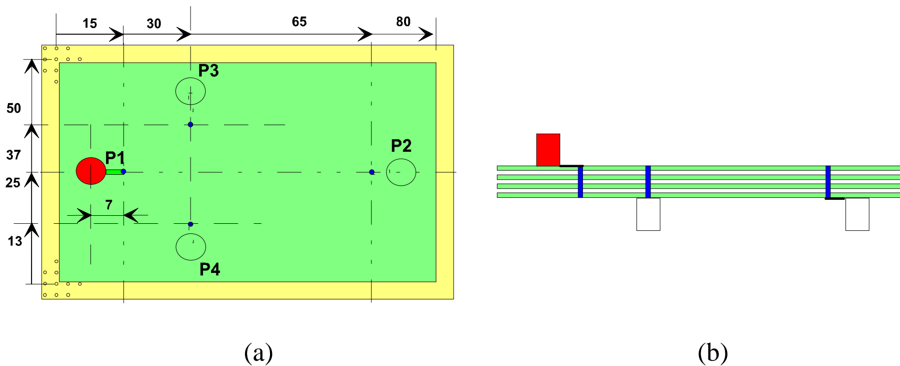

(a) (b)

Fig. 7. Connector and signal via locations for an 8-layer resonator test board. Filled and outline circles indicate connectors on the top and bottom sides of the PCB, respectively. Top and cross-sectional views are shown in (a) and (b), respectively. P1, P2, P3 and P4 are used to indicate measurement interfaces i.e. the connector locations.

Sides of the cavity are closed by through vias arranged in a 2.5 mm grid. Layers 1-4 and 5-8 are additionally connected together by 5 mm blind via grid. This configuration is shown in Fig. 8. Diameter of the ground vias is 0.75 mm. Substrate thickness of the resonant section is nominally 340 µm. This is so called bounding or prepreg layer and its electrical and mechanical properties are not necessarily well defined due to difficulties in manufacturing process (Daigle *et al.* 1993). Nominal copper thickness is 35 µm. Other build-up parameters and an example of measured board dimensions may be seen in Table 10 p 58 and Fig. 33 p 59. FR4 is selected for a substrate material because it is in common use in PCB manufacture. Nominal relative permittivity is 4.4. However, this value depends on the frequency and resin content.

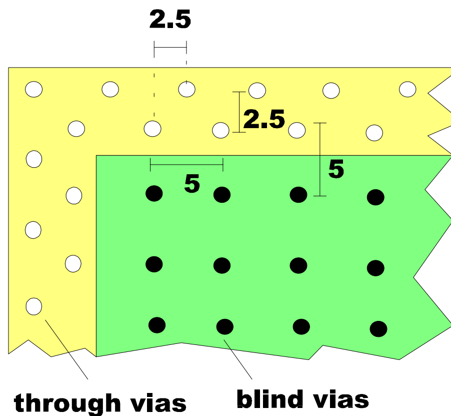

Fig. 8. Top view of a corner of a PCB where location of through and blind ground vias is shown.

3.1.2. Stacked cavities

It is possible that more than one cavity is formed in a multilayer board. One way how this could happen is that cavities are formed on top of each other. This kind of structure is named here as a stacked cavity. For testing purposes a pair of two-layer boards are assembled on top of each other and the mating ground layers are tightly connected together. Substrate thickness for these boards is 0.34 mm corresponding to the height of the centre layer for isolated cavity shown in Fig. 7. Configurations of the ground layers, vias and 3.5 mm coaxial PCB connectors (SMA) are the same as described later for the two-layer boards in section 3.2 p 28-29. Signal via locations are the same as described in Fig. 7. Conductive epoxy is used to connect centre ground layers. Additionally ground via holes at the edges of the board are soldered together. The same process is performed for signal vias. General construction of this stacked cavity is shown in Fig. 9.

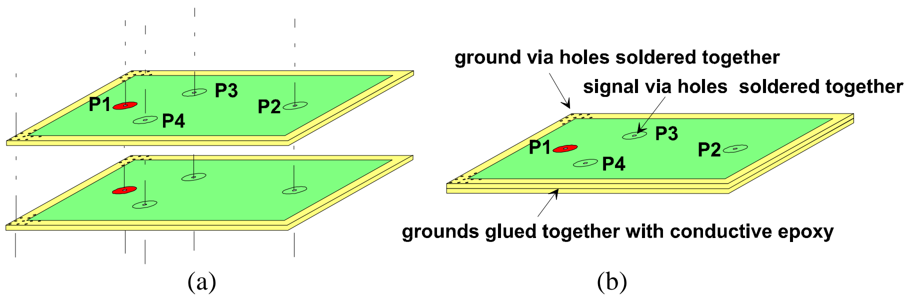

Fig. 9. Construction of a stacked cavity from a pair of two-layer boards. Alignment of the boards is shown in (a) and connection methods in (b).

3.1.3. Transitions between shielded sections

Shielding mechanics may be used to isolate two functional blocks on the same PCB from each other. If needed a signal route between these two blocks can be made through the wall of the shield or below the wall on an internal PCB layer. To assess differences between these methods an 8-layer board build-up similar to that used in the resonator case is used. Configurations of used structures are shown in Fig. 10 and Fig. 11. All layers under the shielding walls and on the sides of the board are connected together with through vias in a 2.5 mm grid pattern except at places where there are signal traces. Additionally there are blind vias in a 5 mm grid pattern to connect layers 1-4 and 5-8 in the centre section, where termination resistors are located. This is a similar configuration to the resonator board and is shown in Fig. 8. In other sections the same grid pattern is applied, but with through ground vias. In case of under wall routing transition to layer 3 is made with a blind via on both sides of the wall. Via diameter is 0.5 mm. Distance from the via centre to the wall is 1.5 mm. Length of the coplanar PCB trace from the connector to the via is 6.5 mm. Vias are then connected together with a coplanar stripline on layer 3. Length of this line is 7.5 mm. Blind via extends to layer 4 where it is left open-ended and

thus may excite the cavity formed between layers 4 and 5. The line is terminated after transition to the other side of the wall to two surface mount 100 ohm resistors of size 0603 in parallel. In case of through wall routing a 5 mm × 5 mm rectangular opening is made in the shielding wall. A similar termination is used as in case of under wall routing. Length of the coplanar line from connector to the termination is 14 mm. The height of the open volume inside shielding mechanics is 5 mm and the thickness of the walls is 3.5 mm. Chassis material is aluminium. Shielding mechanics has two circular holes for connectors. Diameter of the holes is 11 mm. Chassis is connected with pressure to the PCB ground. It should be noted that connectors, signal vias and traces cause the only openings in copper grounds.

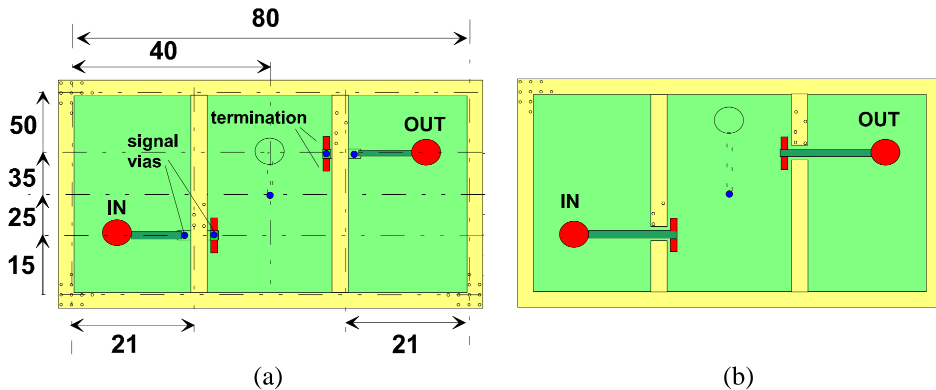

Fig. 10. Top view of the PCB's with (a) routing under shielding wall and (b) through shielding wall. In both cases lines are terminated with two 100-ohm resistors. One additional via with an accompanying PCB trace and a connector is located in the centre of the structure for monitoring of resonances. IN and OUT indicate input and output connector locations, respectively.

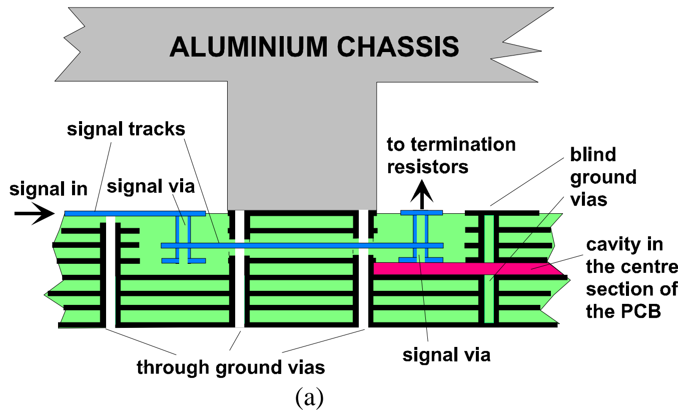

(a)

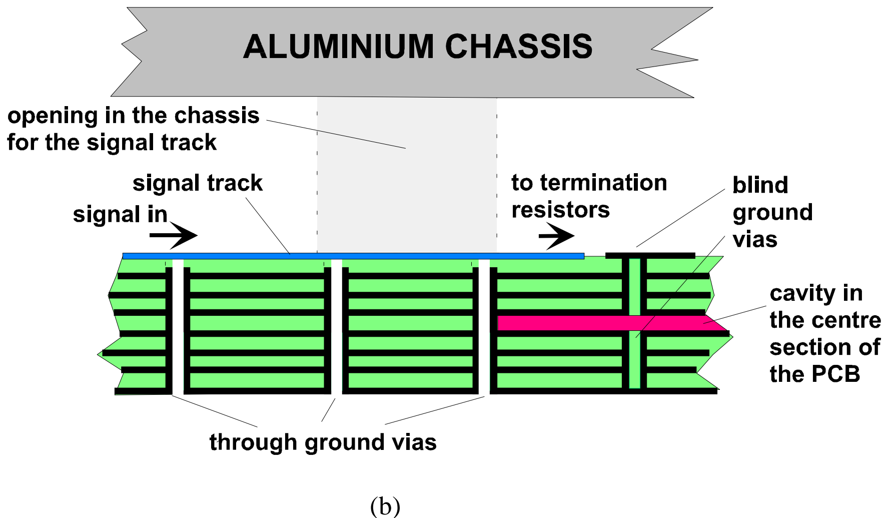

(b)

Fig. 11. Cross-sectional view of the routing methods between two sections. In (a) routing is done inside the PCB and in (b) through a hole in the chassis. Note that in (b) there are no signal vias, which could feed the cavity in the centre section of the PCB.

3.1.4. Coupling between opposite open ended blind vias

Coupling between opposite via ends is tested on an 8-layer board by using blind vias from layer 1 to 4 and 5 to 8. Vias are vertically (i.e. perpendicularly to the PCB plane) aligned. Build-up is similar as in multilayer resonator boards. Via diameter, sleeve and ground access opening at buried layers are 0.5 mm, 1.2 mm and 4.2 mm, respectively. At the top and bottom layers the same parameters are 0.5 mm, 1.1 mm and 3.6 mm. Two arrangements of ground vias are used in the immediate vicinity of a signal via. The first one has six coaxial ground vias at the edge of the ground access opening and second one only four vias located at a radius of 3.5 mm from signal via centre. More ground vias are added around these structures to dampen possible cavity resonances. Top and cross-sectional views are shown in Fig. 12 and Fig. 13, respectively. Interface to the board is accomplished with BMA connectors. Coplanar stripline is used as a signal path from the connector to the via at both sides of the board. Length of this line is 4 mm. To be able to de-embed excess losses from measurements both structures are also built with through signal vias.

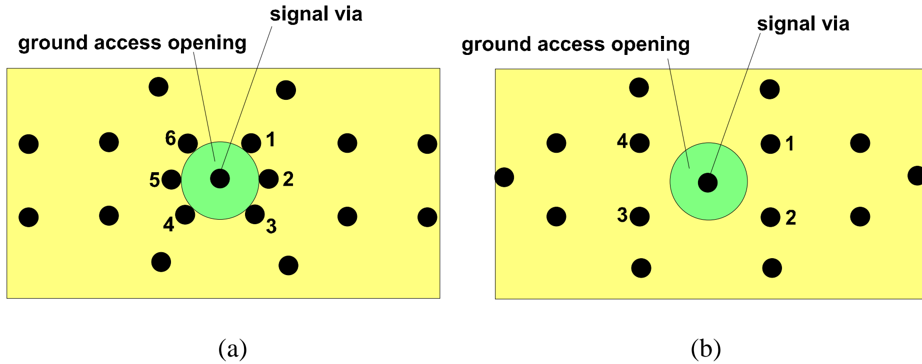

(a) (b)

Fig. 12. Construction of the inner layers of blind via test structures seen from the top. Structures with six coaxial ground vias and four ground vias are shown in (a) and (b), respectively. These vias are numbered in the pictures. The signal via with the ground access opening is shown in the centre of the both pictures. Other black dots indicate locations of the additional ground vias.

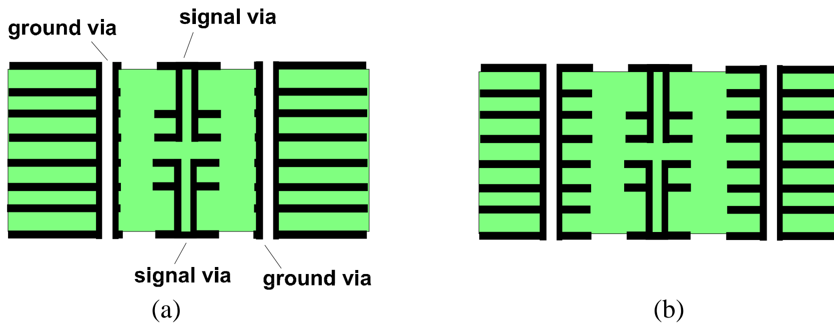

(a) (b)

Fig. 13. Cross-sectional view of the blind via test structures. Structures with six coaxial vias and four vias are shown in (a) and (b), respectively. Only the ground vias immediately surrounding the signal vias are shown.

3.2. Simplified cavities on two-layer boards

3.2.1. Isolated cavities

Two-layer boards are used as simplified models of resonators, which are formed between two layers on multilayer boards. This gives the following advantages: 1) ground vias can be added afterwards more easily and reliably and 2) the price is much lower. To equate between two and multilayer boards it is necessary to use the same PCB parameters in both cases. Here FR4 with nominal thickness of 0.34 mm is used as a substrate material. This is nominally the same as dielectric between layers 4 and 5 on an eight-layer board. Both sides of the two-layer board are metalled and no solder resist is used. Similar

configurations of ground vias at the sidewalls of the cavity as described in Fig. 8 p 24 are used. Naturally blind vias are not used. Ground via diameter is either 0.75 mm or 0.5 mm. At boards with only two signal vias this is 0.5 mm and in all other cases 0.75 mm. Effect of this variation can be considered to be negligible. Different locations of signal vias are tested. First configuration is used to compare eight- and two-layer boards. Via locations for this case are shown in Fig. 7 p 24. Other placements are indicated along measured results. A straight PCB SMA connector is used as an input connector. All ground leads are cut out and the connector jacket is soldered with 360° contact to the PCB ground plane. The centre conductor is cut to match the thickness of the board. Signal pin goes through the cavity and different terminations on the other side of the board may be used. These are similar as described in section 3.1.1 p 23. Signal via diameter with a plated through via hole is 1.6 mm. Cross-sectional view of a SMA connector and different terminations are shown in Fig. 14.

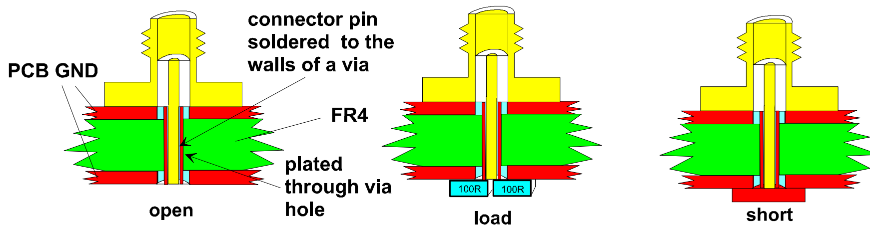

Fig. 14. Cross-sectional view of a SMA connector interface with different terminations. Note that both sides of the board are ground layers indicated by PCB GND.

It is also of interest to study the cavity resonator effect on loss of a through via. This may be done by assembling two SMA connectors on opposite sides of the board and connecting their centre conductors together. For this purpose ground pins of the SMA connectors are cut off and centre leads are shortened so that they fit inside the board. Plated through via hole of diameter 1.6 mm is used to assist soldering of the connector pins together. A cross-sectional view showing the principle how connectors are assembled is given in Fig. 15. This structure may be also used to compare matching effects between terminations to two 100 ohm resistors and SMA 50 ohm load.

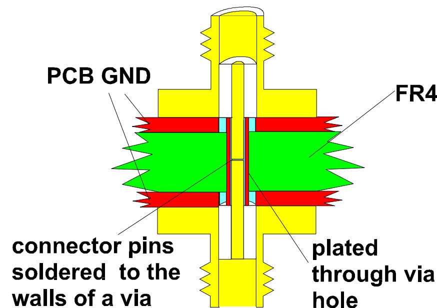

Fig. 15. Cross-sectional view of two SMA-connectors used to test resonator effects on signal path loss.

To enhance coupling, and thus get more dynamic range for the measurements of different methods to increase isolation, we nominally use 1.6 mm thick FR4 substrate. However, in practice thickness is actually 1.5 mm. This structure is also more rigid and easier to handle than thinner versions. Vias are arranged in similar grids as described for other two-layer test boards. Different ground via configurations are studied to increase isolation. A previous study of a coaxial via is used as a starting point (Pillai 1997). Hereafter 1.5 mm board and 0.34 mm board are used to refer to the boards with 1.5 mm and 0.34 mm substrate thickness, respectively.

3.2.2. Coupled cavities

To test coupling between multiple cavities four PCB sections of similar sizes separated with different ground via grids are used. Boundaries of this structure are similar as described in Fig. 8 p 24. Overall view of the structure and arrangement of the vias separating cavities are shown in Fig. 16. Separation S between vias for a single row has the following values: 20 mm, 10 mm, 5 mm and 2.5 mm. These are named resonator 1, 2, 3 and 4 respectively. In case of two rows 5 mm and 10 mm versions for S are built and names resonator 5 and 6 are used, respectively. The inner dimensions of the sections are measured from the centres of the closest vias. Both 1.5 mm and 0.34 mm substrate thicknesses are used. Similar SMA interface as with other two-layer boards is used.

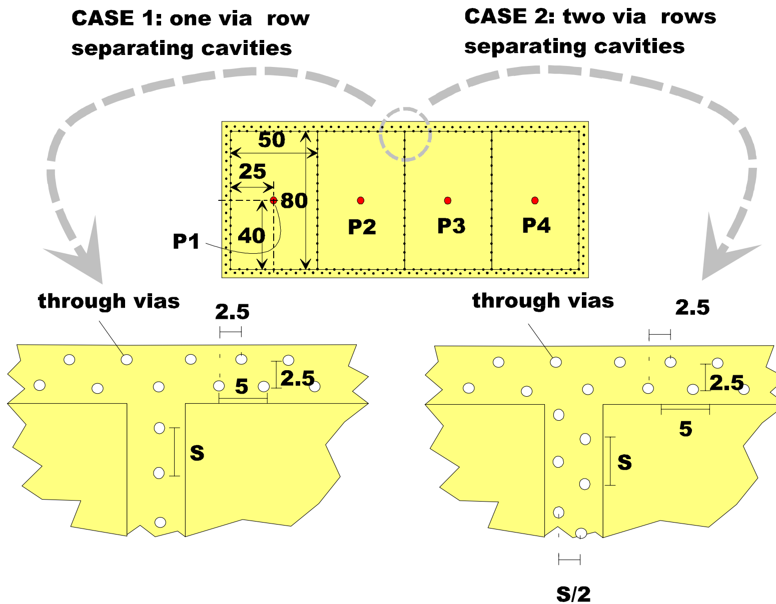

Fig. 16. Coupled resonators at 2-layer boards shown from the top. The whole structure is surrounded by a ground via grid. Separations between different sections are made with either one or two rows of vias.

4. Modelling

4.1. Purpose of modelling in this study

The purpose of modelling in this study is to gain insight into the resonant behaviour and via coupling on multilayer PCB's instead of a rigorous analysis. This approach is reasonable from an EMC point of view, where an ample safety margin to the possible isolation catastrophe is desired. Both analytical and numerical methods are used to reach this goal. Analytical models are used to approximate Q-values and resonant frequencies for a simple rectangular cavity structure. As a practical application splitting of a larger cavity into two smaller ones is discussed. Coupling between vertically aligned blind vias is also described analytically, although the model is then incorporated in Aplac circuit simulator to get S-parameter data. Used numerical means include two-dimensional model for calculation of resonant frequencies and fields, approximation of Q-values, simplified 3-D modelling of a PCB cavity with approximately electric walls in time domain and quasi static analysis of a coaxial via structure. Programming of the numerical schemes is done with Matlab, except the FDTD algorithm, which uses commercial simulator incorporated in Aplac version 7.00.

4.2. Analytical models

4.2.1. Approximation of resonant frequencies and fields

In a real PCB structure studied in this thesis copper planes form top and bottom walls of the cavity and sidewalls are formed by ground via fences. For analytical calculation of the resonant frequencies in unloaded case the cavity is assumed to be rectangular and bounded by electric walls. In this case resonant frequencies are given by

$$f_r = \frac{1}{2\sqrt{\varepsilon\mu}}\sqrt{\left(\frac{m}{L}\right)^2 + \left(\frac{n}{W}\right)^2 + \left(\frac{p}{H}\right)^2}, \qquad (1)$$

where m, n and p are positive integers describing mode and L, W and H are dimensions of the simplified cavity as shown in Fig. 17 (Liao 1987). It can be seen from Eq. (1) that when the permittivity decreases resonant frequency for a given mode increases. This means, that it might be wise to choose a lower relative permittivity for the substrate if resonances are suspected to be a problem. This approach can be considered to be effective if the lowest resonant frequency can be shifted well above the operating frequencies.

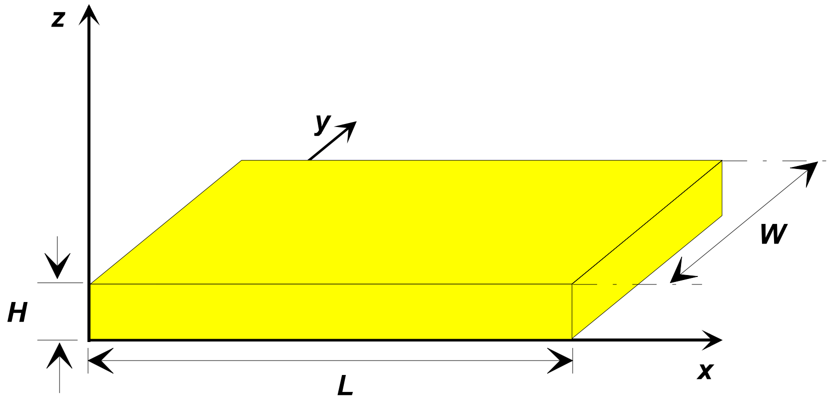

Fig. 17. Geometry of a simplified model of a cavity resonator on a PCB. Vias forming the sidewalls of the cavity are approximated with uniformly metalled surfaces. Only the section of the PCB forming a single cavity is shown.

Some resonant frequencies with different values of relative permittivity are calculated to Table 1, when height of the cavity is assumed to be small compared to the other dimensions. In this case p can be set to zero at the frequency range of interest, which is up to 6 GHz. Due to electric walls m and p can have integer values which are one or higher. Note that if no vias at the sidewalls of the cavity are used resonances may occur even at lower frequencies. This can be explained by using magnetic sidewalls, which allow also either m or n to be zero in addition to p. Used values of permittivity express typical variations for used FR4 materials.

Table 1. Resonant frequencies for different modes and values of relative permittivy, when L is 80 mm, W is 50 mm and H is considered to be small compared to L and W.

			Relative permittivity ε_r				
			4.2	4.3	4.4	4.5	4.6
m	*n*	*p*	Resonant frequency [GHz]				
1	1	0	1.73	1.70	1.69	1.67	1.65
1	2	0	3.07	3.03	2.99	2.96	2.93
1	3	0	4.48	4.43	4.38	4.33	4.28
1	4	0	5.92	5.85	5.79	5.72	5.66
2	1	0	2.34	2.31	2.29	2.26	2.24
2	2	0	3.45	3.41	3.37	3.33	3.30
2	3	0	4.75	4.70	4.64	4.59	4.54
2	4	0	6.13	6.06	5.99	5.92	5.86
3	1	0	3.11	3.07	3.04	3.00	2.97
3	2	0	4.01	3.96	3.92	3.87	3.83
3	3	0	5.18	5.11	5.06	5.00	4.95
3	4	0	6.46	6.39	6.31	6.24	6.18
4	1	0	3.94	3.89	3.85	3.81	3.76
4	2	0	4.68	4.63	4.58	4.52	4.48
4	3	0	5.71	5.65	5.58	5.52	5.46
4	4	0	6.90	6.82	6.74	6.67	6.59
5	1	0	4.80	4.74	4.69	4.64	4.59
5	2	0	5.43	5.36	5.30	5.24	5.19
5	3	0	6.34	6.26	6.19	6.12	6.06

From a nomenclature point of view we have only transverse magnetic TM_{mn0} modes. This is caused by the following reasons: 1) height H of the cavity in PCB is small compared to the other dimensions at frequency range of interest from 3 MHz to 6 GHz and 2) we have selected direction of propagation to be along z-axis (perpendicular to the PCB plane). This means that electric field has only z and magnetic field x- and y-directed components. For a rectangular cavity with electric walls in unloaded case these are given by

$$E_z = D \sin\left(\frac{m\pi x}{L}\right)\sin\left(\frac{n\pi y}{W}\right) , \tag{2}$$

$$H_x = \frac{\mathrm{j}\omega\varepsilon D}{k_c^2}\left(\frac{n\pi}{W}\right)\sin\left(\frac{m\pi x}{L}\right)\cos\left(\frac{n\pi y}{W}\right) , \tag{3}$$

$$H_y = -\frac{\mathrm{j}\omega\varepsilon D}{k_c^2}\left(\frac{m\pi}{L}\right)\cos\left(\frac{m\pi x}{L}\right)\sin\left(\frac{n\pi y}{W}\right) , \tag{4}$$

where D = -2jA, $k_c^2 = (m\pi/L)^2 + (n\pi/W)^2$, A is amplitude coefficient, m and n are integers (1,2, 3, ...) describing mode and W and L are as described in Fig. 17 (Ramo *et al.* 1984). This knowledge can be used while analysing effects of different vias used to feed the cavity. To increase isolation under varying load conditions coupling pin (or loop) should be at a location where both electric and magnetic fields are at minimum. Equations (2) - (4) show that this kind of place is located at the corners of the cavity. Knowledge of the fields can be also used in estimation of Q-values of the PCB resonator. Numerical methods are needed for calculation of the fields, when grounding vias are added inside sidewalls of the structure or the cavity can not be considered to be of simple shape.

If a cavity is divided with a fence of vias, which has small separations compared to wavelength, it may be considered that two smaller cavities are formed. In this case it is desirable to have different resonant frequencies for both cavities so that coupling between them would be as small as possible. Naturally it is even better if all resonances for both cavities are above the frequency range of interest. A cavity, for which the lowest resonant frequencies are shown in Table 1 is considered here as an example. When this cavity is divided into two uneven parts, with lengths of 50 mm and 30 mm PCB geometry like in Fig. 18(a) is formed. In this case resonant frequencies calculated from Eq. (1) p 31 for side A and B are different as shown in Fig. 18(b). Division ratio between lengths (or areas as well) is 30/50 ≈ 0.6. This is quite close to the so called golden number $(\sqrt{5} - 1)/2 \approx 0.618$. Golden number as a division ratio for lengths is tested also for other cavity dimensions and it seems to be a reasonable try in many cases at the frequency range of interest. Naturally as the size of the resonator increases there will be more resonant frequencies at a given range. This may lead to the situation where separation of resonant frequencies is not a fertile process especially when finite Q-values are taken into consideration. However, this kind of situation should not been allowed to arise in the first place.

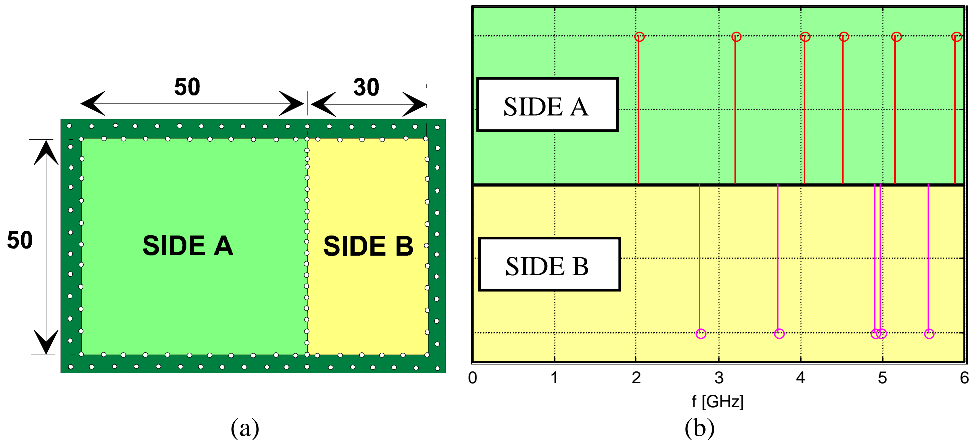

Fig. 18. (a) A PCB cavity, which is divided to two parts with a row of vias and (b) accompanying resonant frequencies for both sides.

4.2.2. Approximation of Q-values

In this section an approximation of the Q-value for a PCB cavity is presented. The main aim of this is to get an idea of the factors limiting Q-values on a PCB. It is noted in section 4.2.1 that only z-directed electric field component exist for PCB resonators at the frequency range of interest. This simplifies calculation of the enclosed energy in the cavity to the form

$$U = 2W_e = \frac{\varepsilon}{2}\int_{\mathrm{V}} |E_z|^2 dv \ , \tag{5}$$

where W_e is time averaged energy stored in the electric field, ε is permittivity of the media filling the cavity and E_z is electric field perpendicular to the PCB plane (Ramo *et al.* 1984). Energy lost in the walls can be calculated by using perturbation theory to give

$$P_c = \frac{R_s}{2}\int_{\mathrm{walls}} |H_t|^2 ds \ , \tag{6}$$

where R_s is surface resistivity described by Eq. (7) and H_t is tangential magnetic field at the surface of the walls.

$$R_s = \sqrt{\omega\mu_0/2\sigma} \ , \tag{7}$$

where ω is angular frequency, μ_0 is permeability of the vacuum and σ is conductivity of the wall material. (Pozar 1998, Ramo *et al.* 1984.) Walls are considered to be formed of vias and bottom and top metallic planes. For approximate calculations in this study only losses caused by copper planes are included. The Q-value resulting from wall losses can be calculated as

$$Q_c = \frac{\omega_{\mathrm{r}} U}{P_c} \ , \tag{8}$$

where ω_r is angular resonant frequency and U and P_c are described by equations (5) and (6), respectively (Ramo *et al.* 1984). A PCB resonator is typically filled with a homogenous dielectric. Hence the dielectric Q-value can be written as

$$Q_d = \frac{1}{\tan\delta} \ , \tag{9}$$

where $\tan\delta$ is a scalar describing the losses inside the dielectric material (Pozar 1998). Radiation losses are assumed to be insignificant and their effect on the total Q-value is not taken into consideration here. This means, that the total unloaded Q can be written as

$$Q_u = \left(\frac{1}{Q_c} + \frac{1}{Q_d}\right)^{-1} , \tag{10}$$

where Q_c and Q_d are described by equations (8) and (9), respectively.

It can be seen that limiting factors for unloaded Q-values are dielectric and wall losses, when radiation loss is not taken into account. In this study FR4 is used as a substrate material. It has quite high loss tangent of about 0.01…0.025 compared to the typical microwave boards. So, maximum for Q_d is about 100 and more typical value would be around 60. Wall losses depend not only on the resonant mode TM_{mn0}, associated frequency, surface area and conductivity of the wall, but also on the roughness of the wall surface. The last one of these may be considered by replacing resistivity R_s with effective resistivity $R_{s,eff}$. Increases of 5…100% in surface conductor resistivity have been reported (Wadell 1991). Amount of increase depends on the ratio of the roughness to the skin depth and is thus frequency dependent. Root mean square surface roughness (RGH_{rms}) for 35 μm thick (1 oz) copper used at test boards has been reported to be around 2.4 μm (Wadell 1991). This would lead to the increase of surface resistance in the order of 20 … 80 % at the frequency range of lowest mode shown in Table 1. Estimations for unloaded Q-values for some modes are shown in Table 2, when Q_d is assumed to be 100. Size of the cavity is 80 mm × 50 mm × 0.34 mm and ε_r is 4.4. Conductivity of the walls is $5.8 \cdot 10^7$ S/m and it is assumed to be independent of frequency. Combination of numerical and analytical methods is used to calculate Q-values. First fields are solved analytically and then Q-values are found numerically as described later in section 4.3.2 p 45-46. Numerical results are compared to the analytical results for ideal rectangular cavity and calculated Q-values agree up to three decimal places. This can be considered accurate enough for the purposes of this study. It can be seen from Table 2 that conductive losses have strong effect on unloaded Q-values. The reason for this is the small height of the cavity.

Table 2. Estimated unloaded Q-values for some modes. Q_d is assumed to be 100 and effect of the copper roughness RGH_{rms} is included. Size of the cavity is 80 mm × 50 mm × 0.34 mm and ε_r is 4.4.

	TM_{110}	TM_{210}	TM_{310}	TM_{410}
f_r [GHz]	1.69	2.29	3.04	3.85
δ_s [μm]	1.61	1.38	1.20	1.07
RGH_{rms}/δ_s	1.49	1.74	2	2.24
Increase in R_s [%]	20…80	25…85	33…90	37…92
Q_c	176…117	197…133	213…149	233…166
Q_u	64…54	66…57	68…60	70…62

Unloaded Q-values for a single double loaded resonator can be related to the loaded Q-values if the external Q-values of both sides are known. Loaded Q can be also calculated from the attenuation through the cavity at resonance when the corresponding external Q-values are known. (Matthaei *et al.* 1980.) In case that the cavity is symmetrically loaded external Q-values and coupling coefficients for both sides are similar. Consequently the loaded Q-value can be written as

$$Q_l = Q_u \left(1 - \frac{1}{10^{(L_A)_r/20}} \right) \quad , \tag{11}$$

where Q_u is the unloaded Q-value and $(L_A)_r$ is the attenuation through the cavity at resonance [dB]. Loaded Q-values with different losses and unloaded-Q-values are shown in Fig. 19. It should be noted that when losses are greater than 40 dB Q_u and Q_l are almost identical. In case that coupling probes with 50 ohms termination are used a PCB cavity has four ports and this approach is not valid.

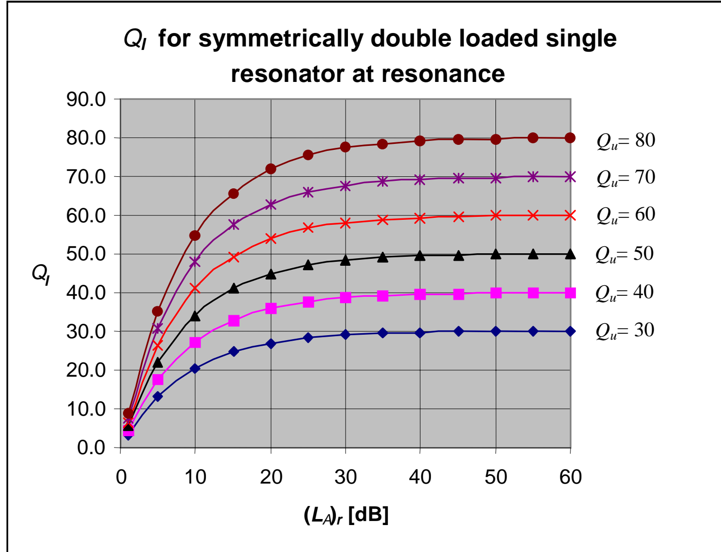

Fig. 19. Loaded Q-values for symmetrically double loaded single cavity as a function of attenuation through the resonator at resonance.

4.2.3. Coupling between opposite open ended blind vias

When two vertically aligned blind signal vias have many coaxially placed through ground vias the structure looks like a gap in a coaxial line. Placement of the ground vias in this fashion is discussed later in section 4.3.4 p 48-51. This approach is further encouraged by modelled results for six coaxial vias in section 4.3.4 and also by earlier study of Pillai (1997). The model for a gap in a coaxial line consist of two parallel capacitors and one series capacitor as shown in Fig. 20. This model assumes that fields concentrate in the dielectric support bead i.e. $\varepsilon_{r,2}$ is greater than $\varepsilon_{r,1}$. (Wadell 1991). We may see this situation arise on PCB's if construction utilises different substrate materials. However, more typically there is a single substrate material and $\varepsilon_{r,2}$ should be close in value to $\varepsilon_{r,1}$. It is further assumed that capacitance values do not change with frequency and $(b\text{-}a) < \lambda$, $s \ll \lambda$, $s \ll (b\text{-}a)$ (Wadell 1991). Effects of any other discontinuities on the line are

neglected. Calculation of model parameters is shown in equations (12)-(15) (Wadell 1991).

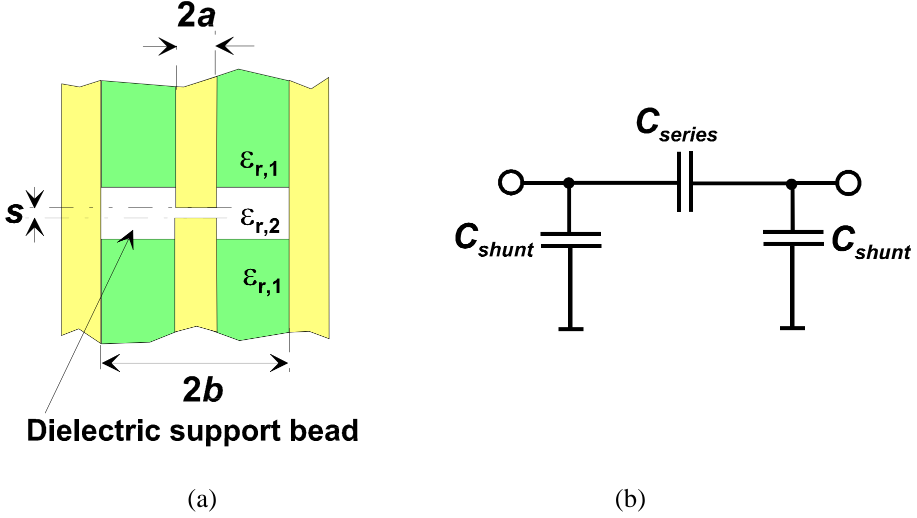

(a) (b)

Fig. 20. Coaxial gap model for vertically aligned blind vias. Line geometry and circuit model are shown in (a) and (b), respectively.

Series capacitance for a coaxial gap model is

$$C_{series} = \frac{27.7795\varepsilon_{r,2}a^2}{s}\,(\mathrm{pF}), \tag{12}$$

where s is length of the gap, a is radius of the centre conductor and $\varepsilon_{r,2}$ is relative permittivity of the support bead. Shunt capacitance for a coaxial gap model is

$$C_{shunt} = 78.7402\varepsilon_{r,2}\pi b C'_{d1}, \tag{13}$$

where b is radius of the outer conductor and $\varepsilon_{r,2}$ is as described in Eq. (12). Parameter C'_{d1} is given by

$$C'_{d1} = \frac{2\varepsilon}{100\pi}(1.477 - \ln 4\alpha), \tag{14}$$

where ε is permittivity of the support bead. Parameter α is calculated from

$$\alpha = 1 - \frac{a}{b}, \tag{15}$$

where a and b are defined in Fig. 20.

The function of the shunt capacitors in case of a PCB has to be questioned, because the outer conductor is not complete and line cross-section is also varied due to the sleeves in the signal via as shown in Fig. 13 p 28. So, we try to approximate coupling with a parallel plate capacitor model where fringing fields are not considered. This yields a simple series connection of capacitance

$$C_{series} = \varepsilon_{r,2}\varepsilon_0 \frac{\pi a^2}{s}, \tag{16}$$

where a and s are defined in Fig. 20, $\varepsilon_{r,2}$ is relative permittivity of the substrate material filling the gap and ε_0 is permittivity of the vacuum (Ramo *et al.* 1984). One problem considering series capacitance values in both models is, that typically a blind via pad area inside the PCB has a hole in the centre due to drilling of the via. However, the via is metalled and it may be expected that this reduces the effect of the hole. Comparison of results between coaxial gap and series capacitor models is shown in Fig. 21. Parameters are selected to be the following: a = 0.6 mm, b = 2.1 mm, s = 0.34 mm and $\varepsilon_{r,2}$= 4.4.

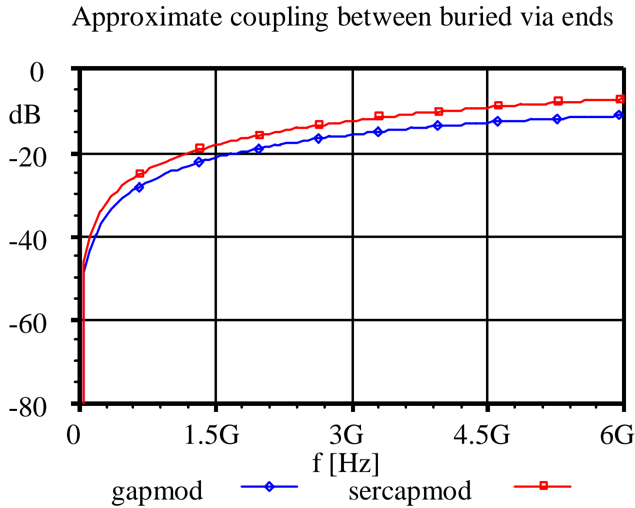

Fig. 21. Comparison of the results between the coaxial gap model (gapmod) and the simple series capacitor model (sercapmod).

4.3. Numerical models

4.3.1. Two-dimensional modelling of PCB cavities in the frequency domain

The PCB cavity is reduced to two dimensions for calculation of resonant frequencies as described in section 2.2.3 p 22. In this study only cavities with walls formed by via fences are considered. From an EMC point of view we are mainly interested in the lowest resonant frequency, which should ideally be well above the PCB's operating frequencies. Modelling may be performed in the frequency domain by using the finite difference method to solve the wave equation for a given geometry (Booton 1992, Sadiku 1992).

For modelling purposes the direction of propagation is selected to be along the z-axis (perpendicular to the PCB plane). This means that we have only TM modes at the frequency range of interest. So, to get field distribution only E_z needs to be solved. To do this either electric or mixed boundary condition at the surfaces of the cavity should be imposed. Cross-section of the PCB including boundaries is divided into the nodes in a rectangular grid. Node spacing is defined by discretization factor h. This naturally also defines the number of nodes in simulation domain. Ground vias inside the cavity walls are treated by setting E_z to zero at the simulation node where the via is located. Division of the calculation domain and treatment of the boundary conditions is shown in Fig. 22.

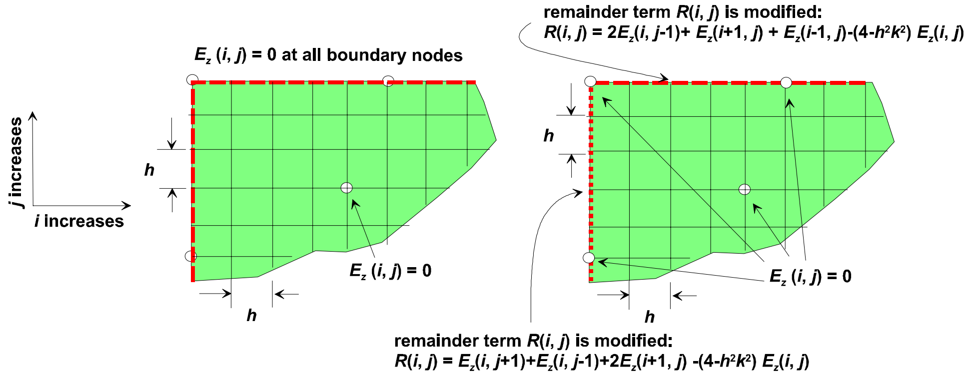

Fig. 22. Division of the calculation domain and treatment of the boundary conditions. The electric field boundary where E_z is set to zero at all boundary nodes is presented at the left side and mixed boundary where the remainder term $R(i, j)$ is modified at all boundary nodes if E_z is not zero (ground via location) at the right side.

Mode, which is converged, depends on the setting of the initial conditions. Imposing E_z to unity at all interior points is known typically to lead to convergence to the lowest mode. (Booton 1992). An initial value for the wave number k has to be also inserted. After this we can successively solve new values for k and E_z by using equations (17) – (19) until the desired accuracy is achieved. These are the same equations as used by Sadiku (1992) except that he has used the Jacobi process in iterations. Computation is started by solving the electric field distribution in the cavity using

$$E_z^{n+1}(i,j) = E_z^r(i,j) + \frac{rR(i,j)}{(4-h^2k^2)}, \quad (17)$$

where $E_z^r(i, j)$ is the most recent value of the electric field at a node (i, j), r is the relaxation coefficient, h is the grid size and k is the most recent value of the wave number. $R(i, j)$ is the residual given by

$$R(i,j) = E_z^r(i,j+1) + E_z^r(i,j-1) + E_z^r(i+1,j) + E_z^r(i-1,j) - (4-h^2k^2)E_z^r(i,j) \quad , \quad (18)$$

where $E_z^r(i, j)$, h and k are the same as described in Eq. (17) and $E_z^r(i, j+1)$, $E_z^r(i, j-1)$, $E_z^r(i+1, j)$ and $E_z^r(i-1, j)$ are the most recent values of E_z at nodes $(i, j+1)$, $(i, j-1)$, $(i+1, j)$ and $(i-1, j)$, respectively. Eq. (17) is scanned typically three or four times over the complete mesh before the updated value for the square of the wave number is calculated (Sadiku 1992). This can be obtained from the electric field distribution in the cavity by using the equation

$$k^2 = -\frac{\sum_{i=1}\sum_{j=1} E_z^r(i,j)\left[E_z^r(i+1,j) + E_z^r(i-1,j) + E_z^r(i,j+1) + E_z^r(i,j-1) - 4E_z^r(i,j)\right]}{h^2 \sum_{i=1}\sum_{j=1}\left(E_z^r(i,j)\right)^2}, \quad (19)$$

where $E_z^r(i, j)$, $E_z^r(i+1, j)$, $E_z^r(i-1, j)$, $E_z^r(i, j+1)$ and $E_z^r(i, j-1)$ are the most recent values for the electric field at nodes (i, j) $(i+1, j)$, $(i-1, j)$, $(i, j+1)$ and $(i, j-1)$, respectively and h is the discretization factor. After this the new electric field distribution in the cavity is calculated by using Eq. (17) with the updated value of the wave number. Then Eq. (19) is used again with the new electric field distribution. This process is continued until the difference between consecutive values of the wave number is within an acceptable tolerance. (Sadiku 1992.) Finally the resonant frequency f_r can be given by

$$f_r = \frac{k}{2\pi\sqrt{\varepsilon\mu}}, \quad (20)$$

where k is the wave number, ε is the permittivity of the media and μ is the permeability of the media.

The magnetic field intensities H_x and H_y can be calculated from the electric field intensities E_z by using source free Maxwell's equation for Ampere's law (Ramo *et al.* 1984). This can be done numerically by using central differencing as described in equations (21) – (22) and by imposing appropriate boundary conditions.

$$H_x(i,j) = \frac{\mathrm{j}\omega\varepsilon}{k^2}\frac{E_z(i,j+1) - E_z(i,j-1)}{2h}, \quad (21)$$

where j is the imaginary unit, ω is the angular frequency, ε is the permittivity of the media, k is the wave number, h is the discretization factor and $E_z(i, j+1)$ and $E_z(i, j-1)$ are electric field values at nodes $(i, j+1)$ and $(i, j-1)$, respectively.

$$H_y(i,j) = -\frac{j\omega\varepsilon}{k^2}\frac{E_z(i+1,j) - E_z(i-1,j)}{2h}, \tag{22}$$

where j, ω, ε, k and h are the same as described in Eq. (21) and $E_z(i+1, j)$ and $E_z(i-1, j)$ are electric field values at nodes (i+1, j) and (i-1, j), respectively.

A PCB cavity, which transverse dimensions are described as in Fig. 7 p 24, is modelled to compare results with different boundary conditions. For electric wall approximation dimensions measured from the inner via rows of Fig. 7 p 24 are used. This leads to a waveguide transverse section of 50 mm × 80 mm. To test a mixed boundary condition via grids as described in Fig. 8 p 24 are used at the sidewalls of the cavity and total size of the structure is then 55 mm × 85 mm. In both simulations h is set to 0.5 mm. Computation is stopped when the difference between successive values for k^2 is smaller than 0.1. Relaxation coefficient r is set to 1.5. Calculated resonant frequencies for the lowest modes are shown in Table 3. For reference, analytic results calculated with electric wall approximation are also shown. The difference between results for mixed and electric boundaries is about 4.4 %. The reason for this is, that the structure with mixed walls is electrically larger, because field is not zero between the ground vias. Correlation between results for analytical and numerical models, which assume electric walls, is good. Simulated modal electric field patterns are shown in Fig. 23.

Table 3. Simulated resonant frequencies for a cavity described in Fig. 7, when electric wall or mixed boundary condition is applied.

Boundary and calculation method	Relative permittivity constant ε_r				
	4.2	4.3	4.4	4.5	4.6
	Resonant frequency f_r [GHz]				
E-wall, numerical	1.7255	1.7053	1.6858	1.6670	1.6487
Mixed, numerical	1.6504	1.6311	1.6124	1.5944	1.5770
E-wall, analytic	1.7251	1.7049	1.6854	1.6666	1.6484

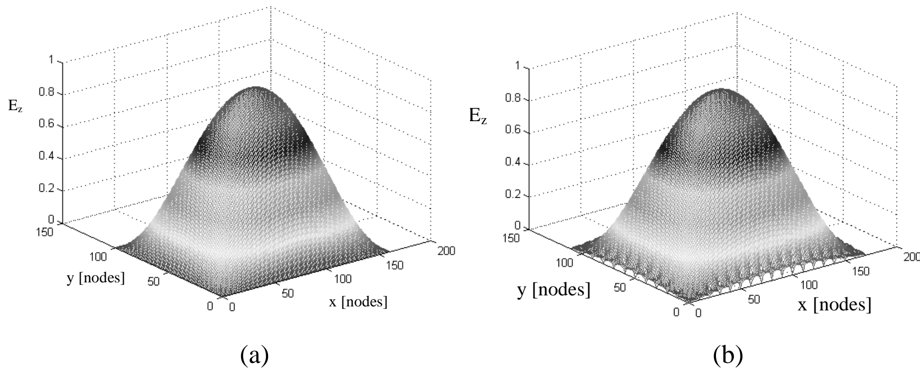

Fig. 23. Simulated modal fields for a PCB cavity which transverse dimensions are described in Fig. 7 p 24. Results with electric and mixed boundaries are shown in (a) and (b), respectively. Discretization setting *h* is 0.5 mm.

Examples of simulated electric field patterns for some structures are shown in Fig. 24. Corresponding resonant frequencies are calculated and shown in Table 4. Remember that these are the lowest resonant frequencies. Measured S-parameter results for the same structures may be seen in Fig. 39 p 65 and Fig. 43 p 69. In modelling the cavity is assumed to have electric boundaries and transverse dimensions of 50 mm × 80 mm. Discretization parameter h is set to 1 mm. Computation is stopped when the difference between successive iterations in k^2 is smaller than 0.1. Relaxation coefficient r is set to 1.5. Calculation time with these settings is about 2 minutes with a personal computer (PC) using 300 MHz Pentium II processor. Results for resonant frequencies when no vias are added correlate well with analytical and numerical results for a cavity with electric walls given in Table 3. Equivalency between numerical results is up to three decimal places, when frequencies are indicated in gigahertzs.

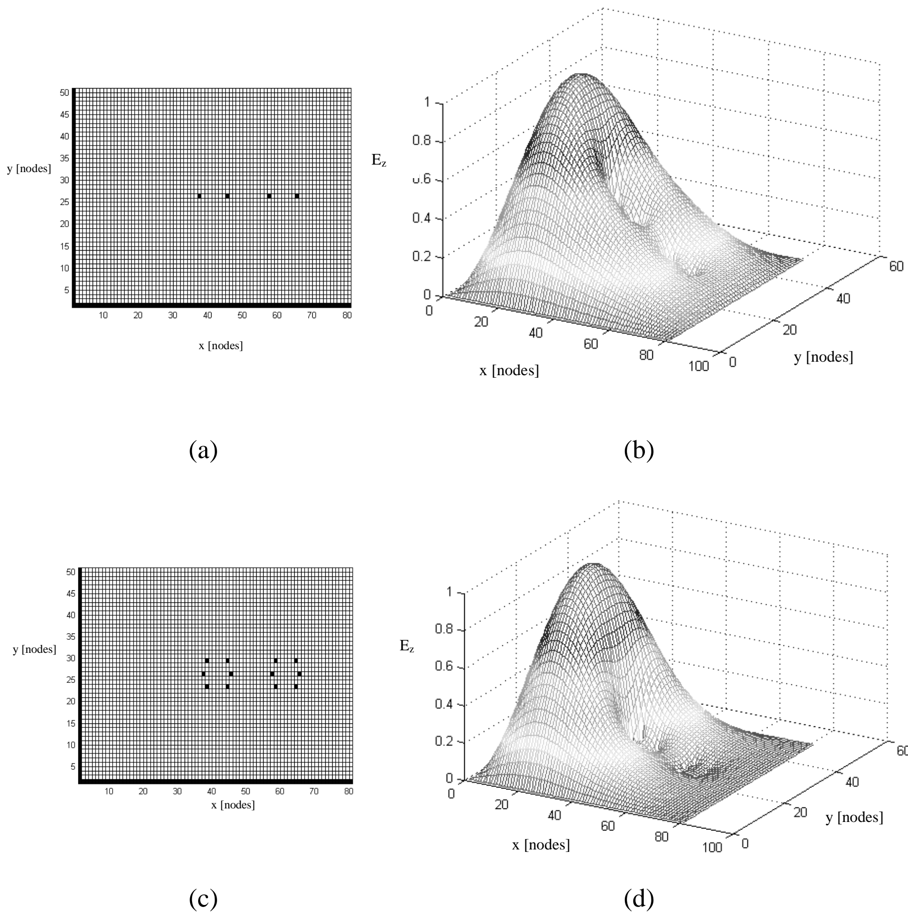

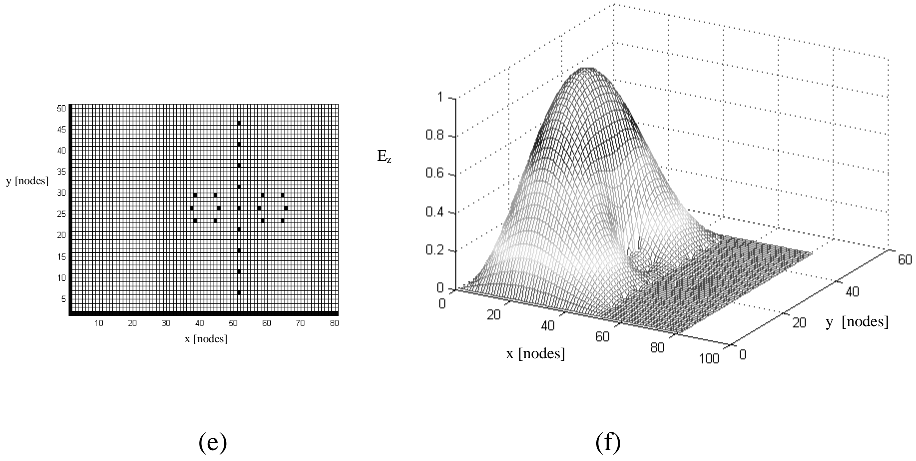

(e) (f)

Fig. 24. Electric field patterns for the lowest mode and associated configurations of additional ground vias. Ground via patterns for four, twelve and 21 vias cases are shown in (a), (c) and (e), respectively. Corresponding modal electric fields are plotted in (b), (d) and (f), respectively.

Table 4. Simulated resonant frequencies with different ground via configurations and values of relative permittivity.

Geometry of Fig. 24	Relative permittivity ε_r				
	4.2	4.3	4.4	4.5	4.6
	Resonant frequency f_r [GHz]				
(a)	2.18	2.16	2.13	2.11	2.08
(c)	2.31	2.29	2.26	2.23	2.21
(e)	2.33	2.30	2.27	2.25	2.22

Coupled resonators described in section 3.2.2 p 30 are modelled as a single waveguide, which includes vias inside the structure. Single via row is used as an example of modelling with *S* set to 20, 10, 5 and 2.5 mm. The same simulation parameters as for 50 mm × 80 mm cavities with additional ground vias are used, except that *h* is 0.5 mm while simulating via row for case where *S* is set to 2.5 mm. Simulated resonant frequencies with various values of relative permittivity are shown in Table 5. It can be seen that when S gets smaller the resonant frequency starts to approach the value for a single 50 mm × 80 mm cavity. Examples of modal patterns of electric field are shown Fig. 25. It may be noted that in Fig. 25(b) fields at different sections are more symmetrical than in Fig. 25(a).

Table 5. Lowest resonant frequencies for a coupled resonator structure with different separations S when single via rows between sections are used.

	Relative permittivity ε_r				
	4.2	4.3	4.4	4.5	4.6
S [mm]	Resonant frequency f_r [GHz]				
20	1.33	1.31	1.30	1.28	1.27
10	1.51	1.49	1.48	1.46	1.44
5	1.64	1.62	1.60	1.59	1.57
2.5	1.69	1.67	1.65	1.63	1.61

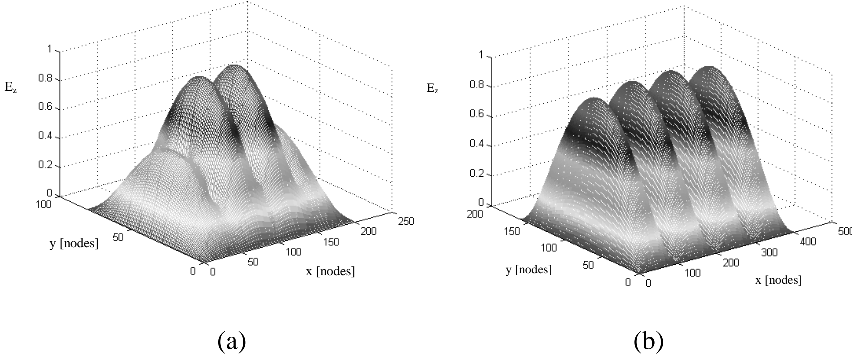

Fig. 25. Modal pattern of electric field at lowest resonance for a coupled resonator structure. Single via rows to separate sections are used and *S* is set to 20 mm in (a) and to 2.5 mm in (b). Discretization setting *h* is 1 mm in (a) and 0.5 mm in (b).

4.3.2. Approximation of unloaded Q-values

Once the field distribution in the cavity is solved either numerically or analytically then the unloaded Q-values can be approximated. First stored energy in the cavity is calculated. The energy corresponding to the numerically solved electric field in the cavity is

$$U = \frac{\varepsilon h^2 H}{32} \sum_{i=1}^{imax-1} \sum_{j=1}^{jmax-1} \left[\left|E_z(i,j)\right| + \left|E_z(i+1,j)\right| + \left|E_z(i,j+1)\right| + \left|E_z(i+1,j+1)\right| \right]^2, \quad (23)$$

where ε is the permittivity of the media filling the cavity, *h* is the discretization constant, *H* is the height of the cavity and *imax* and *jmax* are the largest simulation domain indexes in x- and y-directions, respectively. $E_z(i, j)$, $E_z(i+1, j)$, $E_z(i, j+1)$ and $E_z(i+1, j+1)$ are electric field values at nodes (i, j), $(i+1, j)$, $(i, j+1)$ and $(i+1, j+1)$, respectively. Note that no variation of the fields is assumed in the z-direction and the smallest index used to

indicate location in the simulation domain is one. Energy lost to the conductive walls can be given by

$$P_c = \frac{R_s h^2}{16} \sum_{i=1}^{imax-1} \sum_{j=1}^{jmax-1} \Big\{ \big[|H_x(i,j)| + |H_x(i+1,j)| + |H_x(i,j+1)| + |H_x(i+1,j+1)| \big]^2 + \big[|H_y(i,j)| + |H_y(i+1,j)| + |H_y(i,j+1)| + |H_y(i+1,j+1)| \big]^2 \Big\}, \tag{24}$$

where R_s is surface resistivity described by Eq. (7), *h, imax and jmax* are the same as described for Eq. (23), $H_x(i, j)$, $H_x(i+1, j)$, $H_x(i, j+1)$ and $H_x(i+1, j+1)$ are magnetic field components along x-axis at nodes (i, j), $(i+1, j)$, $(i, j+1)$ and $(i+1, j+1)$, respectively and $H_y(i, j)$, $H_y(i+1, j)$, $H_y(i, j+1)$ and $H_y(i+1, j+1)$ are magnetic field components along y-axis at nodes (i, j), $(i+1, j)$, $(i, j+1)$ and $(i+1, j+1)$, respectively. The meaning of R_s and calculation of Q-values from U and P_c are similar as in section 4.2.2 p 35. Note that Eq. (24) takes only into consideration losses caused by the top and bottom walls i.e. at $z = 0$ and $z = H$.

4.3.3. Three-dimensional modelling of PCB cavities in the time domain

Three-dimensional modelling is of interest, because coupling pins and their terminations can be described unlike in a 2-D model. A commercial FDTD package included in the Aplac circuit simulator is used for these purposes. The advantage of time domain modelling is that a wide range of S-parameter data can be collected from a single sweep. Here modelling is performed for a cavity with approximate electric walls. This simplifies the 3-D model to a thin rectangular cavity shown in Fig. 17 p 32. In other words boundaries of the simulation domain are constructed of perfectly conducting walls instead of via grids, which would lead to an open problem. Losses are incorporated by setting small conductivity to the dielectric material filling of the cavity. Feeding is done with shorted and terminated probes. Modelling of the open-ended probe inside closed boundaries may be possible by terminating it capacitively. An approximation for the terminating capacitance would be however needed and finding it is not necessarily a simple task. In modelling an eight-layer board only the centre section forming a resonator is taken into consideration. This means that transverse dimensions of the resonator are 50 mm × 80 mm, but the height is only 0.34 mm. This leads to the small cell size, which increases calculation time. On a thicker board these kind of problems do not occur as frequently. An example of modelled and measured results for a 1.5 mm board is shown in Fig. 26. The structure to be modelled is the same as in Fig. 37 p 63, but with only ports P2 and P3. A thin wire with radius of 0.25 mm is used to model vias. Two and four ports are used in simulations in case of shorted and terminated probe (via), respectively. The port impedance is 50 ohm. In simulations cell size of 1 mm × 1 mm × 0.5 mm is used. It should be noted here that Aplac necessitates that at least 3 simulation cells are used in all directions. The time step is set to 99% of maximum stable value and simulation is continued for 8000 loops. The relative permittivity of the cavity filling is set to 4.4 and the conductivity to 0.01 S/m. Note that both values are frequency independent in the

simulations. This is a better approximation for the relative permittivity. The conductivity value is selected to take into account dielectric and wall losses slightly above 2 GHz.

The measured and modelled results can be said to agree well from the EMC point of view. Even slightly better results can be achieved with longer simulation times. However, when the number of the loops is increased to 15000 the maximum difference in coupling values compared to the shorter simulation is 2.5 dB. Typically coupling values are less than 0.5 dB higher at the strongest resonant peaks for longer simulation. Larger deviations are mainly concentrated on the notches in the coupling response. Unfortunately typical layer heights on multilayer boards are much thinner than used in this example. Calculation times are approximately a few hours or even more to obtain results with a 300 MHz Pentium II processor. The problem is escalated if there are multiple resonators on top of each other, the size of the cavity is larger or there are dense via fences.

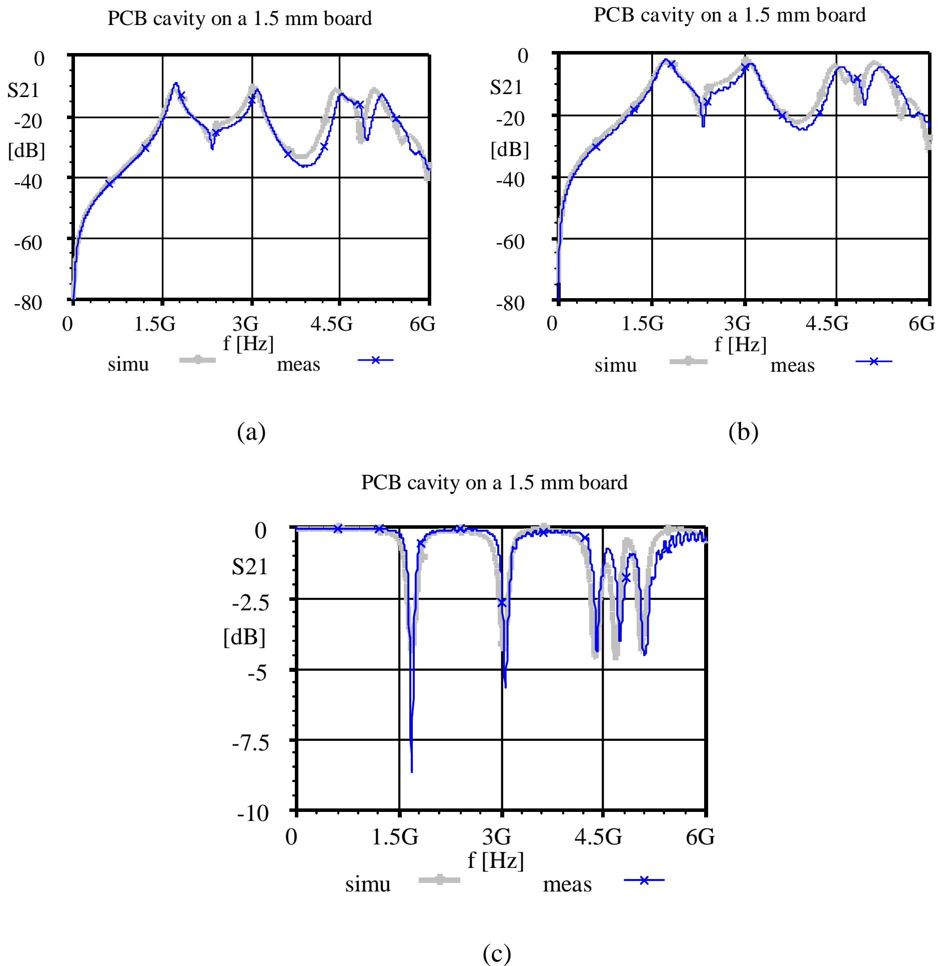

Fig. 26 Simulated and measured coupling between (a) terminated and (b) shorted probes and (c) loss for a via going through a cavity.

4.3.4. *Quasi static modelling of a coaxial via*

In a previous study by Pillai (1997), a coaxial via is introduced. For this structure placement of ground vias is calculated by using a simple equation for a coaxial line to get the desired characteristic impedance (Pillai 1997). Diameter *D* for placement of the ground vias as derived from characteristic impedance equation for a coaxial line (Wadell 1991) can be given by

$$D = d \cdot e^{2\pi Z_0 \sqrt{\varepsilon_r}/\eta_0}, \tag{25}$$

where *d* is inner conductor diameter, ε_r is relative permittivity and η_0 is characteristic impedance of free space. One would however expect that characteristic impedance increases, because the outer conductor is not continuous. This effect should be more evident with two rather than six vias. Naturally these effects depend also on the size of the grounding vias. Increasing diameter decreases distance to the signal via and lowers characteristic impedance. In case that impedance is too high decreasing diameter *D* given by a coaxial equation might lower it. A similar idea is presented for via ground access openings where no ground pins are used (Daigle *et al.* 1993, Watson & Gupta 1996).

Here numerical analysis is used to calculate the characteristic impedance. A coaxial via is assumed to be infinitely long and rectangular pins are used to approximate vias. Analysis is carried out by solving 2-D Laplace equation with finite difference method. Symmetry condition is used to reduce simulation space to one quarter. The coaxial via structure to be solved is shown in Fig. 27.

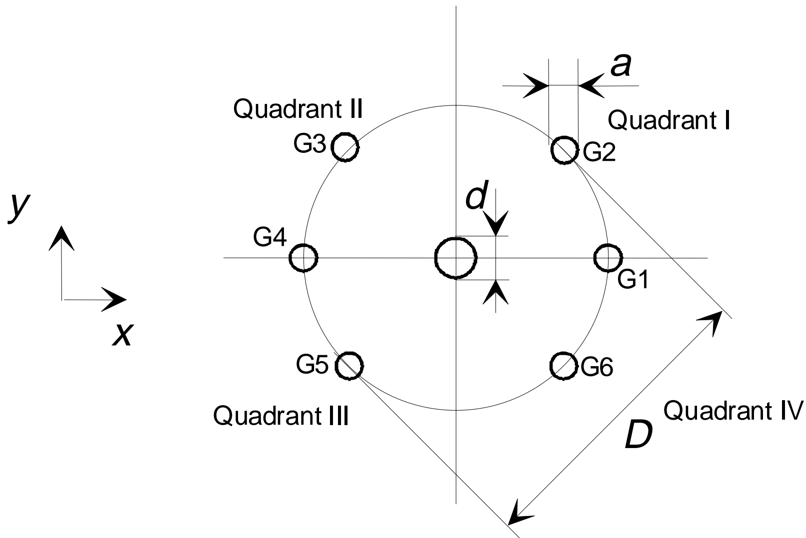

Fig. 27. Top view of a coaxial via structure with possibly differently sized signal and ground vias. Ground vias are numbered from G1 to G6. Signal via is shown in the centre of the picture.

To calculate the characteristic impedance potential distribution is first solved by using over relaxation with Gauss-Seidell iteration. With this method a new value for potential is given by

$$V^{n+1}(i,j) = V^r(i,j) + r\left(\frac{V^r(i+1,j)+V^r(i-1,j)+V^r(i,j+1)+V^r(i,j-1)}{4} - V^r(i,j)\right) \quad (26)$$

where $V^r(i, j)$, $V^r(i+1, j)$, $V^r(i\text{-}1, j)$, $V^r(i, j+1)$ and $V^r(i, j\text{-}1)$ are the most recent values of potential at nodes (i, j), $(i+1, j)$, $(i\text{-}1, j)$, $(i, j+1)$ and $(i, j\text{-}1)$ respectively and r is relaxation coefficient. (Booton 1992). Symmetry conditions for potentials require that

$$V(imax+1, j) = V(imax-1, j) \quad \text{and} \quad (27)$$

$$V(i, jmax+1) = V(i, jmax-1), \quad (28)$$

where *imax* and *jmax* indicate maximum node numbers in quadrant III and $V(imax+1, j)$, $V(imax\text{-}1, j)$, $V(i, jmax+1)$ and $V(i, jmax\text{-}1)$ are potential values at nodes $(imax+1, j)$, $(imax\text{-}1, j)$, $(i, jmax+1)$ and $(i, jmax\text{-}1)$, respectively (Dworsky 1979).

The potential is assumed to be 1 volt in the signal via and zero volts far from the centre conductor and in the ground vias. These assumptions are applied as boundary conditions in addition to symmetry lines. The initial value for potential in dielectric material is selected to be 0.5 V. The total energy per unit length can be approximately written as

$$U = \sum_{i=1}^{imax-1} \sum_{j=1}^{jmax-1} \Delta U, \quad (29)$$

where ΔU is the energy in an area enclosed by four neighbouring simulation nodes. As a per unit length value this can be given by

$$\Delta U = \frac{\varepsilon}{4}\left\{[V(i,j) - V(i+1,j+1)]^2 + [V(i+1,j) - V(i,j+1)]^2\right\}, \quad (30)$$

where ε is permittivity of the substrate material and $V(i, j)$, $V(i+1, j+1)$, $V(i+1, j)$ and $V(i, j+1)$ are potential values at nodes (i, j), $(i+1, j+1)$, $(i+1, j)$ and $(i, j+1)$, respectively. The total capacitance per unit length, when four quadrants are considered is

$$C_{tot} = 8U, \quad (31)$$

where total energy U is calculated from Eq. (29). Voltage at the signal via is normalised to 1 V. Consequently, voltage term is not shown in Eq. (31). (Dworsky 1979). After this characteristic impedance can then be expressed as

$$Z_0 = \frac{\sqrt{\varepsilon_r \varepsilon_0 \mu_0}}{C_{tot}}, \quad (32)$$

where C_{tot} is the total per unit length capacitance calculated from Eq. (31), ε_r is relative permittivity of the substrate, ε_0 is permittivity of the vacuum and μ_0 is permeability of the vacuum. Note that line losses are neglected and the smallest index used to indicate location in the simulation domain is one.

Structures where d = 1.6 mm, a = 0.4, 0.6 or 0.8 mm and ε_r is 4.4 are modelled. The selected value of the relative permittivity is typical for FR4 boards, which are used in measurements. For coaxial approximation D is calculated from Eq. (25) and is approximately 9.2 mm. In simulations different values of D can be given to different vias. Here D_a and D_b are used to indicate the value of D given to placement of vias G1 & G4 and G2, G3, G5 & G6, respectively. Only quadrant III is simulated and the symmetry conditions are used to get the total capacitance. The relaxation coefficient used is 1.5, which is well within the stable range (Dworsky 1979). Computation domain is $m \times n$ nodes excluding symmetry lines. Values of m and n indicate number of nodes in x- and y-directions, respectively. Iteration is stopped when maximum fluctuation of potential values between successive iterations is less than 1 µV. Configurations with two (G1 and G4) and six groundpins (G1 - G6) are modelled. Calculated characteristic impedances for some structures are listed in Table 6.

Table 6. Calculated characteristic impedances for some structures. Note that only quadrant III shown in Fig. 27 is simulated. G4 and G4 & G5 indicate structures with two and six vias, respectively.

Vias in the structure	D_a [mm]	D_b [mm]	a [mm]	h [mm]	$m \times n$	Z_0 [Ω]
G4	9.2	-	0.4	0.2	60×100	61.68
G4 & G5	9.2	9.2	0.4	0.2	60×100	49.82
G4	9.2	-	0.8	0.2	60×100	58.40
G4 & G5	9.2	9.2	0.8	0.2	60×100	46.76
G4 & G5	9.2	9.2	0.8	0.2	120×200	46.84
G4 & G5	9.2	9.2	0.8	0.1	120×200	47.63
G4 & G5	8.4	-	0.8	0.2	60×100	55.56
G4 & G5	8.4	9.4	0.8	0.2	60×100	47.03
G4	8.3	-	0.6	0.1	100×150	56.47
G4 & G5	8.3	9.4	0.6	0.1	100×150	47.92

Characteristic impedances listed in Table 6 are a bit too low because of linear approximation of energy distribution and effect of boundary walls at finite distance. This effect depends on the grid size h and the simulation domain size $m \times n$. Simulated cases with different h, m and n are listed in Table 6. However, what is important is that impedance for two via case is clearly higher than 50 ohms. This can be considered to be caused by coaxial approximation in case where outer conductor is far from complete circular boundary. In practice this would mean that if only two ground vias are used they should be closer to the centre conductor than indicated by coaxial approximation to get 50 ohms impedance level. When a via passes through the ground plane we have to consider ground access opening also. In two via case this might be considered as a transition from one type of transmission line to another. Six vias on the other hand seem to approximate coaxial transmission line quite well, which is desirable for good shielding and impedance

match. We can also see from Table 6, that when the diameter of ground via increases the characteristic impedance decreases. Difference between coaxial line approximations when either two or six ground vias are used can be investigated visually from plots of potential distributions in quadrant III shown in Fig. 28. It can be seen that potential is not as closely confined for two vias as for six vias case.

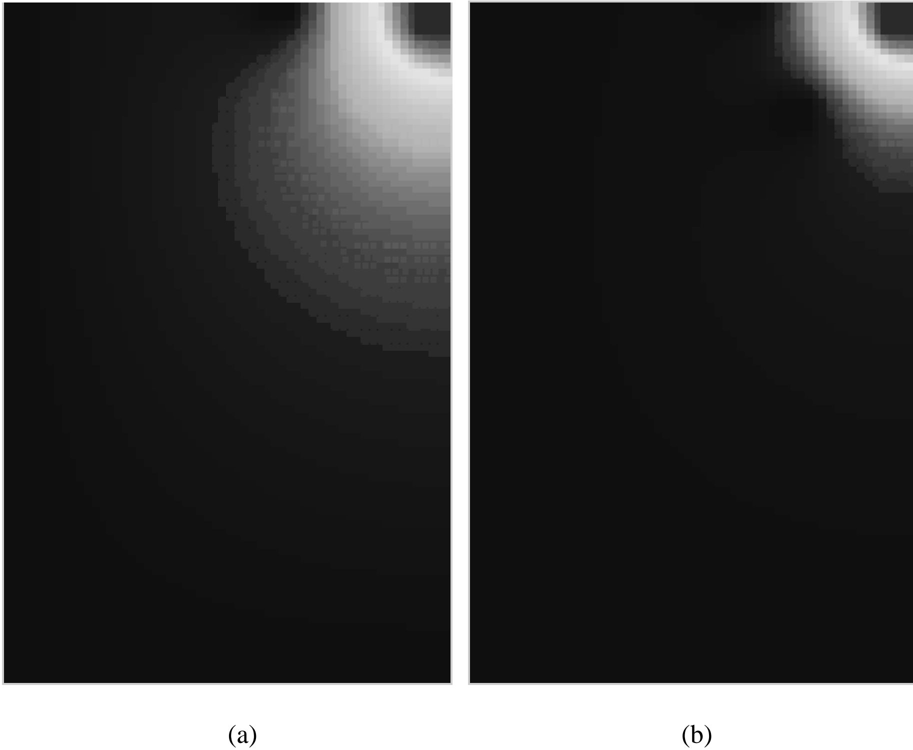

(a) (b)

Fig. 28. Plots of simulated potentials in quadrant III. Two and six vias cases are shown in (a) and (b), respectively. In these simulations $D_a = D_b = 9.2$ mm, $a = 0.8$ mm, $h = 0.2$ mm, $m = 60$ and $n = 100$.

5. Measured results

5.1. Description of the measurement methods

5.1.1. Coupling measurements

S-parameter measurements are used to study coupling and matching of different via configurations. All measurements are made with a Hewlett Packard 8503C network analyzer and 85047A S-parameter set. The PCB to be measured is located on a wooden chair. The measurement room is neither shielded nor anechoic. In most cases there is no significant effect due to external coupling or reflections, because main coupling path is inside the PCB. The frequency range used is from 3 MHz to 6 GHz. This range is interesting, because it spans typical operating frequencies of mobile communications and high-speed data transmission systems. Full two port calibration is used for error correction. Intermediate frequency bandwidth (IFBW) is varied from 10 Hz to 100 Hz according to the isolation needs. Using 100 Hz IF bandwidth is substantially faster, but it also causes more noise to measurements. This means that the dynamic range of the measurements is reduced. Isolation is typically better than 75 dB or 85 dB up to 6 GHz for 100 Hz and 10 Hz IFBW, respectively. The measurement cables used have to be able to achieve desired isolation also. For these purposes Sucoflex 104PE cables from Huber-Suhner are used. The cable length is 1 m. The number of points at which measurement samples are taken is either 1601 or 801. This means about 3.75 MHz and 7.5 MHz frequency resolution for 1601 and 801 points, respectively. Taking into consideration that Q-values of resonators to be measured are limited to a few tens this is good enough from an EMC point of view. Source power of the network analyzer is set to 20 dBm. This can be safely done, because the test sample contains no active circuits.

The network analyzer is selected to be used instead of a spectrum analyzer to automate measurements. In case that higher isolation than 85 dB up to 6 GHz is needed it can be achieved with spectrum analyzer and an RF generator. Also using isolation calibration with averaging increases the dynamic range when a network analyzer is used, but the measurement acquisition time is substantially slower. Using a thicker substrate material than in typical RF multilayer boards also increases dynamic range in resonator

measurements. This is caused by increased coupling although resonant frequencies do not change from an EMC point of view.

Graphical plots in Hewlett Packard graphics language (HPGL) format and two port S-parameter data are used to store measured results. Most of the graphs are then plotted by using Aplac. These should not be considered as a simulated data unless otherwise stated.

5.1.2. Q-value measurements

Loaded Q-value for given resonant frequency can be written as

$$Q_l \approx \frac{f_r}{\Delta \mathrm{f}}, \tag{33}$$

where f_r is the resonant frequency and Δf is the 3 dB bandwidth of the resonance (Kajfetz & Guillon 1986). When the measurement bandwidth widens accuracy in Q-value measurements deteriorates. From an EMC point of view, where mainly isolation is of interest this error can be considered to be negligible.

5.2. Measurements on multilayer boards

5.2.1. Isolated cavities

The multilayer board structure described in section 3.1.1 p 23-24 is measured to compare coupling and Q-values between different terminations. S-parameter data is measured between ports P1 and P2 of Fig. 7 p 24. Ports P3 and P4 are left unconnected. Matching is also tested in a similar configuration, but only in case where terminating resistors are assembled. Measured results are shown in Fig. 29. Q-values for the four lowest resonances are calculated using Eq. (33) and listed in Table 7. From the EMC point of view the resonant frequencies match well with the analytically calculated values shown in Table 1 p 33. Measurements with open-ended probes and signal traces shielded are also done to check the effect of possible leakage outside the PCB. The difference compared to unshielded measurements is negligible. This indicates that leakage inside the PCB is the dominating effect on isolation. Matching response shows spikes at resonant frequencies and in overall high coupling values with each probe are noted. Differences in coupling effects tend to get smaller at the high frequency end. At lower frequencies coupling is strongest with shorted and weakest with open-ended probes. Corresponding loaded Q-values are highest for open-ended and lowest for shorted probe. This means that below first resonance isolation increases at slowest rate for shorted probe, with respect to decreasing frequency. For example if 60 dB isolation is needed it can be achieved only at frequencies below approximately 690 MHz. First resonance occurs at about 2.4 times this

frequency indicating, that ample safety margin to the first resonance may be needed. This kind of behaviour can be expected from PCB resonators with FR4 substrate, because unloaded Q-values are already below 100.

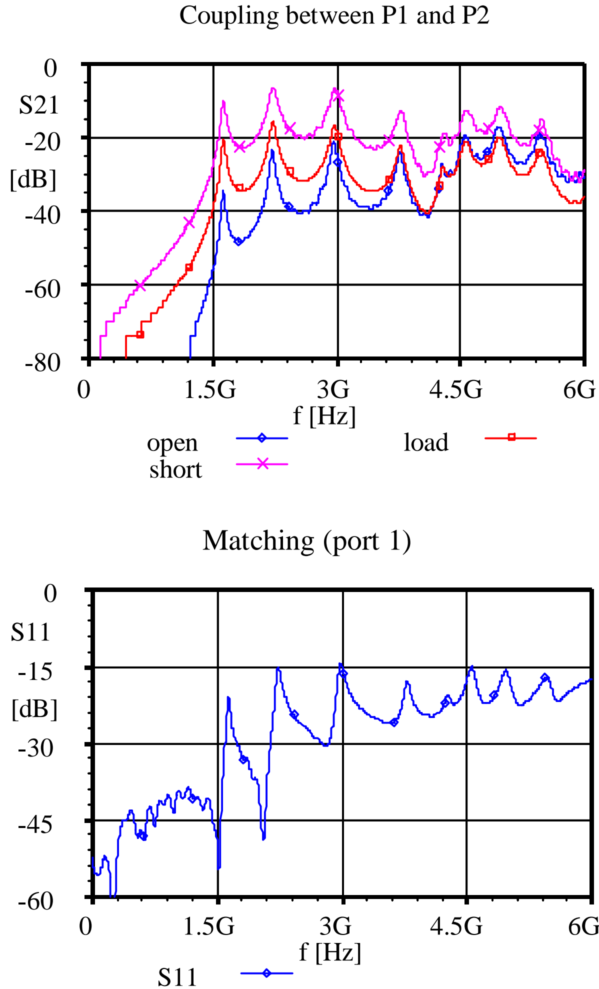

Fig. 29. Measured coupling and match on an eight-layer board. Terminations used are open, load (50 ohms) and short.

Table 7. Loaded Q-values for different resonant frequencies and terminations for the cavity on an 8-layer board.

	1.63 GHz	2.22 GHz	2.97 GHz	3.77 GHz
open	46	49	48	55
load	40	34	36	47
short	34	25	29	37

Unloaded Q-values may be solved from loaded Q-values by using Eq. (11) p 37 when the loss through the cavity at resonance is known. This can be found from the curves shown in Fig. 29. Calculated unloaded Q-values are shown in Table 8 for different resonant frequencies. These Q-values are slightly below the theoretically evaluated values shown in Table 2 p 36.

Table 8. Unloaded Q-values calculated from the measured results for the cavity on an 8-layer board.

	1.63 GHz	2.22 GHz	2.97 GHz	3.77 GHz
open	47	53	53	59
short	51	50	55	48
average	49	51	54	54

5.2.2. Stacked cavities

Measurements between ports P1 and P2 are made for the structure shown in Fig. 9 p 25 to test effect of a stacked cavity on coupling. Ports P3 and P4 are left unconnected. Measured results are shown in Fig. 30. Coupling is increased about 6 dB compared to the single resonator inside an eight-layer board except in the case, where the probe is left open-ended. Resonance effects in matching response are higher in case of two stacked resonators. The coupling increase compared to the results for single two-layer cavity shown later in Fig. 34 p 60 is similar as for an eight-layer board for shorted and terminated (100R//100R) probes, but about 11 dB increase for open-ended probe may be noted. Calculated Q-values with different probe terminations are listed in Table 9. Note that resonant frequencies are the same as those in Table 8. Consequently the resonant frequencies may be approximated analytically with Eq. (1) p 31 for this structure also, although we have two cavities on top of each other.

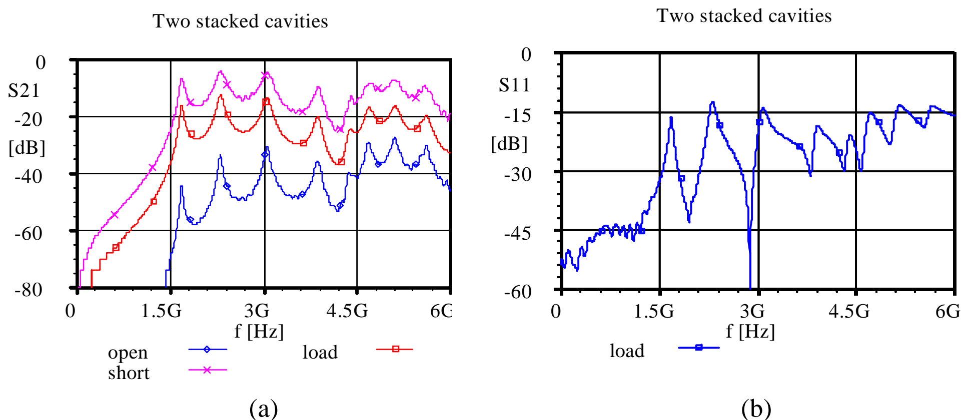

Fig. 30. Measured (a) coupling and (b) match for two stacked cavities.

Table 9. Loaded Q-values for different resonant frequencies and terminations for the stacked cavity structure.

	1.63 GHz	2.22 GHz	2.97 GHz	3.77 GHz
open	51	42	44	38
load	30	24	27	35
short	22	15	18	38

5.2.3. Transitions between shielded sections

Both matching and isolation are measured for structures described in section 3.1.3 p 25-27. Measured results are shown in Fig. 31. The matching response of through wall routing is more even than under wall routing. However, both curves show better than –25 dB match up to 2.6 GHz and it should be remembered that the effect of the BMA connector is also included in both responses. Under wall routing has more resonances and they start from lower frequencies, but Q-values and coupling are lower than for the 5.6 GHz peak encountered in through wall routing. Coupling values are quite low in both cases.

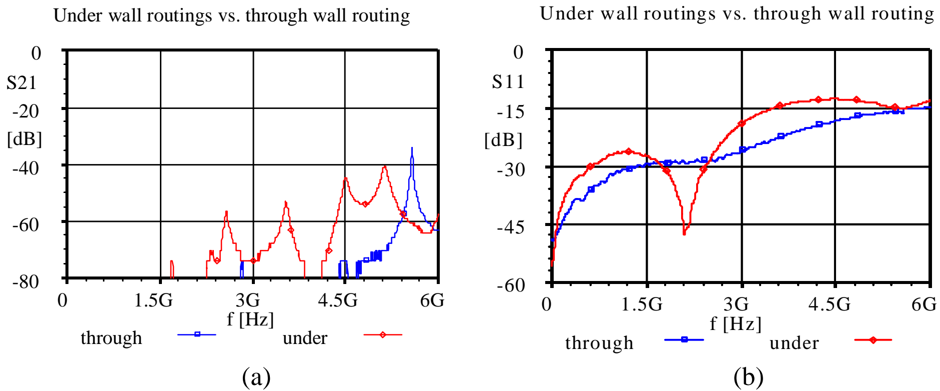

Fig. 31. Comparison of coupling and match between under and through shielding wall routings. Coupling is shown in (a) and matching in (b).

5.2.4. Coupling between opposite open ended blind vias

Arrangements to be tested are described in section 3.1.4 p 27-28. Measured results are shown in Fig. 32. Here excess losses are de-embedded by subtracting through via responses from those measured for blind vias. The overall shape of the coupling curves for structures in Fig. 12(a) and (b) p 28 is quite similar, but isolation for six coaxial vias is slightly lower. The difference is below 2 dB over the whole frequency range and has generally rising trend. Response curves start to deviate from the simple capacitance

models described in section 4.2.3 p 37-39 slightly above 3 GHz. The single series capacitance model seems to describe coupling values better when nominal board parameters are used in calculations. This can be seen by comparing modelled and measured results shown in Fig. 21 p 39 and Fig. 32, respectively.

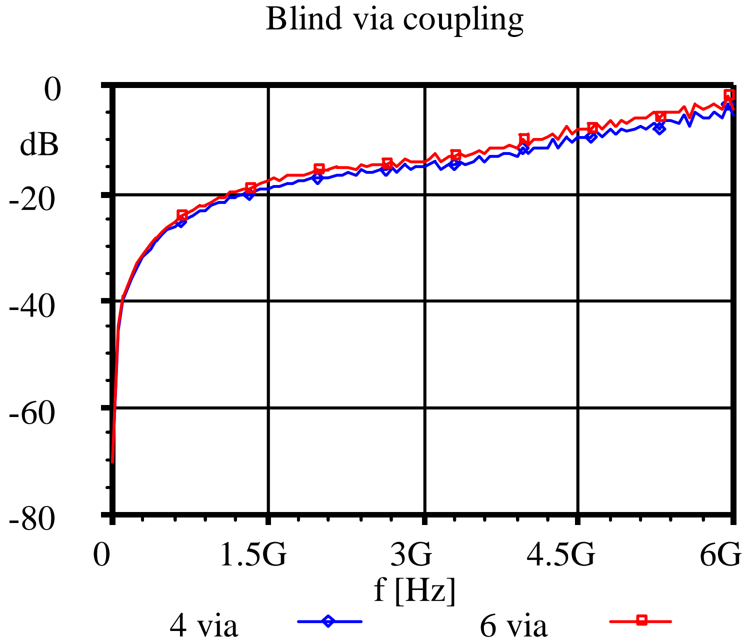

Fig. 32. Coupling between vertically aligned open ended blind vias.

Cross-sectional measurement for one PCB sample from the location of open-ended vias is also made. The purpose of this is to get an idea of the actual PCB structure. Cross-sectional view of the measured PCB is shown in Fig. 33. It can be seen that via ends inside the PCB have holes instead of complete pad areas. In addition to this it can be seen that the signal via has pad areas on all layers except 2 and 7. The effect of these on modelling is discussed in section 4.2.3 p 39. Surrounding coaxial vias are visible on the left and right edges of the picture. Blind vias are quite well aligned and offset seen in Fig. 33 is only about 30 µm. Height of the substrate between layers 4 and 5 at blind via location is measured to be 0.35 mm, which is quite close to the nominal value, but it is not guaranteed that this would be the case on boards used for coupling measurements. Measured dimensions are shown in Table 10.

Table 10. Measured and nominal board parameters for an eight-layer structure at the location of a blind via. The same identification numbers (Id.) for dimensions are used as in Fig. 33.

Id.	Nom. [μm]	Meas. [μm]	Description
1	2922	3040	thickness of the board
2	508	490	thickness of the substrate between layers 1 and 2, left side
3	170	170	thickness of the substrate between layers 2 and 3, left side
4	508	480	thickness of the substrate between layers 3 and 4, left side
5	340	340	thickness of the substrate between layers 4 and 5, left side
6	508	490	thickness of the substrate between layers 5 and 6, left side
7	170	140	thickness of the substrate between layers 6 and 7, left side
8	508	490	thickness of the substrate between layers 7 and 8, left side
9	508	490	thickness of the substrate between layers 1 and 2, right side
10	170	170	thickness of the substrate between layers 2 and 3, right side
11	508	480	thickness of the substrate between layers 3 and 4, right side
12	340	340	thickness of the substrate between layers 4 and 5, right side
13	508	500	thickness of the substrate between layers 5 and 6, right side
14	170	140	thickness of the substrate between layers 6 and 7, right side
15	508	480	thickness of the substrate between layers 7 and 8, right side
16	713	700	height between layers 1 and 3 at the left edge of the blind vias
17	713	700	height between layers 1 and 3 at the right edge of the blind vias
18	508	490	thickness of the substrate between layers 3 and 4 at the left edge of the blind vias
19	508	490	thickness of the substrate between layers 3 and 4 at the right edge of the blind vias
20	340	350	thickness of the substrate between layers 4 and 5 at the left edge of the blind vias
21	340	350	substrate thickness between layers 4 and 5 at the right edge of the blind vias
22	508	500	thickness of the substrate between layers 5 and 6 at the left edge of the blind vias
23	508	500	thickness of the substrate between layers 5 and 6 at the right edge of the blind vias
24	713	660	height between layers 6 and 8 at the left edge of the blind vias
25	713	660	height between layers 6 and 8 at the right edge of the blind vias
26	0	30	offset between blind via holes
27	0	50	offset between blind via pad areas

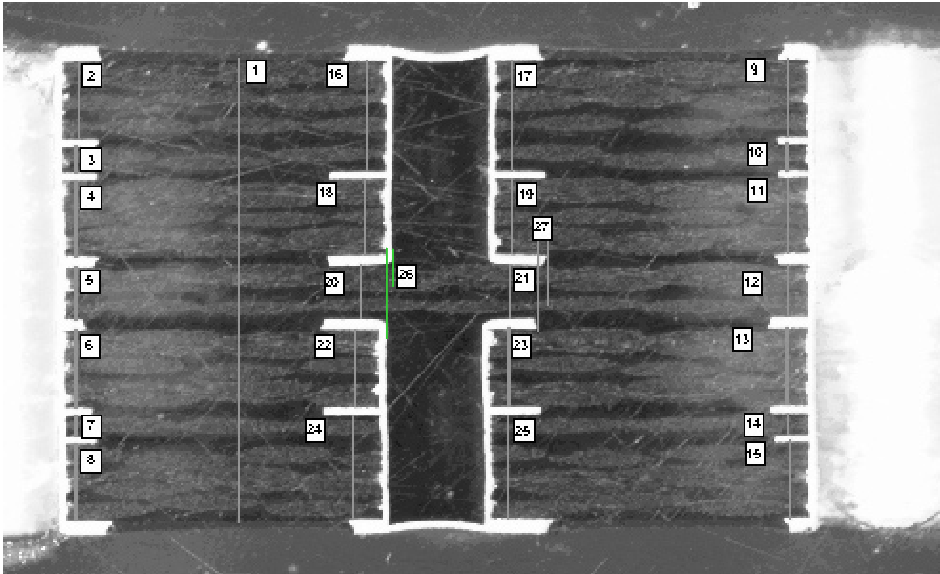

Fig. 33. Cross-sectional view of vertically aligned blind vias on an eight-layer board. Note that the same identification numbers for different dimensions are used as in Table 10.

5.3. Measurements on two-layer boards

5.3.1. Isolated cavities

The purpose of these measurements can be classified to the following groups: 1) comparisons of coupling between eight- and two-layer boards, 2) comparisons of coupling between 0.34 mm and 1.5 mm thick two-layer boards 3) studying how to reduce resonant effects and 4) verifying simulation models.

To compare coupling on two- and eight-layer boards probes at locations P1 and P2 as shown in Fig. 7 p. 24 are used. Ports P3 and P4 are left unconnected. The cavity on an eight-layer board is described in chapter 3.1.1 p 23-24. A two-layer version with substrate thickness of 0.34 mm is then built according to the guidelines described in section 3.2.1 p 28-30. Fig. 34 shows the coupling and matching results for both two- and eight-layer boards. Corresponding Q-values for two-layer board are shown in Table 11. It can be seen that the coupling results when the probe is either terminated to approximately 50 ohms or shorted correlate quite well. In case that the probe is left open-ended two-layer board has typically about 20 dB less coupling. Corresponding resonant frequencies are slightly different, but the Q-values are quite similar. Both matching responses show spikes

at resonant frequencies. Note that effect of connectors and terminating resistors is included in the responses shown.

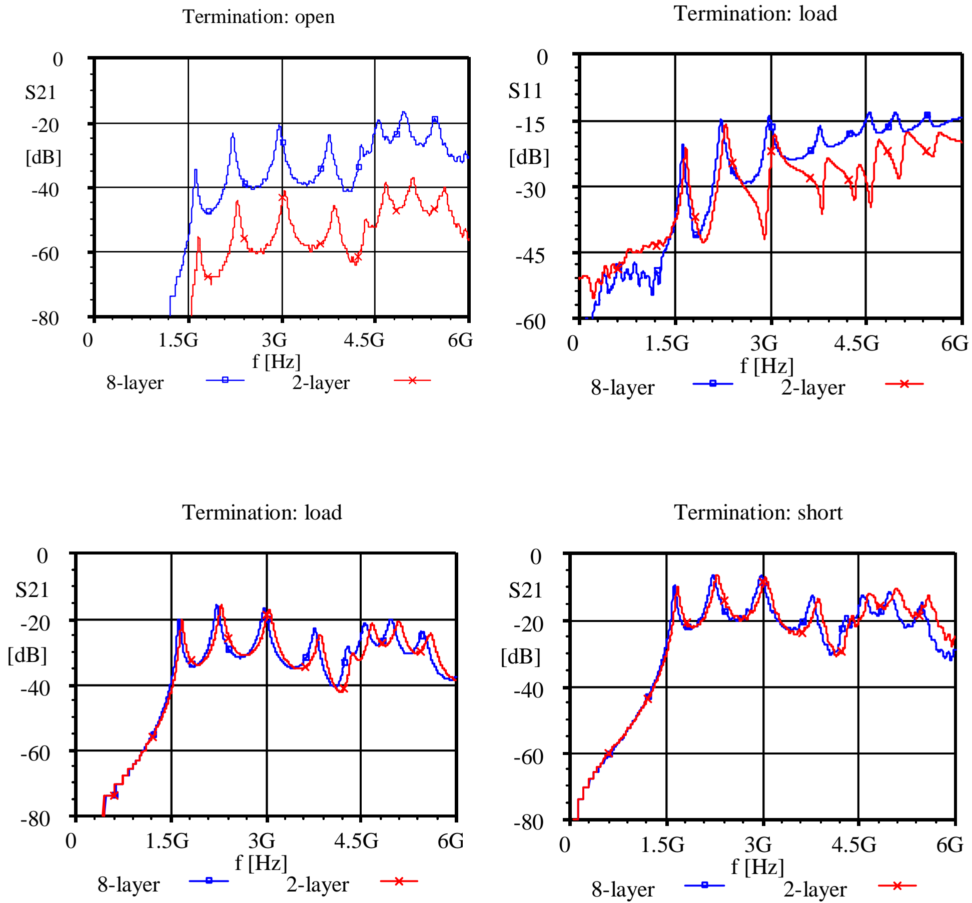

Fig. 34. Comparison of coupling and match between eight and two-layer boards with the same dimensions and probe locations. Probe terminations open, load (50 ohm) and short are used in coupling and only load in matching measurements.

Table 11. Loaded Q-values for different resonant frequencies and terminations on a 0.34 mm thick two-layer board.

	1.68 GHz	2.30 GHz	3.05 GHz	3.90 GHz
open	48	42	54	57
load	36	31	34	38
short	31	26	30	42

To increase coupling on two-layer boards the substrate thickness is changed from 0.34 mm to nominally 1.6 mm. Measurements however show that this thickness is actually 1.5

mm. The probe locations are the same as marked with P1 and P2 in Fig. 7 p 24. Ports P3 and P4 are left unconnected. Comparison between 0.34 mm and 1.5 mm boards is shown in Fig. 35. Q-values for 1.5 mm board are shown in Table 12. Resonant frequencies shown in Table 12 are averages of those for open, load and short terminations. Coupling is stronger on the thicker board especially when the probe is left open ended. Resonant frequencies are slightly lower on the 0.34 mm board and loaded Q-values are also higher. Matching responses show resonances in both cases, but the 1.5 mm board has a higher reflection level.

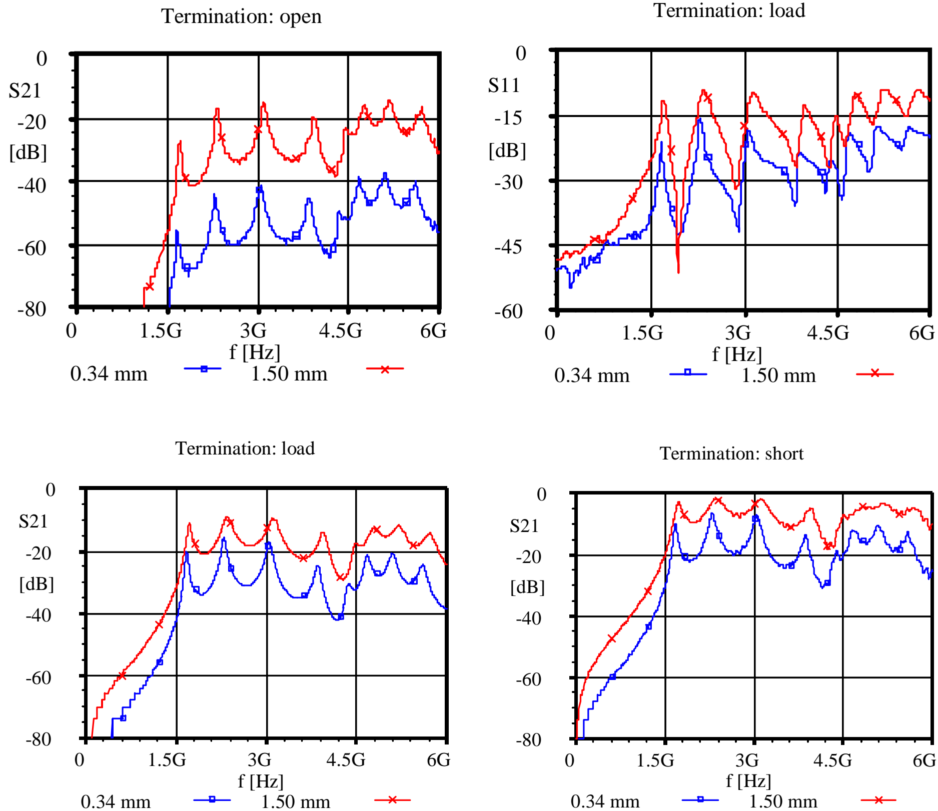

Fig. 35. Comparisons of coupling between 0.34 mm and 1.5 mm thick two-layer boards. Probe terminations open, load (50 ohm) and short are used.

Table 12. Loaded Q-values for different resonant frequencies and terminations on a 1.5 mm thick two-layer board.

	1.72 GHz	2.36 GHz	3.11 GHz	3.94 GHz
open	50	51	45	55
load	24	15	17	32
short	15	9	10	23

To check the validity of the assumption that a PCB section surrounded by a via grid can be modelled as a cavity with uniformly metalled walls coupling between ports P1 and P2 shown in Fig. 36(a) is measured. The measurement is performed on a 1.5 mm thick board for the cases, where sidewalls of the cavity are metalled or formed by vias. Different probe terminations are used in measurements. Metallization of the walls is done by soldering a copper tape, which covers uniformly the sidewalls of the cavity to the PCB ground at both sides. Naturally the board is first cut to the required dimensions of 80 mm × 50 mm. The measured results in case of an open-ended probe are shown in Fig. 36(b). It can be seen that coupling values are almost identical, but resonant frequencies for a cavity with metalled walls are somewhat higher. The typical difference is about 2 %. Similar results can be seen with other terminations. Modelled field patterns and resonant frequencies for these structures in case of the lowest resonance are shown in Fig. 23 p 42 and Table 3 p 42, respectively. Loaded Q-values for the four lowest resonances with different terminations are calculated to Table 13. It can be seen that Q-values in both cases are typically similar.

The wavelength inside a FR4 PCB is about 24 mm at 6 GHz. This is a bit less than ten times the separation Δ between the vias shown in Fig. 36(a). So, we may estimate that when the separation between the vias is in the order of 0.1λ or less the electric wall approximation for the via fence is valid. However, we have to remember that in the measured case the vias are not aligned in a single row and if this is done the results may change. This change can be assumed to be negligible for the purposes of this study.

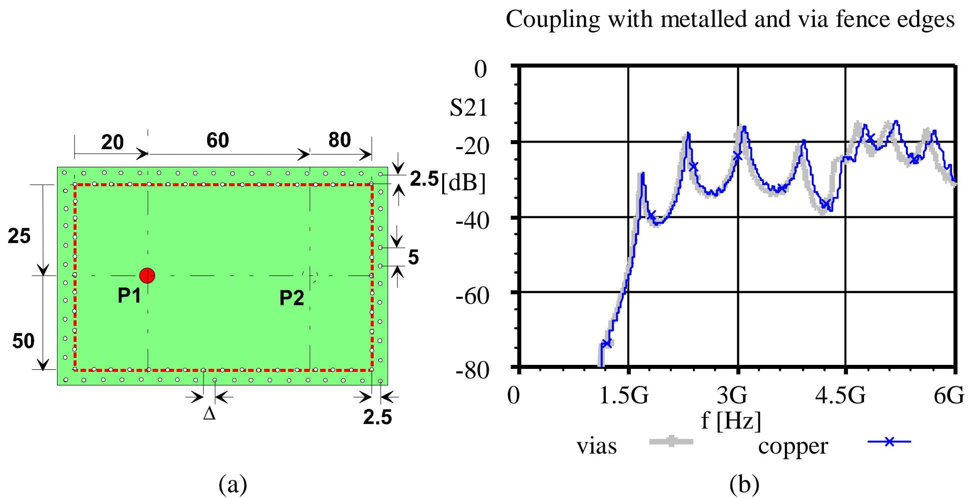

Fig. 36. Comparison of cavities with metalled and via fence sidewalls. Measured structures and the results are shown in (a) and (b), respectively. When sidewalls of the cavity are metalled the board is first cut to the dimensions of 80 mm ×50 mm. The line of the cut is marked with a wide dotted line in (a).

Table 13. Comparison of loaded Q-values between cavities where sidewall is formed by a via grid or copper metallization. Subscripts via and cop refer to these constructions, respectively.

	$Q1_{via}/Q1_{cop}$ $f_r \approx$ 1.7 GHz	$Q2_{via}/Q2_{cop}$ $f_r \approx$ 2.3 GHz	$Q3_{via}/Q3_{cop}$ $f_r \approx$ 3.1 GHz	$Q4_{via}/Q4_{cop}$ $f_r \approx$ 3.9 GHz
open	49/46	41/47	42/38	41/59
load	24/23	22/15	17/19	29/23
short	13/15	8/9	10/11	23/21

Measurements this far are used to make comparisons between different types of PCB's. Further measurements are made on a 1.5 mm thick two-layer board to find out effects of different methods to suppress resonances. Multiple coupling structures are experimented with two-layer boards and one used to test most methods for suppression of resonances is shown in Fig. 37. In some measurements one of the ports P1, P2 or P3 may not exist on the board. This is stated separately along description of the quantity to be measured. The sidewalls of the cavity are closed with similar ground via grids as described in Fig. 8 p 24. The first measurements without additional ground vias or other suppression methods are performed between ports P2 and P3, while P1 is left unconnected. These results are shown in Fig. 38 and they form a reference to which we can compare measured coupling values, when various suppression methods are used. Simulated coupling values for the same structure with terminated (50 ohms) and shorted coupling probes are shown in Fig. 26(a) and (b) p 47, respectively. Measured and simulated values of S_{21} agree well from the EMC point of view. Note that due to board resonances coupling does not necessarily decrease when separation between vias is increased. This can be seen by comparing the results in Fig. 35 with those in Fig. 38.

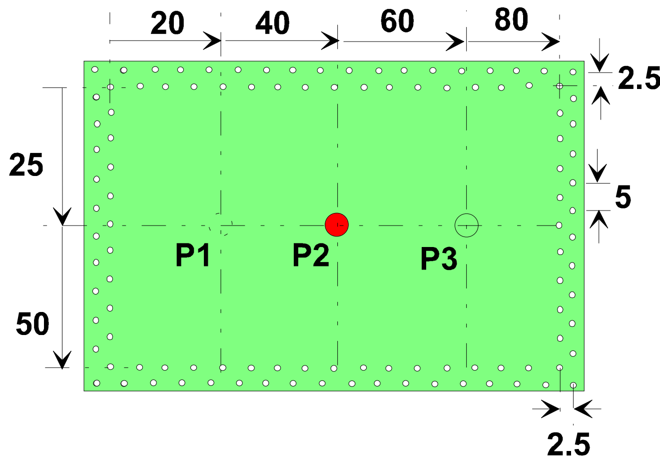

Fig. 37. Top view of the coupling structure used to test suppression of resonances. Large and small circles indicate locations of the connectors and ground vias, respectively.

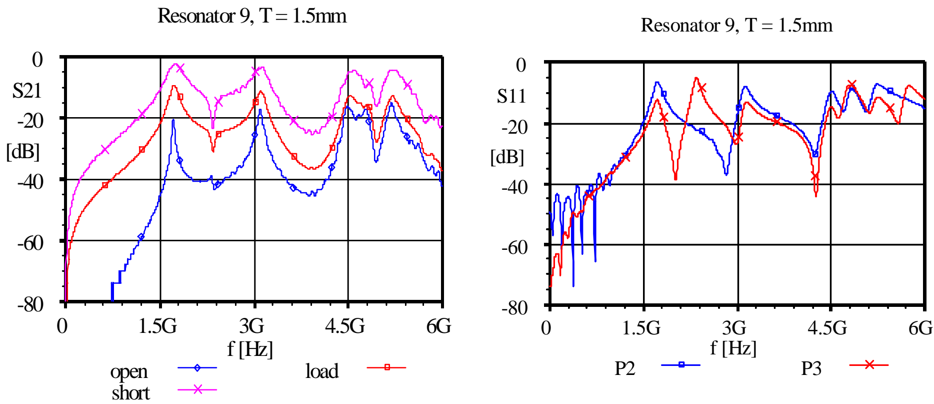

Fig. 38. Coupling and match on the suppression test board (named resonator 9), when no grounding vias are added.

When two grounding vias are added on the centre line along the resonator length on both sides of the centre pin at 1 mm distance from SMA edge ($D_a \approx 8.3$ mm) some suppression of the resonances can be achieved as shown in Fig. 39(a). Distance D_a is less than about 9.2 mm calculated for a coaxial via by using Eq. (25) p 48, when $d = 1.6$ mm and $\varepsilon_r = 4.4$. This is to reduce the effect of only 2 ground vias in a coaxial via structure. Ground vias are implemented by drilling a hole with a diameter of 0.8 mm on a PCB. After this copper wire is put through that hole and soldered to the PCB ground at the both sides of the board. Finally excess length of the wire is cut out. Diameter of the wire is 0.6 mm. Resonances shift to higher frequencies, when vias are added as might be expected due to perturbation of fields. Also a reduction of coupling can be seen, but due to shifting resonances coupling at some frequencies may be even higher than without grounding vias. This effect is not seen during simulations under non-resonant conditions (Pillai 1997). When four more vias are added at the SMA connector corners ($D_b \approx 9.4$ mm), which is slightly further than coaxial approximation states, we may still suppress coupling, but resonances do remain, thus causing potently unexpected coupling problems. This is shown in Fig. 39(b). Modelled results for these structures are shown in Fig. 24(b) and (d) p 43 and Table 4 p 44.

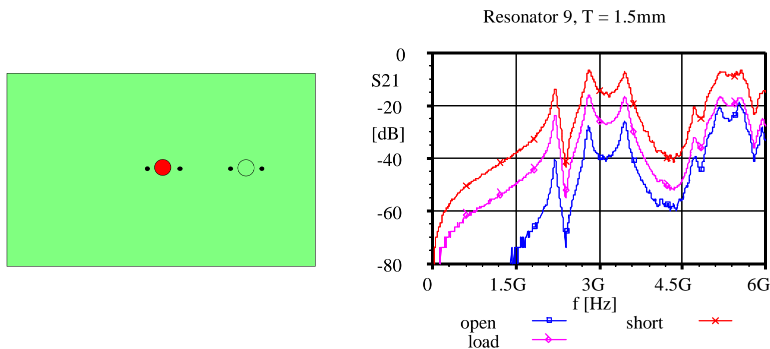

(a)

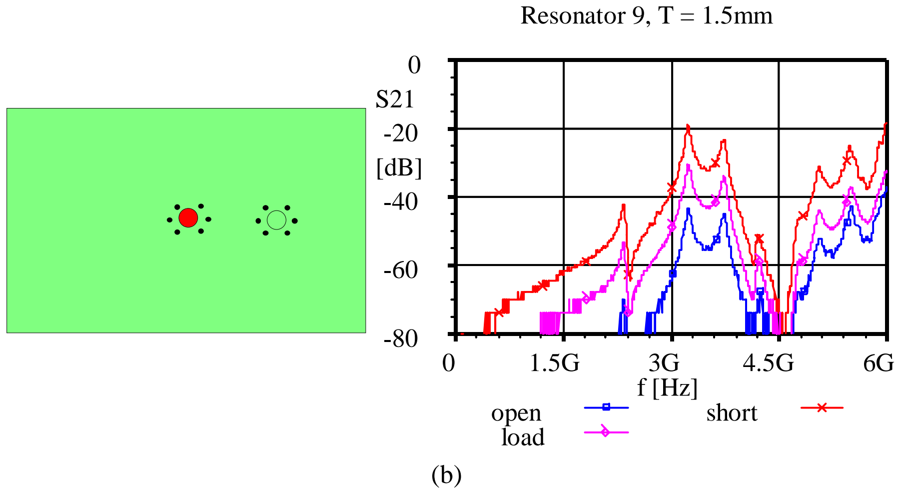

(b)

Fig. 39. Suppression of coupling when (a) two or (b) six ground vias are added at approximately coaxial distance from the signal vias. Locations of the connectors and additional ground vias are shown in the geometrical drawings by using large and small circles, respectively. Vias along the sidewalls of the cavity are not shown.

The effect on matching when probe is terminated to two 100 ohm resistors is shown in Fig. 40. It can be seen that a six via structure gives good match even under resonant conditions. Differences in responses between port P2 and P3 may be explained by the asymmetrical probe locations. For example when no ground vias are added the first resonance at about 1.72 GHz causes higher fluctuation on port P2. The probable reason for this is that electric field is at its maximum in the centre of the board. If we consider then the second resonance at about 2.36 GHz the situation is reversed and the resonance in port P2 is not even seen, probably due to electric field minimum at that location.

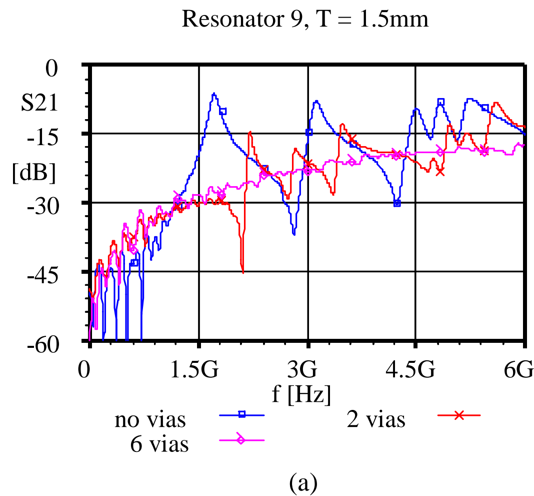

(a)

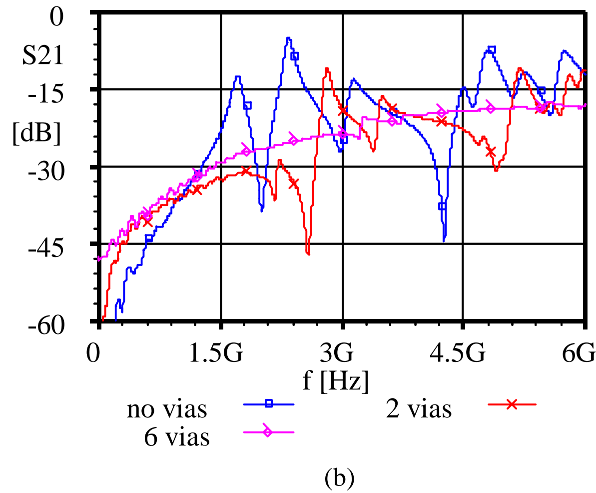

(b)

Fig. 40. Matching of (a) port P2 and (b) P3 on the suppression test board with different ground via configurations.

The resonance effect on loss along the signal path, which goes through the cavity, is measured in two-layer boards with substrate thickness of 1.5 mm and 0.34 mm. For these purposes the signal via at the centre of the resonator is used. This corresponds to the pin location P2 in Fig. 37 p 63. Unused ports are left unconnected. These are P1 and P3 for 0.34 mm and P3 for 1.5 mm board. The principle of SMA connector assembly for through signal path is shown in Fig. 15 p 29. Losses in case of different ground via configurations are shown in Fig. 41. In case that no ground vias are added resonances cause losses as high as 2.7 dB and 8.5 dB on 0.34 mm and 1.5 mm boards, respectively. Simulated results for the 1.5 mm board show also high loss peaks, although they are typically not as sharp as the measured peaks seen in Fig. 26(c) p 47. Two vias can improve this situation a little, but still loss peaks of about 0.8 dB even on thinner board do exist. In case that six coaxial vias are used loss peaks are suppressed on the 0.34 mm board and only small peaks are left on the 1.5 mm board. Matching when six coaxial vias are used is shown in Fig. 42. Responses for terminations using a 50 ohm SMA load and two 100 ohm resistors correlate well. However, it should be noted that the latter termination is measured in case, where also port P3 is terminated. These two measurements are performed on a PCB with a substrate thickness of 1.5 mm. In the case of a 0.34 mm substrate better match is achievable and S_{11} is lower that –23 dB up to 6 GHz, when the SMA load is used for termination.

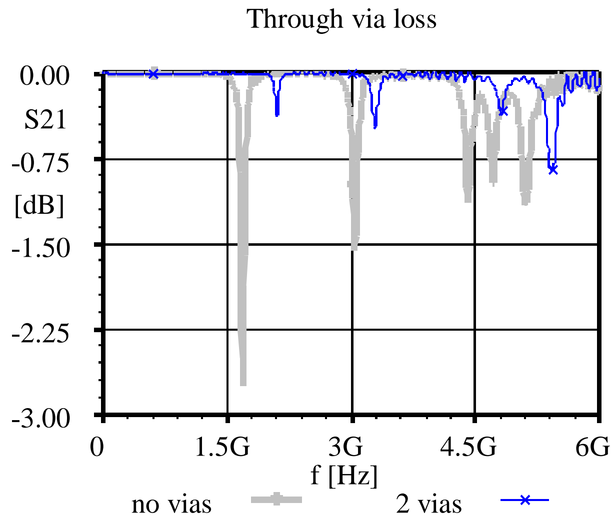

(a)

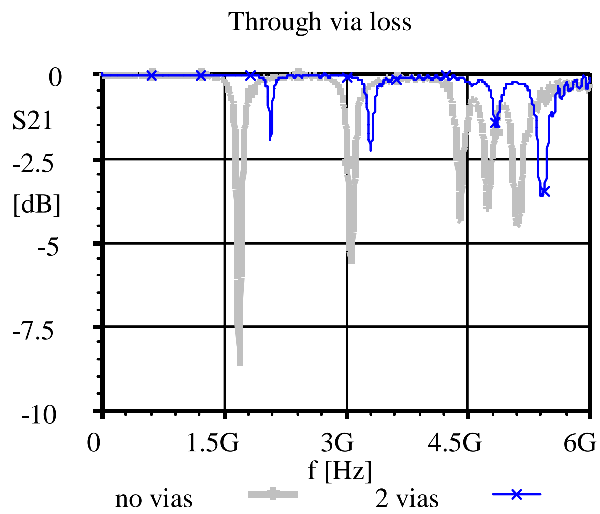

(b)

Fig. 41. Loss measurement for a via going through a cavity. Results for 0.34 mm and 1.5 mm thick boards are given in (a) and (b), respectively. In case that six coaxial vias are used loss peaks are suppressed on the 0.34 mm board and only small peaks are left on the 1.5 mm board

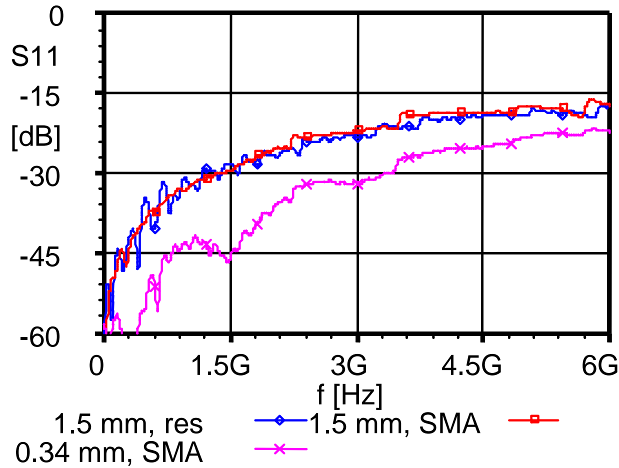

Fig. 42. Matching when the coaxial via structure is used. Substrate thicknesses of 0.34 mm and 1.5 mm are used. Termination is made either with two 100 ohm resistors (res) or with SMA 50 ohm load (SMA).

To further increase isolation different additional ground via configurations are tried. First division of the cavity into two uneven parts with lengths of 30 mm and 50 mm is made as described in section 4.2.1 p 34. A via fence with either a 5 mm or a 2.5 mm grid pattern is used for this purpose. Measured results are shown in Fig. 43. Compared to the case where only six coaxial vias are used an additional 20 to 30 dB reduction of maximum coupling level is achieved at frequencies below 3 GHz depending on the ground via grid used. However, resonances above 3 GHz increase coupling to the levels of –30 dB and -40 dB for 5 mm and 2.5 mm grid, respectively. This is still lower than for six coaxial vias where maximum coupling is about –20 dB. Simulated results for this structure with 5 mm via grid are shown in Fig. 24(f) p 44 and Table 4 p 44.

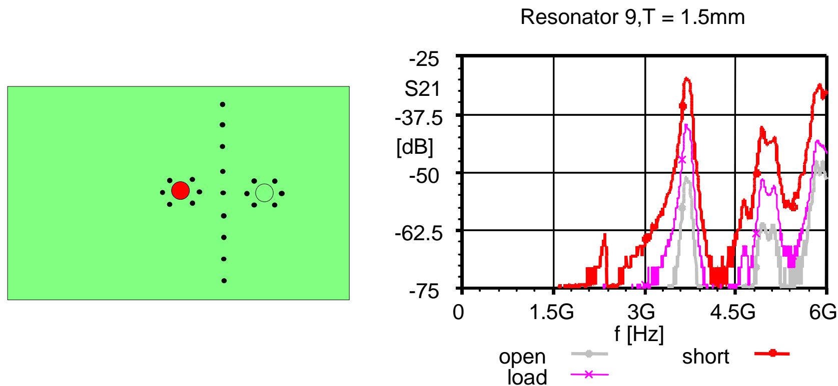

(a)

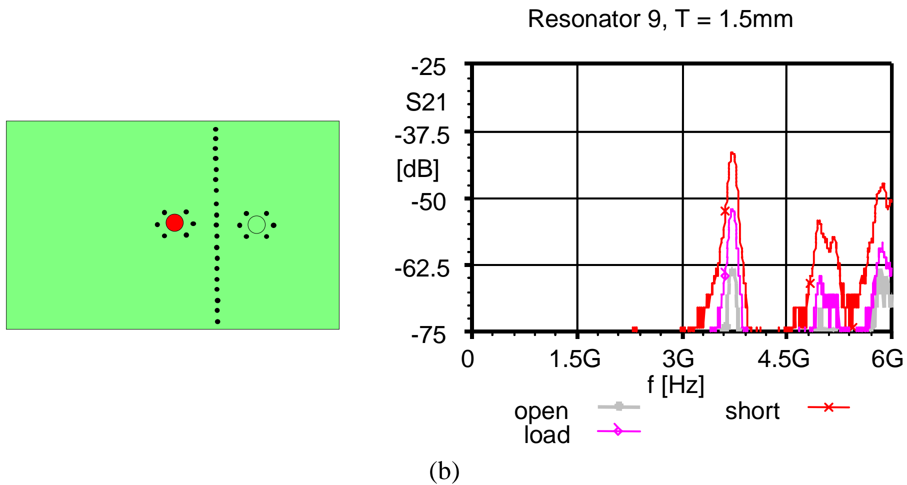

Fig. 43. Separation of the cavity into the two differently sized sections. This is made with a ground via fence with (a) 5 mm and (b) 2.5 mm grid.

To further study reduction of coupling the following steps in addition to the usage of a coaxial via are made 1) the cavity is filled with a 10 mm ground via grid and 2) ground via fences with 5 mm grid are added with row separations of 5 mm. Adding a 10 mm via grid causes lowest resonant frequency to rise, but high coupling of about – 30 dB is still seen above 4.5 GHz as shown in Fig. 44. To reduce effect of this three via rows are added. The centre row is located at an equal distance of 10 mm from both signal vias. It can be seen from Fig. 45 that the coupling level is now lower than –75 dB for short-circuited and –80 dB for a resistor terminated probe. Response for an open-ended probe is below the noise floor shown in Fig. 45(b).

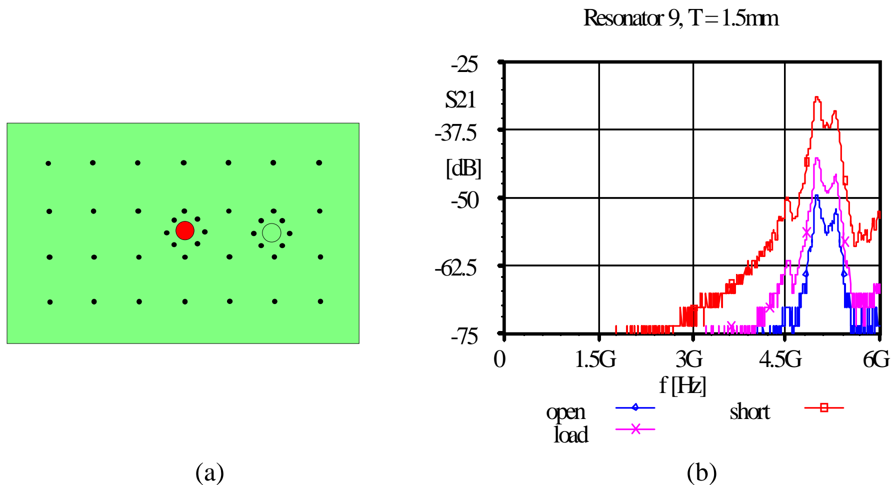

Fig. 44. Reduction of coupling with filling of the cavity with 10 mm grid in addition to coaxial vias. Via locations are shown in (a) and coupling in (b).

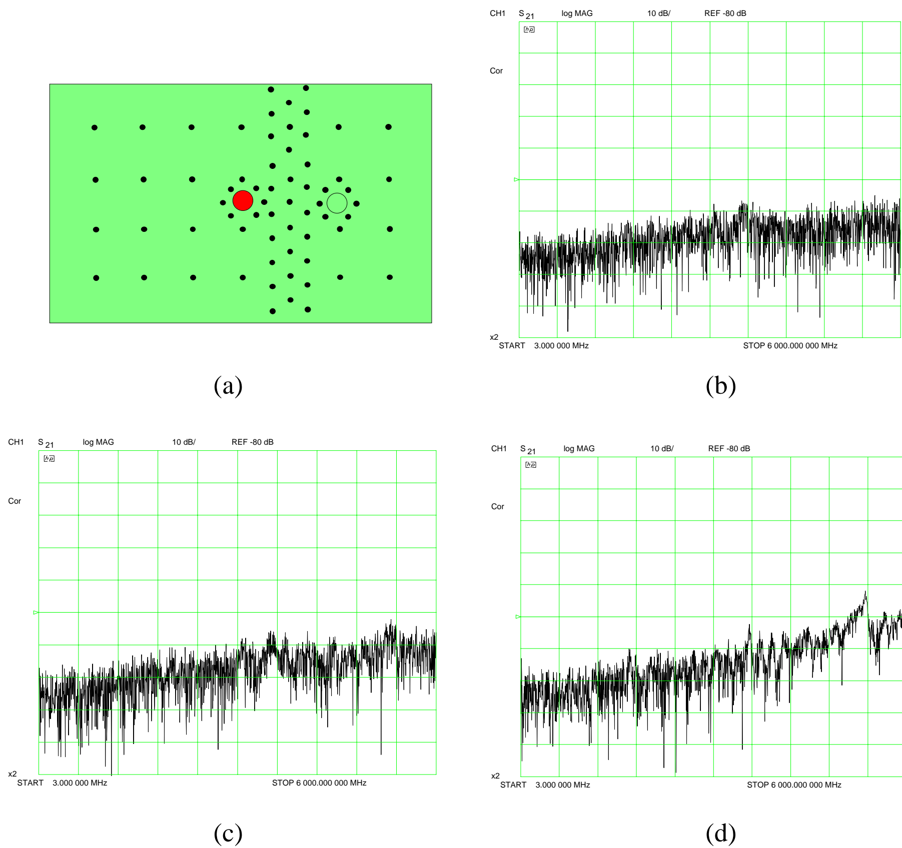

Fig. 45. Reduction of coupling when a cavity is filled with a 10 mm ground via grid in addition to coaxial vias and three rows with 5 mm grid added in between resonators. The frequency range is from 3 MHz to 6 GHz, the amplitude scale is 10 dB/ div and the reference value of -80 dB is located 5 divisions from the bottom line. Ground via locations are shown in (a), noise floor in (b) and coupling with terminated (approximately 50 ohms) and shorted probes in (c) and (d), respectively.

In section 4.2.1 p 34 a via position in a corner of a cavity is described as advantageous especially considering the lowest modes. This is due to low fields at the corners of a rectangular cavity. To test the effects in practice two vias are located at the opposite corners of a 50 mm × 80 mm cavity at 5 mm distance from both side walls. Reduction of coupling compared to the case described in Fig. 38 p 64 may be up to 45 dB, depending on the probe termination, for the lowest resonance. With rising frequency this advantage starts to fade. Measured results are shown in Fig. 46.

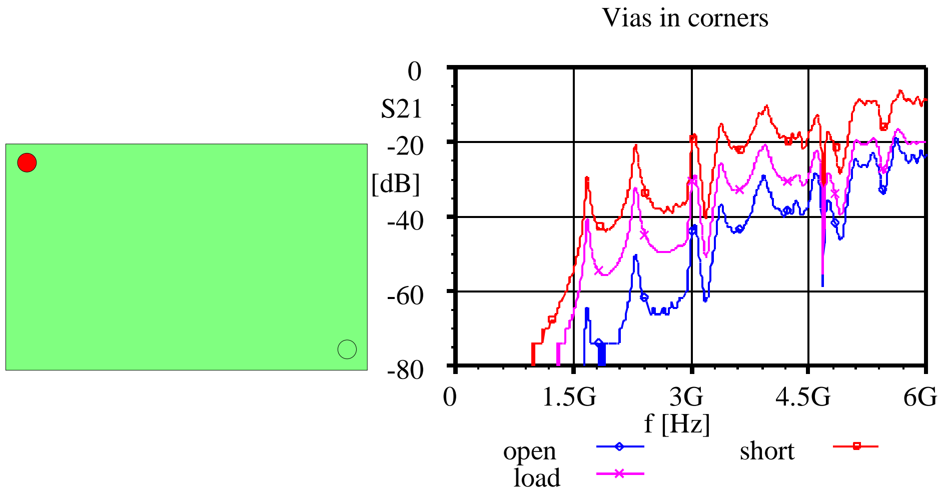

Fig. 46. Measured coupling, when the vias are located in the opposite corners of the cavity.

It is also possible to use metalled holes instead of vias to divide resonators. If we consider coupling between ports P2 and P3 of the structure described in Fig. 37 p 63 and cut a 1.2 mm diameter hole through the cavity along the centre line between signal vias and then metal it, we may reduce coupling to the measurement noise floor. Copper tape is used for metallization. Tape is soldered to the PCB grounds at both sides of the boards along whole length of the hole. Port P1 does not exist on the board. Interestingly here only coupling in case of an open-ended probe deviates some decibels from the noise floor at worst. This coupling may be suppressed to the noise floor by shielding open ends by constructing a case from copper tape. If the same hole is cut to the PCB, but left without metallization coupling can still exist and the lowest resonance seems to closely correspond to that of a cavity with transverse dimensions of 50 mm × 80 mm. Measured results are shown in Fig. 47.

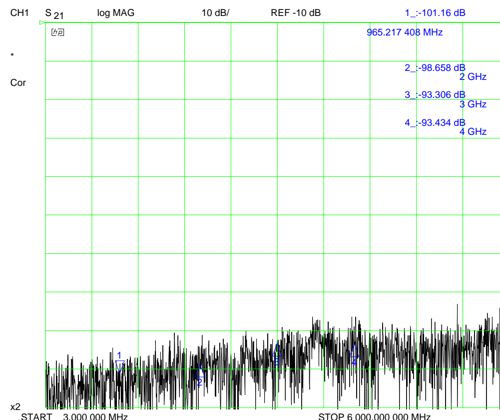

(a)

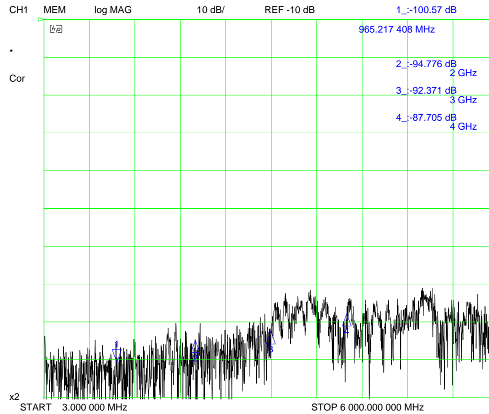

(b)

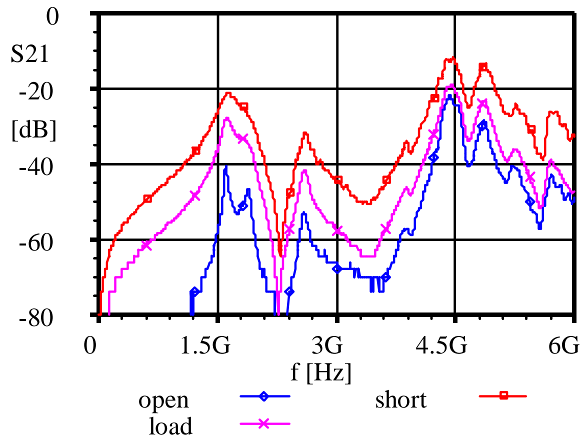

(c)

Fig. 47. Shielding hole cut between signal vias along the whole length of the resonator. Noise floor is shown in (a) and then coupling with metalled wall and open-ended probe in (b). The coupling values for terminated and shorted probes are below the noise floor. The same will happen also in the case of an open-ended probe if it is shielded. In (c) coupling is shown, when the hole is not metalled. In all measurements the frequency range is from 3 MHz to 6 GHz, although in (c) horizontal scale starts from 0 Hz. In both (a) and (b) vertical scale is 10 dB/ div, reference level position is at the top of the figure and corresponding value is – 10 dB.

5.3.2. Coupled cavities

Measurements for structures described in section 3.2.2 p 30 are performed to find out the effects of different via grids separating 80 mm × 50 mm sections. Coupling probes are left open-ended. Coupling between ports P1 and P2 over the whole measurement bandwidth is shown in Fig. 48. Ports P3 and P4 are left unconnected. It can be seen that the lowest coupling occurs with via grid of resonator 4 or 6. These correspond to the single or double row with S of 2.5 mm and 5 mm respectively. Generally coupling has also a tendency to increase when frequency rises. The reason for this is probably, that the ratio λ/S decreases and the coupling to the cavity increases with respect to the rising frequency.

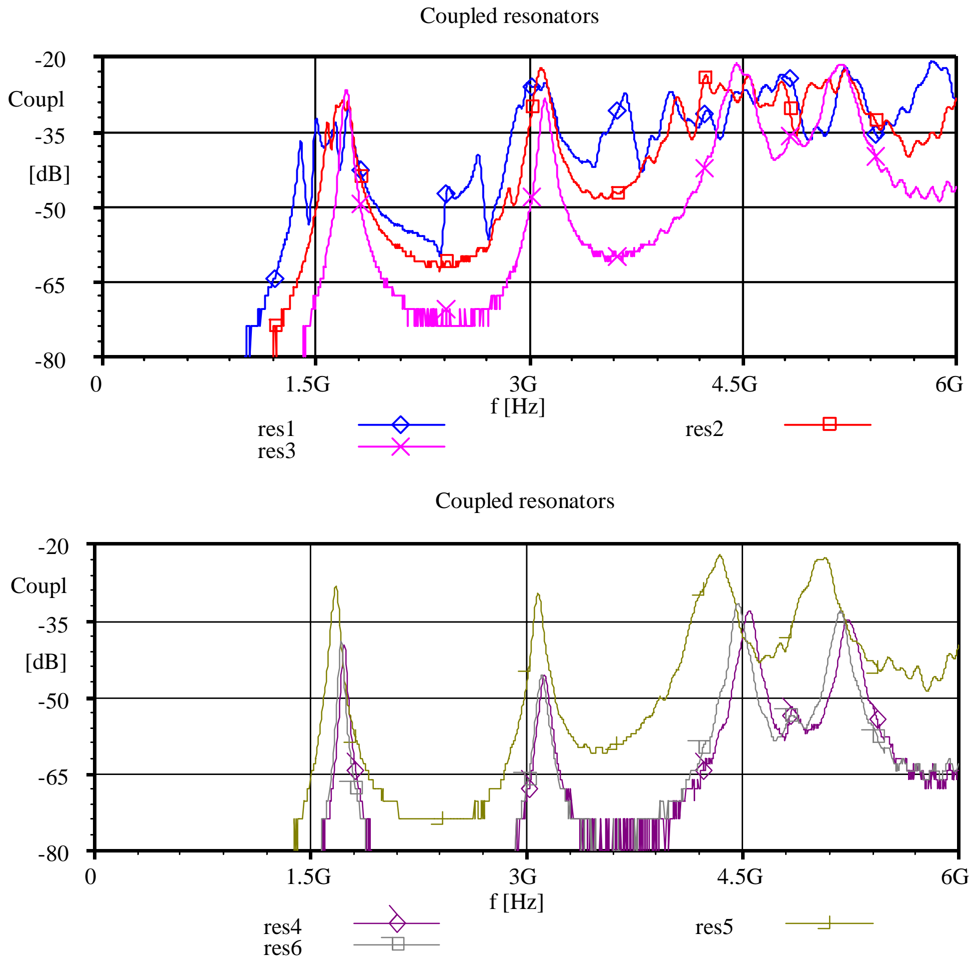

Fig. 48. Coupling from port P1 to port P2 at full measured frequency band from 3 MHz to 6 GHz when coupling probes are left open-ended.

The same results are shown in Fig. 49 with reduced span around first resonances. From here we can see that in case of resonators 4 and 6 coupling is quite low and produces only a single peak. Peak for resonator 6 is at a bit lower in frequency. This can be explained by two via rows of resonator 6, which makes the structure a little larger although the total number of vias is the same in both cases. A similar frequency shift effect can be seen between resonators 3 and 5. In their case coupling is however much higher. Resonators 1 and 2 do not show clear single peaks and their resonant response starts from lower frequencies than in other cases. The lowest resonant frequency in each case is shown in Table 14. We can see that the resonant frequency has a rising trend with respect to decreasing separation between vias. Simulated results in Table 5 p 45 show a similar trend although the resonant frequencies are a bit lower in value. Simulated modal field patterns for the lowest resonance with a single via row, when S is either 20 mm or 2.5 mm are shown in Fig. 25 p 45.

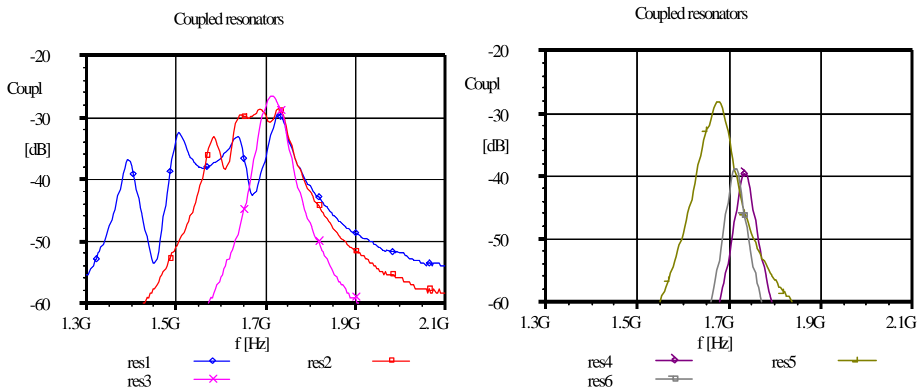

Fig. 49. Measured coupling from port P1 to port P2 at the vicinity of first resonances.

Table 14. Lowest resonant frequency for resonators 1-6 for coupling between ports P1 and P2.

	RES1	RES2	RES3	RES4	RES5	RES6
f_r [GHz]	1.39	1.58	1.71	1.74	1.68	1.72

To check effects of structural symmetry coupling between ports P2 and P3 is also measured and the results for the first resonance are shown in Fig. 50. Coupling for resonators 1 and 3 differ remarkably from measurements between ports P1 and P2. Less effect is found between results for resonators 3-6. However, coupling levels tend to be a bit higher in the symmetric case i.e. measurements between ports P2 and P3. Additionally two close resonant peaks for resonator 3 can be seen indicating overcoupling.

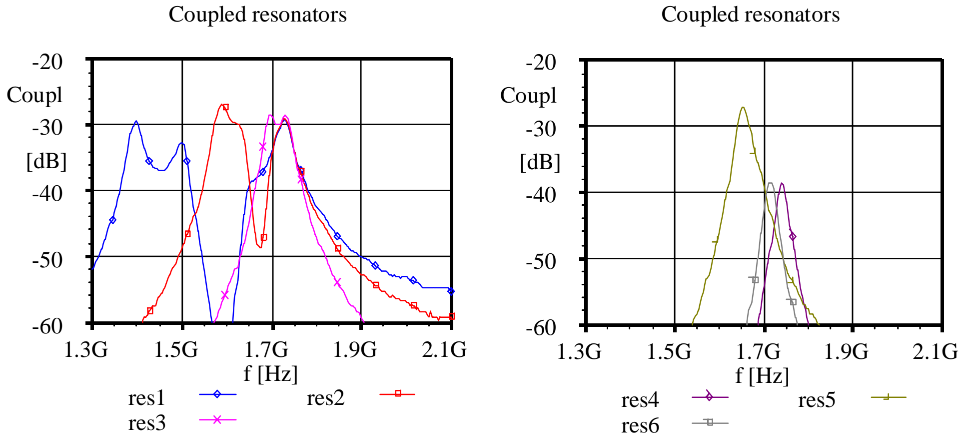

Fig. 50 Measured coupling from port P2 to port P3 in the vicinity of the first resonances.

Coupling values over the frequency range 1.3 GHz to 2.1 GHz between ports P1 and P3 are shown in Fig. 51. Ports P2 and P4 are left unconnected. Coupling for resonators 4 and 6 is decreased about 20 dB and the Q-value is notably increased compared to the measured results between ports P1 and P2. Similar effects for resonators 3 and 5 can be seen, but the changes are less dramatic. Maximum coupling values for resonator 1 and 2 change only negligibly. A quite similar trend can be seen when changing receiving end from port P3 to port P4 and leaving P2 and P3 unconnected. Measured results are shown in Fig. 52. Note that vertical scales of the figures on the left and right sides in Fig. 52 are different, because coupling level for resonator 4 and 6 is much lower than in other cases. Coupling results in the vicinity of the first resonances are summarised in Table 15 and Fig. 53. In Fig. 53 also maximum coupling values in case, that 0.34 mm substrate is used are shown for comparison. It can be seen that isolation values vary between 1.5 mm and 0.34 mm boards, but relative changes for different probe locations are quite similar. Coupling between ports P1 and P4 is under the measurement noise floor for 0.34 mm board for resonators 4 and 6. Separation Δ of the vias along width of the resonator compared to the wavelength at which leakage is measured is shown in Table 15. Relative permittivity ε_r is assumed to be 4.4. It can be seen that separations in the order of $\lambda/10$ or larger do not give much isolation increase when more via rows are added between measurement points.

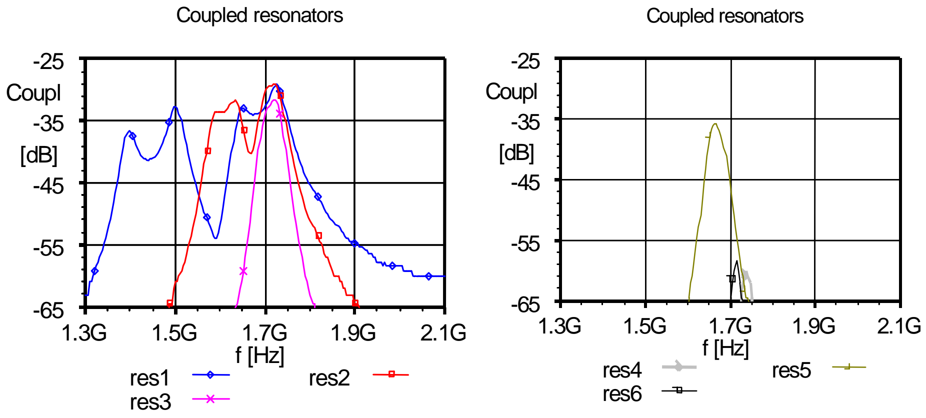

Fig. 51. Measured coupling between ports P1 and P3 at the vicinity of first resonances.

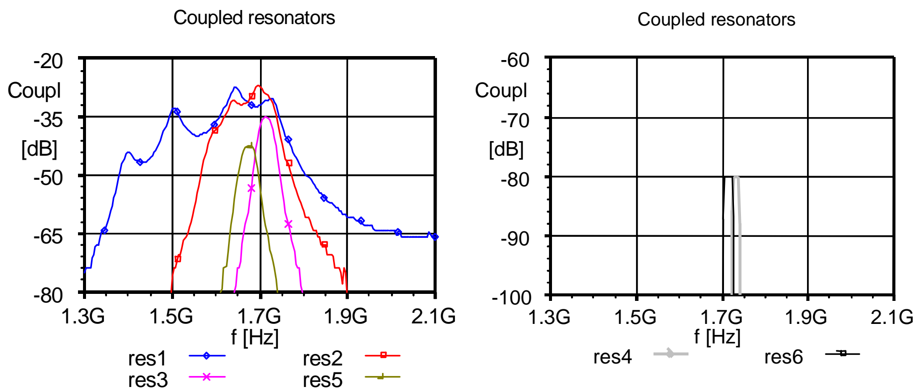

Fig. 52. Coupling between ports P1 and P4 at the vicinity of first resonances.

Table 15. Maximum coupling and associated frequencies for coupled resonators, when substrate thickness is 1.5 mm. Frequency range considered is from 1.3 GHz to 2.1 GHz. RES1-6 indicate different ground via configurations. Parameter Δ is equal to S or S/2 for single and double via rows, respectively.

	RES1	RES2	RES3	RES4	RES5	RES6
S_{21} [dB]	-29.5	-28.5	-26.6	-39.6	-28.2	-39.7
S_{31} [dB]	-29.1	-29.2	-31.4	-60.0	-35.7	-58.4
S_{41} [dB]	-27.4	-27.0	-35.1	-80.0	-42.2	-80.0
S_{23} [dB]	-29.2	-26.9	-28.4	-38.6	-27.1	-38.5
f_{S21} [GHz]	1.73	1.73	1.71	1.74	1.68	1.72
f_{S31} [GHz]	1.73	1.72	1.72	1.74	1.66	1.72
f_{S41} [GHz]	1.65	1.70	1.72	1.73	1.68	1.71
f_{S23} [GHz]	1.73	1.59	1.70	1.74	1.66	1.72
Δ/λ_{S21}	0.24	0.13	0.06	0.03	0.06	0.03
Δ/λ_{S31}	0.24	0.12	0.06	0.03	0.06	0.03
Δ/λ_{S41}	0.23	0.12	0.06	0.03	0.06	0.03
Δ/λ_{S23}	0.24	0.11	0.06	0.03	0.06	0.03

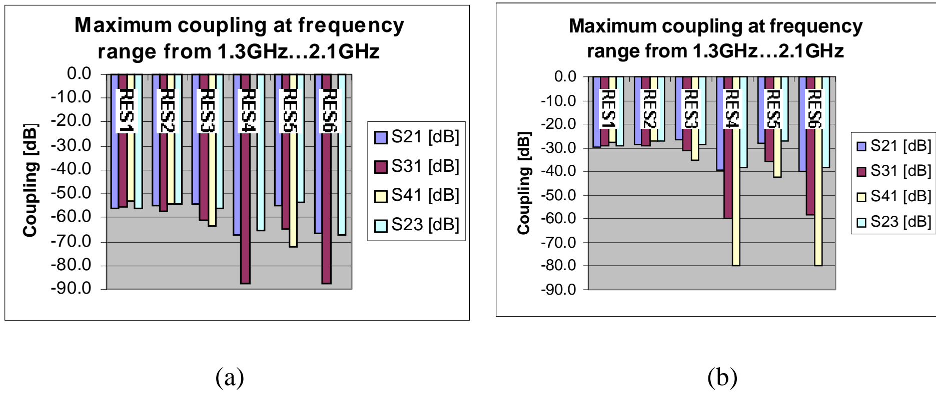

(a) (b)

Fig. 53. Maximum coupling values for (a) 0.34 mm and (b) 1.5 mm boards at frequency range from 1.3 GHz to 2.1 GHz.

6. Discussion

6.1. Measurement accuracy

The main effect to the measurement accuracy when high dynamic range is desired comes from the achievable isolation of the measurement device, which is in this case a network analyzer. Isolation between ports of the measurement device is reduced when frequency rises. This is however partially compensated by the fact that coupling in the resonator test boards tends to increase with rising frequency. Now with a 30 Hz IFBW coupling which is higher than –85 dB can be measured over the whole frequency range. Note that this already takes into consideration the effect of the measurement cables. When it is further taken into consideration that a thicker substrate is used to increase coupling this can be thought to be quite adequate for most purposes. One additional point effecting isolation is that leakage from signal lines or via terminations (especially open-ended) on the PCB may exist. This is minimised by installing input and output terminations at the opposite sides of the board. Additional shielding is used when it is felt to be necessary. Naturally calibration inaccuracy have to be taken into consideration also, but from an EMC point of view it can be though to be negligible. This can be reasoned by the fact that there should be sound safety margin considering isolation. However, it should be noted that calibration is performed at the end of the measurement cables. So, response of board connectors is included in measurements. This can be considered to have quite negligible effect from isolation point of view with same reasoning as for calibration.

6.2. Modelling accuracy

Basic inaccuracy of the models comes from the simplification of a physical structure and then from the inability of a model to exactly characterise desired phenomena.

In case of analytical and numerical models for PCB resonators it is assumed that a structure can be described as a waveguide thus forming a closed problem. This is not entirely true, because part of the fields may leak from the board edges much like in a case of a microstrip antenna. However, in this study consideration is given mainly to the

structures that have via grids at the edges of the structure thus reducing leakage. So, a closed boundary seems to be still a reasonable approximation at least from the EMC point of view. No perturbing effects due to signal vias are considered except in 3-D modelling. For calculation of resonant frequencies effect of these is quite negligible for purposes of this study. In 2-D numerical models ground vias are modelled as a single node point in a simulation domain and their finite conductivity is not taken into consideration. Also any other losses are neglected in the calculation of fields both in analytical and 2-D numerical models. This can be considered as a reasonable approximation for EMC purposes. When Q-values are approximated no effect of the vertical dielectric surfaces or vias is taken into consideration. This can be reasoned by the fact that most losses can be attributed to the FR4 dielectric filling and typically large top and bottom ground (or power) plates in comparison to the sidewalls or vias. The geometry is also simplified when ground vias are approximated to be rectangular in modelling of a coaxial via. In coaxial gap model of opposite open-ended vias outer conductor is assumed to be complete and in simplified model no fringing fields are taken into consideration. In addition to this a typical blind via end has a hole in a pad area due to drilling of the via hole. Pad areas also cause changes in centre conductor cross-section.

The finite difference schemes used are basically of second order accuracy. This means, that truncation errors in finite difference approximations are proportional to the h^2, where h is the grid size.

The usefulness of quasi-static models reduces when the frequency rises. The reason for this is, that the fields in the structures have more complicated forms than the approximation is able to describe. The effect of this can be well seen in static capacitance models for coupling between open-ended vias at frequencies above 3 GHz, where behaviour of the modelled coupling values starts to deviate from the measured results.

6.3. Comments on measured and modelled results

Comparisons between measured results on two and eight-layer boards show quite good correlation except in the case of an open-ended probe. This may be explained by a probe going through multiple layers before termination, which enables higher capacitive coupling to the cavity. Further evidence for this is that in case of an open-ended probe coupling through two stacked cavities is lower than for a single cavity inside an eight-layer board. Resonant frequencies are also slightly lower for an eight-layer board. This may be again due to multiple layers causing a resonator to be a bit larger although the centre section is dominating in resonances. Also tolerances of FR4 dielectric material may cause deviations. Differences in match may be explained by similar comments and also by the effect of different connectors, PCB traces and nonideal terminating resistors. Despite these differences similarities are still high enough that methods to improve isolation may be studied on a two-layer board.

When 1.5 mm instead of 0.34 mm thick substrate for two-layer board is used coupling values are increased especially in case of an open-ended probe. Loaded Q-values decrease, which is natural consequence of increasing coupling. However, we should remember that unloaded Q-value for a thicker cavity is not so much effected by conductor

losses as a thinner layer version, thus increasing Q. On the other hand the dielectric loss tangent of FR4 board already reduces unloaded Q-value to be not higher than 100 and more typical values are probably around 60. Also possible leakage from the board may be higher in the case of a thicker substrate. In spite of this high coupling is still available inside a PCB. Resonant frequencies for 1.5 mm boards are somewhat higher than for 0.34 mm boards. This is probably due to differences in values of relative permittivity. Also some deviations in resonant frequencies on 1.5 mm boards can be noted. This may be explained again by slightly different values of relative permittivity. The reason for this is probably that, PCB's with thicker substrates were purchased from two different manufacturers. However, these shifts in resonances are negligible from an EMC point of view.

Differences between measured and calculated resonant frequencies are no more than a few percent for both analytical and numerical methods. This is tolerable from the EMC point of view, when the effect of dielectric material tolerance is also taken into consideration. Theoretically calculated unloaded Q-values seem to have reasonable correlation with measurements in a way that unloaded Q-values show a limit to the achievable Q of the board. It should be remembered here that roughness of the copper and dielectric loss tangent are not necessarily exactly specified quantities.

Simulated coupling values in case of a 1.5 mm thick substrate correspond quite well with measurements, when no ground vias are added inside the sidewalls of the cavity. This is shown in Fig. 26 p 47. However, one would expect measured resonant frequencies to be lower because sidewalls of the resonator are formed by via grids instead of ideally conductive walls as in the simulations. This may be attributed to the inaccuracy of the simulation or on the other hand deviations in relative permittivity of the substrate material. FDTD simulation method has been used also in other studies to model coupling between vias, when no resonances are present and also to model power plane resonances (Pillai 1997, Van den Berghe *et al.* 1998).

Coupling due to unshielded open ends is measured with metalled shielding hole, but not in the situation, where multiple ground vias are used as shown in Fig. 45(a) p 70. However, the metalled shielding hole is shown to reduce coupling in the case of terminated (100R//100R) and shorted probes more than the via grids of Fig. 45(a) p 70. In both cases signal via locations are the same. When the metalled shielding hole is used resonant cavities of dimensions 50 mm × 50mm and 30 mm × 50 mm are formed. These in turn may enhance radiation. In the case of multiple vias being used resonances are further suppressed such that radiation is below the noise floor.

Comparison of the measured results in Fig. 31 p 56 for routings between shielded sections show that the version with traces inside the PCB has more resonances. These are caused by the cavity inside the PCB. The resonance peak for through wall routing is due to a cavity formed by the ground plane of PCB and the shielding mechanics. Transverse dimensions of both structures are approximately the same, but FR4 has a higher relative permittivity than air and thus lower resonant frequencies. Difference in Q-values may be mainly attributed to the dielectric loss tangent of FR4 and the small height of the resonator inside the PCB. Resonance caused by the shielding mechanics and the ground plane is not seen in response of routing inside the PCB. The reason for this is probably that coupling to the corresponding mode is poor due to only via end with terminating resistors in a cavity. Resonances inside the PCB are caused by a cavity formed between

layers 4 and 5, which is coupled by blind via ends. These extend to layer 4 although the actual signal strip is on layer 3. This is due to the manufacturing method, where blind vias may be formed only between even number of layers. So, a via from layer 1 to 4 is possible, but not from 1 to 3. Coupling to the resonator is quite weak due to the probe location at the edge of the resonator. In case that resonances inside the PCB are suppressed and proper care is taken in matching this routing might be even better than through wall routing.

Measured and modelled results for coupling between vertically aligned blind vias correlate within some decibels up to 3 GHz. Deviation at higher frequencies is probably caused by the fact that the dynamic wave nature of the board starts to be important and the simple static capacitance model is no longer adequate. It is also interesting to note that these models seem to give reasonable approximations although pad areas at the ends of the vias inside PCB have holes. Below 3 GHz the simplified model with only a series capacitor seems to match measured coupling values better, when nominal board parameters are used in calculations. This can be reasoned by the fact that the outer conductor is not complete and inner conductor cross-section is reduced immediately after pad areas so the effect of parallel capacitors should probably be reduced. The difference between measured results for structures in Fig. 12(a) and (b) p 28 may be due to tolerances of the PCB parameters. These include 1) substrate thickness, 2) alignment of the vias and 3) relative permittivity. Here the first point is probably the most important. Additionally BMA connectors and their assembly may also cause deviations. It has also to be remembered that through via is used in subtracting excess losses from the measured results. This does take into consideration also loss due to via section between layers 4 and 5 of the PCB, which is not strictly correct. The error caused by this can be considered to be negligible when PCB tolerances and overall loss caused by connectors, coplanar microstrips and other portions of vias are taken into consideration. Another possible explanation for higher coupling when six coaxial vias are used is that 4 via structure may exhibit more leakage inside PCB. However, the difference is below 2 dB across the whole frequency range and from an EMC point of view this is quite negligible. The main point here is that vertically aligned vias may cause excessive coupling, which has capacitive behaviour at lower frequencies. This means that great care should be taken in PCB design to avoid these kinds of structures.

6.4. Improvement of isolation

Ideally no PCB resonances should exist at the frequency range of interest. In practice an ample safety margin between operating frequencies and the lowest resonant frequency may be needed because of finite Q-values of the resonances as described in section 5.2.1 p 53-54. Broadness of the resonances may be estimated already in the design phase by modelling Q-values as described in sections 4.2.2 p 35-37 and 4.3.2 p 45-46. Resonances can be naturally suppressed if the size of the PCB used is small compared to the wavelength at the frequency range of interest. This can be checked by using Eq. (1) p 31 to find resonant frequencies in case that a PCB is rectangular. Otherwise the 2-D numerical model described in section 4.3.1 p 40-45 may be applied. Again the effect of

the finite Q-values has to be considered. Here it is good to remember that selecting a substrate material with lower relative permittivity increases wavelength inside the board. Consequently resonant frequencies, which are proportional to $1/(\sqrt{\varepsilon_r})$ will increase. If a PCB is not electrically small it can be divided to smaller sections with via fences. These sections should be so small that no resonances exist at the frequency band of interest. In case that this is not possible neighbouring sections should have different resonant frequencies. Measured example of this kind of structure is shown in Fig. 43 p 69. Separation between vias in a fence should be small compared to the wavelength. If we take into consideration the measured results shown in Fig. 53 p 77 and Table 15 p 77 it seems that 0.1 λ, which is often considered to be small, is not necessarily small enough. The reasoning for this is that isolation between different sections of the coupled resonators varies only slightly, when the separation between vias is in the order of 0.1 λ or more. What we would expect is that isolation increases, when more via fences are added between measurement ports. Indeed this kind of behaviour can be seen in the measured results, when separation Δ between vias is in the order 0.06 or 0.03 λ. Eq (1) p 31 or numerical model in section 4.3.1 p 40-45 may be used for calculation of resonant frequencies for different sections. The latter can be applied in a more general case, while the former is restricted to modelling of rectangular sections. If via fences can not be inserted on the board, separate vias could be used to increase resonant frequencies. One way to do this is to establish a via grid on a PCB as shown in Fig. 44 p 69. Naturally it is even better if separate vias in addition to via fences are used. Measured results for this kind of structure are shown in Fig. 45 p 70. The lowest resonant frequency for these kind of structures may be estimated by using the 2-D numerical model presented in section 4.3.1 p 40-45. Also in some cases a wall may be formed by a hole or a slit cut into a PCB. The hole or slit should have metalled surfaces. This should clearly outperform isolation achievable by vias. In the measurements the coupling values for this kind of structure were below the noise floor as described in Fig. 47 p 72. Note that to achieve this the open-ended probe had to be shielded.

The approach described above focused on suppressing resonances of the board. In many practical cases this is not necessarily possible. The reasons may be for example that vias consume space that may be used for component placement and vias also increase costs. However, increased costs may be a small price to pay of a product that works correctly and which arrives on the market in good time. But if a cheap way to work under resonances is needed then one should at least attempt to suppress coupling to the resonator. This may be done by placing a signal via so, that fields are at their minimum. An example of this is to locate the signal via at the corner of the cavity as shown in Fig. 46 p 71. This is advantageous, because both electric and magnetic fields are at a minimum especially for lowest resonances as discussed in section 4.2.1 p 34. Hence suppression may be achieved regardless of the probe termination. Another obvious way is not to route signals so that they may couple to a cavity inside the PCB. An example of this is shown in Fig. 10 p 26 and Fig. 11 p 27, where the signal is routed either inside the PCB or through the shielding wall on a top layer. If the latter option is used no signal vias are used, which could feed the cavity inside the PCB. Unfortunately a resonator formed by the shielding mechanics and the PCB is still possibly coupled as can be seen from Fig. 31(a) p 56. Also a coaxial via structure may be used to decrease coupling to the resonator and increase resonant frequencies. An example of the effect of the coaxial vias on the modal field

pattern is shown in Fig. 24 p 44. The improvement of isolation in this case can be seen by comparing coupling responses in Fig. 38 p 64 and Fig. 39 p 65. Coaxial vias enhance also match and decrease loss along the signal path as shown in Fig. 40 p 66 and Fig. 41 p 67. Crosstalk effects for this kind of structure have been simulated by using a FDTD model (Pillai 1997). Although no resonance effects were modelled in Pillai's study FDTD is capable of doing this as shown in this study and also by Van den Berghe *et al*. (1998).

7. Conclusions

The main purpose of this thesis was to study coupling between vias on multilayer boards and to show how isolation could be improved. Special attention was given to the coupling due to PCB resonances and vertically aligned blind vias. Measurements and modelling were used as research methods. The problem was approached from an EMC point of view. So, high accuracy of measurements or models was not the objective.

Both analytical and numerical means were used in modelling. Analytical methods included calculation of resonant frequencies, fields and Q-values for simple rectangular structures. Cavity was reduced to two-dimensions for numerical calculation of the same quantities in analytically difficult cases. Simple analytic capacitance models with Aplac circuit simulator were used for approximation of coupling between vertically aligned open-ended blind vias. The quasi-static model was used to study a coaxial via structure. Three-dimensional FDTD simulator of Aplac was used to model coupling between vias. For measurements test structures were build for resonators and vertically aligned open-ended vias on multilayer boards. Simplified resonator structures were also built on two-layer boards to test different methods to increase isolation. FR4 was used as a substrate material in these structures.

Measured and calculated resonant frequencies correlate within a few percent. Q-value calculations showed that the main limiting factors are small height of the cavity inside the PCB and the relatively high loss tangent of FR4 substrate material. It was shown that high coupling may occur due to PCB resonances and termination of a via has a high effect on coupling. Increasing via separation and coaxial via structure suggested in other studies to increase isolation were noted to be not necessarily effective enough. However, good match and low through loss was noted for a coaxial via even under resonant conditions. Several methods to reduce coupling due to cavity resonances of a PCB were presented based on measurements, models and ideas from closely related studies. These included proper location of a via, coaxial via structure, via fences, metalled holes or slots in a PCB, decreasing relative permittivity, proper division ratios of large cavities and separately located ground vias. Coupling due to vertically aligned blind vias was shown to be high. A simple capacitance model was used to successfully approximate this up to the frequencies where the dynamic wave nature of the board starts to be important.

From a PCB designers point of view these results mean that when board size is large compared to the wavelength the possibility of resonances has to be taken into account.

Here small means size, which causes PCB resonances to be well above operating frequencies. Whether this happens or not can be checked by using either analytical or numerical model to calculate the lowest resonant frequency. Broadness of the resonances may be estimated by modelling Q-values. Also this may be done either analytically or numerically. Analytical models shown in this study are applicable to rectangular PCB structures, while 2-D numerical models are valid in a more general case. The advantage of these methods is that they are simple and typically fast compared to 3-D numerical models. The drawback is that they do not give the actual coupling values between vias. In case that these are needed a 3-D FDTD model may be applied as described in this study. However, simulations with this model even for a modest structure with dimension of 80 mm × 50 mm can take several hours. So, 3-D FDTD modelling of large PCB's like motherboards is quite likely to be out of the question during the design phase. Suppression of resonances can be accomplished basically by two means: 1) not to design a resonator in the first place and 2) minimising coupling to the possibly formed resonator. Several ways to carry out both of these options were shown in this thesis. Also placement of the vias has to be carefully selected especially if blind or buried vias are used to avoid coupling between via ends.

References

Bird TS (1996) Cross-coupling between open-ended coaxial radiators. IEE Proc.-Microw. Antennas Propag. 143(4): 265-271.

Booton RC Jr. (1992) Computational Methods for Electromagnetics and Microwaves. John Wiley & Sons, Inc., New York, p 24-36, 52-56.

Chen C, Tsai MJ, Alexopoulos NG (1996) Optimization of aperture transitions for multiport microstrip circuits. IEEE Transactions on Microwave Theory and Techniques 44(12): 2457-2465.

Clayton PR (1992) Introduction to Electromagnetic Compatibility. John Wiley & Sons, Inc., New York, p 402-404.

Coetzee JC, Joubert J (1996) Full-wave characterization of the crosstalk reduction effect of an additional grounded track introduced between two printed circuit tracks. IEEE Transactions on Circuits and Systems-I: Fundamental Theory and Applications 43(7): 553-558.

Daigle RC, Bull GW, Doyle DJ (1993) Multilayer microwave boards: manufacturing and design. Microwave Journal, April: 87-97.

Das NK (1996) Methods of suppression or avoidance of parallel-plate power leakage from conductor-backed transmission lines. IEEE Transactions on Microwave Theory and Techniques 44(2): 169-181.

Dawirs HN (1969) Equivalent circuit of a series gap in the center conductor of a coaxial transmission line. IEEE Transactions on Microwave Theory and Techniques, February: 127-129.

Dworsky LN (1979) Modern Transmission Line Theory and Applications. John Wiley & Sons, Inc., New York, p 137-152

Fujimoto K, James JR (1994) Mobile Antenna Systems Handbook. Artech House, Boston, p 536-545.

Gu Q, Tassoudji MA, Poh SY, Shin RT, Kong JA (1994) Coupled noise analysis for adjacent vias in multilayered digital circuits. IEEE Transactions on Circuits and Systems I: Fundamental Theory and Applications 41(12): 796-803.

Hoffman RK (1987) Handbook of Microwave Integrated Circuits. Artech House, Norwood, p 394 – 403.

Howell JQ. (1973) A quick accurate method to measure the dielectric constant of microwave integrated circuit substrate. IEEE Transactions on Microwave Theory and Techniques, March: 142-143.

Kajfetz D, Guillon P (1986) Dielectric Resonators. Artech House, Inc., Dedham, p 53-60.

Kiang JF (1990) On resonance and shielding of printed traces on a circuit board. IEEE Transaction on Electromagnetic Compatibility 32(4): 269-276.

Landbrooke PH, Potok HN, England EH (1973) Coupling errors in cavity-resonance measurements on MIC dielectrics. IEEE Transactions on Microwave Theory and Techniques, August: 560-562.

Li M, Ma KP, Hockanson DM, Drewniak JL, Hubing TD, Van Doren TP (1997) Numerical and experimental corroboration of an FDTD thin-slot model for slots near corners of shielded enclosures. IEEE Transactions on Electromagnetic Compatibility 39(3): 225-232.

Liao SY (1987) Microwave Circuit Analysis and Amplifier Design. Prentice Hall Inc., New Jersey, p 304-305

Matthaei G, Young L, Jones EMT (1980) Microwave Filters, Impedance-Matching Networks, and Coupling Structures. Artech House, Inc., Norwood, p 660-662.

Montrose M (1996) Printed Circuit Board Design Techniques for EMC Compliance. IEEE Press, p 30-38, 61-62, 93-94.

Napoli LS, Hughes JJ (1971) A simple technique for the accurate determination of the microwave dielectric constant for microwave integrated circuit substrates. IEEE Transactions on Microwave Theory and Techniques, July: 664-665.

Parker JC (1997) Via coupling between parallel rectangular plates. IEEE Transactions on Electromagnetic Compatibility 39(1): 17-23.

Pillai ER (1997) Coax via - a technique to reduce crosstalk and enhance impedance match at vias in high-frequency multilayer packages verified by FDTD and MoM modeling. IEEE Transactions on Microwave Theory and Techniques 45(10): 1981-1985.

Ponchak GE, Chen D, Yook JG, Katehi LB (1998) Characterization of plated via hole fences for isolation between stripline circuits in LTCC packages. Proc. IEEE MTT-S Symposium, Baltimore, MD.

Pozar DM (1998) Microwave Engineering. John Wiley & Sons, Inc., New York, p 313-318

Ramo S, Whinnery JR., Van Duzer T (1984) Fields and Waves in Communication Electronics. John Wiley & Sons, Inc., New York, p 27-28, 392-395, 489-495

Robinson GH (1971) Resonant frequency calculation for microstrip cavities. IEEE Transactions in Microwave Theory and Techniques, July: 665-666.

Sadiku M (1992) Numerical Techniques in Electromagnetics. CRC Press Inc., Boca Raton, p 173-176.

Wadell BC (1991) Transmission Line Design Handbook. Artech House, Boston, p 47-49, 97-99, 267-268, 447.

Waldron RA (1967) The Theory of Waveguides and Cavities. Maclaren & Sons Ltd., London, p 19.

Van den Berghe S, Olyslager F, De Zutter D, De Moerloose J, Temmerman W (1998) Study of the ground bounce caused by power plane resonances. IEEE Transactions on Electromagnetic Compatibility 40(2): 111-119.

Watson PM, Gupta KC (1996) EM-ANN models for microstrip vias and interconnects in dataset circuits. IEEE Transactions on Microwave Theory and Techniques 44(12): 2495-2503.

Yook JG, Chandramouli V, Katehi LPB, Sakallah KA, Arabi TR, Schreyer TA (1997a) Computation of switching noise in printed circuit boards. IEEE Transactions on Components, Packaging, and Manufacturing Technology- Part A 20(1): 64-75.

Yook JG, Katehi LPB, Sakallah KA, Martin RS, Huang L, Schreyer TA (1997b) Application of system level EM modeling to high-speed digital IC packages and PCB's. IEEE Transactions on Microwave Theory and Techniques 45(10): 1847-1856.